FREQUENCY-INDEPENDENCE AND SYMMETRY PROPERTIES OF CORRUGATED CONICAL HORN ANTENNAS WITH SMALL FLARE ANGLES

M.E.J. JEUKEN
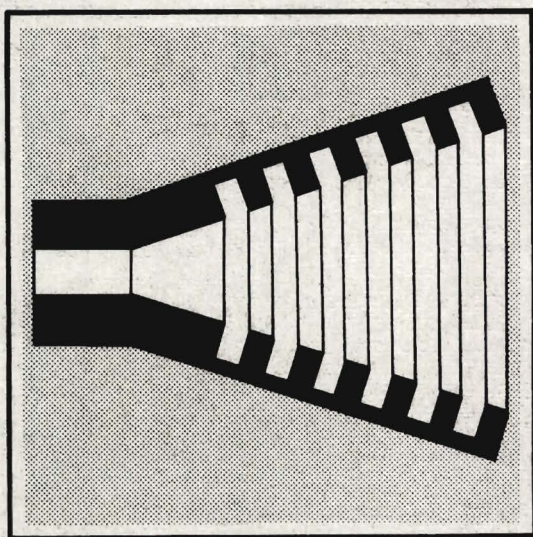
FREQUENCY-INDEPENDENCE AND SYMMETRY PROPERTIES OF CORRUGATED CONICAL HORN ANTENNAS WITH SMALL FLARE ANGLES

Dit proefschrift is goedgekeurd
door de promotor
Prof.Dr.Ir.A.A.Th.M. van Trier

een aandenken aan mijn vader
aan mijn moeder
aan mijn vrouw

CONTENTS

CHAPTER 1

FEEDS FOR REFLECTOR ANTENNAS

1.1   Introduction

The parabolic reflector is a popular antenna in the microwave region.
This is the frequency range from 1 GHz to 300 GHz. In this range the
parabolic reflector is used as an antenna for radar, line-of-sight
communications, satellite communications and as an instrument for
radio-astronomical investigations.

The principle of this reflector antenna is that a spherical wave de-
parts from the focal point of the parabola towards the reflector, which
reflects the wave and concentrates a large part of the energy in a
small angle along the axis of the parabola. As a source of the sphe-
rical waves use is mostly made of a small horn antenna.

Such a source is called a feed. It is obvious that the performance of
the reflector antenna depends mainly on the feed used. For instance,
the illumination of the reflector and the spill-over energy along the
rim of the reflector depend on the radiation pattern of the feed.

It is well-known that for a reflector antenna no unique definition of
the bandwidth can be given [1]. However, generally speaking, we can
say that the bandwidth of a reflector antenna is chiefly determined
by the properties of the feed.

The precise requirements which have to be satisfied by the feed depend
on the application for which the antenna will be used.
Let us summarise the most relevant properties of the feed in the four
applications mentioned at the beginning of this section.
For a radar antenna a high gain is necessary, because the range of a
radar system is proportional to the square root of the antenna gain.
This high gain can be obtained if a reflector antenna is used with a
diameter, which is large compared with the wavelength. Moreover, one
should choose the illumination of the reflector in such a way that a
high efficiency is obtained. This requirement implies that the illu-
mination should be as uniformly as possible and the spill-over energy
along the rim of the reflector as low as possible. A radiation pattern

with these two properties is called a sector shaped radiation pattern. The radiation pattern of a conventional feed, such as an open radiating waveguide, deviates considerably from a sector shaped radiation pattern. Therefore modern research on feeds is mainly carried out with the aim to improve the radiation pattern of conventional feeds. For a radar antenna it is sufficient that the feed possesses a sector shaped radiation pattern in a rather small frequency range, because the bandwidth of a radar antenna is small.

In addition, sometimes a radar antenna should transmit and receive circularly polarised waves in order to prevent the detection of echoes from such targets as rain and snow [1]. It is clear that in this case the feed should be able to transmit and receive circularly polarised waves without disturbing the other properties discussed above.

An antenna for line-of-sight communications should meet the same high requirement with regard to the gain as a radar antenna. The bandwidth of this antenna system is much larger, because the antenna is used for telephone and T.V. traffic. In the frequency spectrum above 1 GHz several frequency bands have been allocated for this kind of communications. Which of the frequency bands mentioned above are used in a line-of-sight communication system depends on the local situation. In order to use the frequency bands as effectively as possible the feed must be suitable for operation in two perpendicular modes of polarisation [2]. In that case it is very desirable that the radiation patterns in two perpendicular planes are the same for the two modes of polarisation. It is obvious that a symmetrical radiation pattern with respect to the antenna axis meets this requirement.

One of the most recent applications in the microwave field is communication by means of satellites, for instance, the famous Early Bird (= Intelsat I), Intelsat II and Intelsat III and in the near future the Intelsat IV, which are employed for intercontinental telephone and T.V. traffic. Again the antenna for satellite-communications should be suitable for broadband operation, because of the large amount of information that must be handled with this system. In order to get an idea about the bandwidth which is required in these modern communication systems, it should be noted that a groundstation used for communications with Intelsat III must be suitable for receiving in the frequency band 3700 - 4200 MHz and transmitting in the 5925 -

8

6425 MHz band. Besides, the gain and the figure of merit, which is de-
fined as the ratio of the antenna gain and the system noise tempera-
ture, should meet very stringent requirements. Especially in connec-
tion with the low noise requirement a cassegrain antenna is used ex-
clusively. In order to obtain high aperture efficiency and low spill-
over and diffraction losses at the subreflector the principle of dual
shaping has been proposed [3]. In this case it is necessary for the
radiation pattern of the feed to be symmetrical with respect to the
antenna axis in the desired frequency band. The reflectors can be ad-
justed only for one frequency. Therefore it is a coercive demand that
the phase pattern is also independent of the frequency in the desired
frequency band and symmetrical with respect to the antenna axis as
well. However, owing to the principle of dual shaping, it is not nec-
essary that the feed possesses a sector shaped radiation pattern. A
complete list of requirements which should be met by a feed in an an-
tenna of a groundstation can be found in [4] .

The purpose of a radio-astronomical antenna is to detect and to study
celestial radio sources. In order to prevent interference with other
users of the frequency spectrum, several frequency bands have been
allocated to radio-astronomical research. An example is the frequency
band situated between 1400 MHz and 1427 MHz. So the bandwidth which is
needed is small. Radio-astronomical investigations require a high re-
solution and a high sensitivity. A high resolution is obtained with a
large reflector antenna, while a high sensitivity requires that the
system noise temperature is low. So the antenna noise temperature must
be low, for in most cases low noise receivers are used. The low tempe-
rature is obtained by using a carefully designed feed and applying an
edge illumination of about 20 dB, including the space attenuation. If
the antenna is used for studying the polarisation characteristics of a
radio source, it is necessary that the cross-polarisation in the main
beam should be as low as possible [5]. It can be shown quite easily
that this low cross-polarisation can be realised with a feed with a
symmetrical radiation pattern with respect to the antenna axis [6].In
that case the electric field in the aperture of the reflector has a
constant direction.

Summarising one can say that in general a good feed should possess one or more of the following properties:

(i)   a flat or sector shaped radiation pattern in the forward direction in order to illuminate a reflector as effectively as possible;

(ii) a power radiation pattern and a phase radiation pattern both of which are symmetrical with respect to the antenna axis;

(iii) the feed should possess the two properties mentioned above in a frequency band as large as possible.

In the next section a survey of the recent literature concerning feeds for reflector antennas is given. In this survey special attention is devoted to the three properties of feeds mentioned above.

1.2   Survey of the recent literature concerning feeds

High aperture efficiency and high spill-over efficiency can be attained with a feed which has a sector shaped radiation pattern. The problem of synthesising a sector shaped radiation pattern has attracted the attention of several investigators in the antenna field. A remarkable effort has been made by Koch [7]. He started by observing that the radiation pattern on a field basis is approximately the Fourier transform of the aperture field. The next consideration was that an ideal sector shaped pattern can be realised with an aperture field of the form $J_1 (x) / x$; x is the normalised radius of the circular aperture. The following task was to generate a field to approximate this situation. This was done by means of a central waveguide and five conductors with circular cross-section arranged coaxially. A further improvement of the system was published one year later [8] by the same author.He claimed to have succeeded in synthesising a sector shaped radiation pattern. However, up till now no information concerning the bandwidth of this antenna is available.

A purely experimental approach of the same problem has been followed by Geyer [9]. He designed a feed for an antenna for line-of-sight communications. He was able to improve the radiation pattern of a circular horn radiator by placing one or more annular one-quarter wave chokes around the aperture. Then the radiation pattern in the H-plane,

the E-plane and the 45°-plane became equal in a relative frequency band of 1 : 1.2. There is still need for a theoretical explanation of his results. Besides, it is desirable that more design information is available. The same problem has been also tackled by Thust [10]. He placed mushroom-shaped elements on the flange of a horn radiator. They pointed in the direction of the antenna axis. In this way a more or less sector shaped pattern was realised in the frequency band 5.925 GHz to 6.425 GHz. In this case too, it will be difficult to give a theoretical explanation of the phenomena observed.

In the antenna research work discussed hitherto the main effort was devoted to the design of a sector shaped radiation pattern. This was of more importance than obtaining also a completely symmetrical radiation pattern.

In some applications, however, a radiation pattern which is as symmetrical as possible is of the utmost importance. As an example we recall that the application of the dual shaping principle demands a symmetrical radiation pattern and a phase pattern which is symmetrical with respect to the antenna axis as well. The first effort to design a horn antenna with equal beamwidth in all planes through the antenna axis was undertaken by Potter [11]. He was able to improve the radiation pattern of a conical horn antenna by applying two modes. Somewhere in the feed the TM_{11}-mode is generated apart from the dominant TE_{11}-mode. If the right phase and amplitude relations in the aperture are applied to these two modes, a radiation pattern is obtained with equal beamwidth in the E-plane, H-plane and 45°-plane. The theory of mode generation as given by Potter has been extended by Nagelberg and Shefer [12] and by Reitzig [13]. From their work and the paper of Potter it is impossible to get a clear insight into the bandwidth which can be obtained with this dual-mode technique. In an effort to improve the radiation pattern of the dual-mode conical horn antenna Ludwig [14] used four modes. His aim was to synthesise a symmetrical pattern with a prescribed dip in the forward direction. It can be proved that a feed with this radiation pattern gives rise to a very high aperture efficiency. Ludwig obtained some beautiful results; especially the splitting of the beam is very remarkable. Again, the question of bandwidth was not discussed by him. In addition it is obvious that the problem of mode generation and control is very difficult. Moreover,

11

completely new methods of measurement should be developed.
Therefore, it is not surprising that one has looked for new means for
generating a prescribed aperture field. A promising approach to the
problem has been given by Minett and Thomas [15] . They studied
the electromagnetic field in the focal region of a parabola on which
a plane wave is incident along the axis of the parabola. From their
considerations they concluded that a symmetrical radiation pattern can
be obtained with a circular horn antenna in which a hybrid mode propa-
gates. In spite of their unsatisfactory theoretical considerations,
they found experimentally a symmetrical radiation pattern, at least
for one frequency. In an accompanying paper, Rumsey [16] published
some calculations concerning symmetrical radiation fields. Also
Simmons and Kay [17] studied the same problem. They found that it was
possible to get a symmetrical radiation pattern by placing transverse
fins in a conical horn with large flare angle. Surprisingly, they re-
ported that the radiation pattern of this antenna is also independent
of the frequency in a relative frequency band of 1 : 1.6. If the fins
are removed the symmetry disappears but the radiation pattern remains
virtually independent of the frequency. A theoretical understanding
of this important phenomenon has not been found up till now. Besides,
there is a need for more practical information, which can be used by the
designer of this kind of antenna.

The phenomenon that the far-field radiation pattern of the horn anten-
na proposed by Simmons and Kay is independent of the frequency, is
completely new. Classical theory of the horn antenna predicts that the
beamwidth is smaller according as the frequency is higher [18], [19].
There is only one example of a horn antenna with a radiation pattern
which is more or less independent of frequency. This is the well-known
horn-paraboloid antenna, which possesses broadband properties in the
near field of the antenna [20]. This type of antenna has been used as
a feed in the German groundstation antenna for satellite communica-
tions [21]. A disadvantage of the feed is that it must be very large
even if the focal distance is only one-quarter of the diameter of the
parabolic reflector. The second disadvantage is the fact that some
distortion of the field occurs, caused by the parabolic reflector. Re-
cently some improvements of the radiation pattern have been realised
by Trentini et al. [22]. They used Potter's dual-mode technique [11],

12

which implies that the improvements which are reached, probably are restricted to a small frequency band.

1.3 Formulation of the problem

From the first section it is obvious that a good feed must have a combination of qualities which of course depend on the application of the antenna. Much work on feeds has been done, as can be seen from section 1.2. However, most of the work has an experimental character and consequently there is little insight into the precise operation of many antennas. Therefore, the designer of this kind of antennas does not have much useful information at his disposal. With special reference to the application in the field of satellite communications there is a need for a horn antenna which can handle linearly and circularly polarised waves. Because a conical horn antenna can handle these two modes of polarisation, it is very suitable for this application. In the very limited amount of literature on conical horn antennas [23], [24] there is no indication that the conical horn antenna possesses frequency-independent properties, with the exception of the article of Simmons and Kay [17]. One of the results of the present study is that the conical horn antenna can be used as a broadband antenna, provided that the dimensions of the antenna are chosen in the right way. It is the purpose of the present study to collect theoretical and experimental tools which can be used by the designer of broadband conical horn antennas. In chapter 2 the attention is not only devoted to the power pattern of these antennas but also to the phase pattern. The phase pattern is very important if the antenna is used as a feed in a reflector antenna. In chapter 3 a theory is developed which is concerned with a symmetrical radiation pattern. Both the theoretical and the experimental aspects of this problem are studied in some detail.

CHAPTER 2

FREQUENCY-INDEPENDENT CONICAL HORN ANTENNA

2.1   The radiation pattern of a horn antenna

The calculation of the radiation pattern of a horn antenna starts with Maxwell's equations

$$\text{curl } \underline{E}(\underline{r},t) + \frac{\partial \underline{B}(\underline{r},t)}{\partial t} = 0 , \qquad \text{div } \underline{B}(\underline{r},t) = 0 ,$$

$$\text{curl } \underline{H}(\underline{r},t) - \frac{\partial \underline{D}(\underline{r},t)}{\partial t} = \underline{I}(\underline{r},t) , \text{ div } \underline{D}(\underline{r},t) = \rho(\underline{r},t) , \tag{2.1}$$

where the current distribution $\underline{I}(\underline{r},t)$ and the charge distribution $\rho(\underline{r},t)$ are connected by the equation div $\underline{I}(\underline{r},t) + \frac{\partial \rho(\underline{r},t)}{\partial t} = 0$.

In vacuum equations (2.1) reduce to the following two:

$$\text{curl } \underline{E}(\underline{r}) = - j\omega\mu_o \underline{H}(\underline{r}) ,$$

$$\text{curl } \underline{H}(\underline{r}) = j\omega\varepsilon_o \underline{E}(\underline{r}) . \tag{2.2}$$

In the derivation of (2.2) use has been made of the relations $\underline{D}(\underline{r},t) = \varepsilon_o \underline{E}(\underline{r},t)$ and $\underline{B}(\underline{r},t) = \mu_o \underline{H}(\underline{r},t)$. Furthermore a time dependence $\exp(j\omega t)$ has been assumed together with the following relations

$$\underline{E}(\underline{r},t) = \text{Re}\left(\underline{E}(\underline{r}) \ e^{j\omega t}\right) ,$$

$$\underline{H}(\underline{r},t) = \text{Re}\left(\underline{H}(\underline{r}) \ e^{j\omega t}\right) . \tag{2.3}$$

For the sake of completeness the following relations are also given:

$$\underline{I}(\underline{r},t) = \text{Re}\left(\underline{I}(\underline{r}) \ e^{j\omega t}\right) ,$$

$$\rho(\underline{r},t) = \text{Re}\left(\rho(\underline{r}) \ e^{j\omega t}\right) . \tag{2.3'}$$

The calculation of the radiation pattern of a horn antenna has been greatly facilitated by the use of a representation theorem. The theorem can be formulated in the following way [25].

15

Consider the electromagnetic field $\underline{E}(\underline{r})$, $\underline{H}(\underline{r})$ originating from the source distributions $\underline{I}(\underline{r})$ and $\rho(\underline{r})$ enclosed by S_1 (Fig. 2.1) Then the electromagnetic field in a point P in the region between the two closed surfaces S_1 and S_2 is given by the expressions
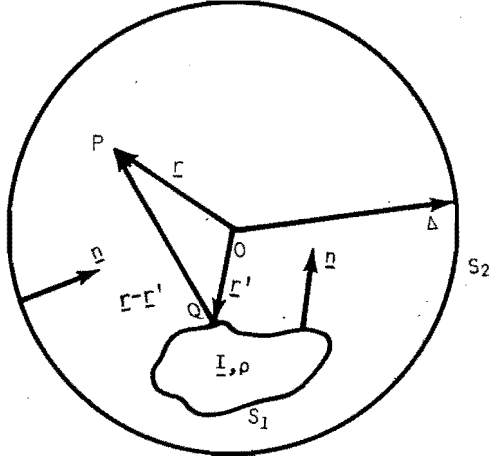
Fig. 2.1.   Illustration for calculating the electromagnetic field in P; sources are within S_1.

$$\underline{E}(\underline{r}) = \text{curl}_P \int_S \{\underline{n} \times \underline{E}(\underline{r}')\} \psi(\underline{r},\underline{r}') \, dS +$$

$$+ \frac{1}{j\omega\varepsilon_o} \text{curl}_P \, \text{curl}_P \int_S \{\underline{n} \times \underline{H}(\underline{r}')\} \psi(\underline{r},\underline{r}') \, dS$$

(2.4)

and $$\underline{H}(\underline{r}) = \text{curl}_P \int_S \{\underline{n} \times \underline{H}(\underline{r}')\} \psi(\underline{r},\underline{r}') \, dS +$$

$$- \frac{1}{j\omega\mu_o} \text{curl}_P \, \text{curl}_P \int_S \{\underline{n} \times \underline{E}(\underline{r}')\} \psi(\underline{r},\underline{r}') \, dS$$

(2.5)

with

$$\psi(\underline{r},\underline{r}') = \frac{1}{4\pi} \frac{e^{-jk\,|\underline{r}-\underline{r}'|}}{|\underline{r}-\underline{r}'|} \quad \text{and } k = \omega(\varepsilon_o\mu_o)^{\frac{1}{2}} \text{ and } S = S_1 + S_2.$$

The operator curl_p acts on the coordinates of the point P. The electromagnetic field in P can be found if the tangential electric field and the tangential magnetic field on the closed surfaces S_1 and S_2 are known. Let us choose for S_2 a sphere with radius Δ, which becomes infinite. The sources $\underline{I}(\underline{r})$ and $\rho(\underline{r})$ of the electromagnetic field are found within the finite surface S_1. Then it can be proved [26] that the contribution of the integral over S_2 to the electromagnetic field in P vanishes. Now the integration in (2.4) and (2.5) can be restricted to the surface S_1. The radiation pattern of a horn antenna can now be calculated in the following way. (Fig. 2.2)
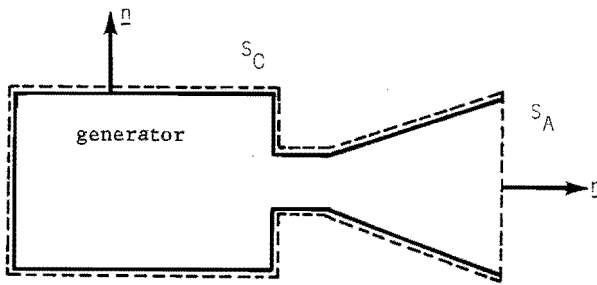
Fig. 2.2.   Horn antenna and generator.

As a closed surface S_1, we choose $S_1 = S_C + S_A$.
S_C consists of the outside surface of the antenna (the signal source
     included).
S_A is the aperture of the horn antenna.
In order to make possible the calculation of the radiation pattern of an antenna it is necessary to formulate some assumptions concerning the tangential electric and the tangential magnetic field on S_1.
The assumptions are:

(i)   the outside of the antenna is perfectly conducting; consequently
      $\underline{n} \times \underline{E}(\underline{r}') = \underline{0}$ on S_C;
(ii) the currents on the outside of the antenna and the signal source
      are negligible; consequently $\underline{n} \times \underline{H}(\underline{r}') = \underline{0}$ on S_C;
(iii) the aperture field is the same as would exist in that place if
      the horn antenna was not truncated; this implies that the higher
      modes, which are excited at the aperture, are negligible.

These assumptions give rise to the following comment:

(i)   this assumption offers no problems in practice, because for the
      construction of the horn antennas copper and aluminium have been
      used;

(ii) the currents on the outside of the horn antenna act as sources for the
      radiation field; this assumption implies, however, that the contribu-
      tion of these currents to the radiation in the forward direction can
      be neglected.

(iii) this assumption seems to be reasonable, provided the diameter of
      the aperture is large compared with the wavelength. If the aper-
      ture field is zero at the rim of the aperture, then the effect of
      the truncation will be negligible. This situation occurs for the
      antennas, which are discussed in chapter 3 of this study. Neg-
      lecting the higher modes at the aperture is not allowed in gener-
      al, especially if the diameter of the aperture is of the order of
      a wavelength. However in this study we are dealing with horn an-
      tennas having a large diameter compared with the wavelength.

In general it is impossible to predict the effect of any of the above
assumptions on the radiation pattern. Justifying these assumptions can
only be done by comparing the experimental results with computations
based on the above assumptions. Summarising we can say that the equa-
tions (2.4) and (2.5) have been reduced to (Fig. 2.3):
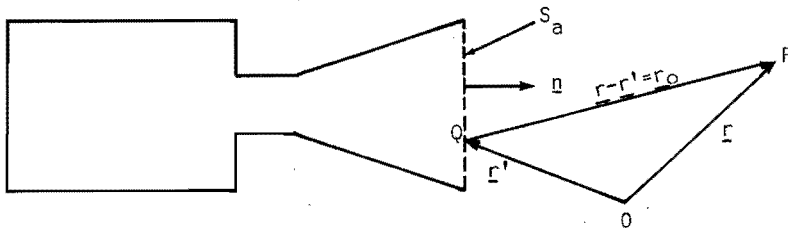
Fig. 2.3.   Horn antenna with observation point P.

$$\underline{E}(\underline{r}) = \text{curl}_P \int_{S_A} \{\underline{h} \times \underline{E}(\underline{r}')\} \, \psi(\underline{r},\underline{r}') \, dS +$$

$$+ \frac{1}{j\omega\varepsilon_o} \text{curl}_P \, \text{curl}_P \int_{S_A} \{\underline{n} \times \underline{H}(\underline{r}')\} \, \psi(\underline{r},\underline{r}') \, dS \; , \tag{2.6}$$

$$\underline{H}(\underline{r}) = \text{curl}_P \int_{S_A} \{\underline{n} \times \underline{H}(\underline{r}')\} \, \psi(\underline{r},\underline{r}') \, dS +$$

$$- \frac{1}{j\omega\mu_o} \text{curl}_P \, \text{curl}_P \int_{S_A} \{\underline{n} \times \underline{E}(\underline{r}')\} \, \psi(\underline{r},\underline{r}') \, dS \; . \tag{2.7}$$

The next step is to carry out the vector operations curl_P and $\text{curl}_P \, \text{curl}_P$. Because the operators act only on the coordinates of the observation point P and not on the source point Q, it is allowed to interchange the integration and the vector operations. Then we find

$$\underline{E}(\underline{r}) = \int_{S_A} \left(-jk \left(1 + \frac{1}{jkr_o}\right) \frac{e^{-jkr_o}}{4\pi \, r_o} \left[\underline{r}_o^{(1)} \times \{\underline{n} \times \underline{E}(\underline{r}')\}\right] \right) dS +$$

$$+ \frac{1}{j\omega\varepsilon_o} \int_{S_A} \left\{ k^2 \left(-1- \frac{3}{jkr_o} + \frac{3}{(kr_o)^2}\right) \frac{e^{-jkr_o}}{4\pi \, r_o} \left(\underline{r}_o^{(1)} \times \left[\underline{r}_o^{(1)} \times \{\underline{n}\times\underline{H}(\underline{r}')\}\right]\right) \right\} dS +$$

$$+ \frac{1}{j\omega\varepsilon_o} \int_{S_A} \left[2jk \left(1 + \frac{1}{jkr_o}\right) \frac{e^{-jkr_o}}{4\pi \, r_o^2} \{\underline{n} \times \underline{H}(\underline{r}')\} \right] dS \quad , \tag{2.8}$$

$$\underline{H}(\underline{r}) = \int_{S_A} \left(-jk \left(1 + \frac{1}{jkr_o}\right) \frac{e^{-jkr_o}}{4\pi \, r_o} \left[\underline{r}_o^{(1)} \times \{\underline{n} \times \underline{H}(\underline{r}')\}\right] \right) dS +$$

$$- \frac{1}{j\omega\mu_o} \int_{S_A} \left\{ k^2 \left(-1- \frac{3}{jkr_o} + \frac{3}{(kr_o)^2}\right) \frac{e^{-jkr_o}}{4\pi \, r_o} \left(\underline{r}_o^{(1)} \times \left[\underline{r}_o^{(1)} \times \{\underline{n}\times\underline{E}(\underline{r}')\}\right]\right) \right\} dS +$$

$$- \frac{1}{j\omega\mu_o} \int_{S_A} \left[2jk \left(1 + \frac{1}{jkr_o}\right) \frac{e^{-jkr_o}}{4\pi \, r_o^2} \{\underline{n} \times \underline{E}(\underline{r}')\} \right] dS \tag{2.9}$$

with the following definitions:

$$\underline{r} - \underline{r}' = \underline{r}_0 \ ,$$

$$\underline{r}_0^{(1)} = \frac{\underline{r}_0}{r_0} \ , \tag{2.10}$$

$$r_0 = (\underline{r}_0 \cdot \underline{r}_0)^{\frac{1}{2}} \ .$$

The region surrounding the antenna at a distance of a few wavelengths is named the reactive near-field region. This region is of no importance and is excluded in the following considerations. On the assumption that $kr_0 \gg 1$, the formulae (2.8) and (2.9) are reduced to the following more simple form:

$$\underline{E}(\underline{r}) = \frac{-jk}{4\pi} \int\limits_{S_A} \left\{ \underline{r}_0^{(1)} \times \left\{ \underline{n} \times \underline{E}(\underline{r}') \right\} - Z_0 \left(\underline{r}_0^{(1)} \times \left[\underline{r}_0^{(1)} \times \left\{ \underline{n} \times \underline{H}(\underline{r}') \right\} \right] \right) \right\} \frac{e^{-jkr_0}}{r_0} dS \ ,$$

$$\tag{2.11}$$

$$Z_0 \underline{H}(\underline{r}) = \frac{-jk}{4\pi} \int\limits_{S_A} \left(Z_0 \left[\underline{r}_0^{(1)} \times \left\{ \underline{n} \times \underline{H}(\underline{r}') \right\} \right] + \underline{r}_0^{(1)} \times \left[\underline{r}_0^{(1)} \times \left\{ \underline{n} \times \underline{E}(\underline{r}') \right\} \right] \right) \frac{e^{-jkr_0}}{r_0} dS$$

with

$$\tag{2.12}$$

$$Z_0 = \left(\frac{\mu_0}{\varepsilon_0} \right)^{\frac{1}{2}} \ .$$

The formulae (2.11) and (2.12) are the mathematical formulation of Huygens' principle, which says that every surface-element of the aperture acts as a source of a spherical wave. So the electromagnetic field in a point P is composed of the contributions of spherical waves departing from the various points of the aperture.

Next we restrict ourselves to the situation where S_A is a flat circular surface and in addition we suppose that the origin of the coordinate system coincides with the centre of the circle (Fig.2.4)

The expressions (2.11) and (2.12) are very complicated. However, depending on the distance of P to the aperture, appropriate approximations are possible. In order to carry out these approximations it is necessary to express $\underline{r}_0^{(1)}$, in the spherical unit vectors $\underline{a}_r$, $\underline{a}_\theta$, $\underline{a}_\phi$.

20
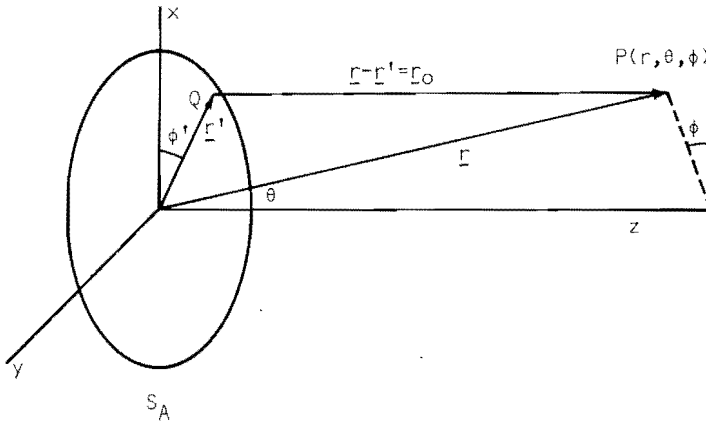
Fig. 2.4.   Circular aperture and coordinate system.

Then we find [27]

$$\underline{r}_o^{(1)} = \underline{a}_r\left[\frac{r}{r_o} - \frac{r'}{r_o} \sin\theta \cos(\phi - \phi')\right] - \underline{a}_\theta\left[\frac{r'}{r_o} \cos\theta \cos(\phi - \phi')\right]$$

$$+ \underline{a}_\phi \left[\frac{r'}{r_o} \sin(\phi - \phi')\right] .$$ (2.13)

Now we write for r_o

$$r_o = r - r' \sin\theta \cos(\phi - \phi') + \frac{(r')^2}{2r}\left[1 - \sin^2\theta \cos^2(\phi - \phi')\right]$$

$$+ 0\left[\frac{(r')^3}{r^2}\right] .$$ (2.14)

This expression has been obtained by applying a binominal expansion of
(2.10) [27] and is more precise than the one derived with Newton's
iteration formula for finding a square root of a given number [28].
If we assume that the diameter D of the aperture is at least a few
wavelengths, then a large part of the energy will be concentrated in a
rather small angle around the antenna-axis (z-axis) and the estimation

$$\left|\sin^2\theta \cos^2(\phi - \phi')\right| \ll 1 \quad \text{is valid.}$$

The following considerations now give rise to the far field region ap-
proximation. If the distance r_o of point P to a point Q of the aper-

21

ture is large, two approximations in the factor $\exp(-jkr_0)/r_0$ can be carried out. The first is that in the denominater r_0 is replaced by r. The second approximation is that the numerator is replaced by $\exp[+jk(-r+r'\sin\theta\cos(\phi-\phi'))]$.

In the far field region approximation it is also allowed to approximate $\underline{r}_0^{(1)}$ by $\underline{a}_r$, as can be verified from (2.13). After these approximations we find for the expressions (2.11) and (2.12)

$$\underline{E}(\underline{r}) = \frac{-jk}{4\pi} \frac{e^{-jkr}}{r} \underline{a}_r \times \int_{S_A} \left(\{\underline{n} \times \underline{E}(\underline{r}')\} + \right.$$

$$\left. -Z_0 \left[\underline{a}_r \times \{\underline{n} \times \underline{H}(\underline{r}')\} \right] \right) e^{jkr' \sin\theta \cos(\phi-\phi')} \, dS \qquad (2.15)$$

and

$$Z_0\underline{H}(\underline{r}) = \frac{-jk}{4\pi} \frac{e^{-jkr}}{r} \underline{a}_r \times \int_{S_A} \left(Z_0 \{\underline{n} \times \underline{H}(\underline{r}')\} + \right.$$

$$\left. +\underline{a}_r \times \{\underline{n} \times \underline{E}(\underline{r}')\} \right) e^{jkr' \sin\theta \cos(\phi-\phi')} \, dS \, . \qquad (2.16)$$

These are the formulae which describe the electromagnetic field at a largedistance of an aperture. An interesting feature is that the integral does not depend on the distance r, but only on the angles θ and ϕ (Fig. 2.4). So we can write for (2.15) and (2.16)

$$\underline{E}(\underline{r}) = \frac{-jk}{4\pi} \frac{e^{-jkr}}{r} \underline{F}(\theta,\phi) \, , \qquad (2.17)$$

$$Z_0\underline{H}(\underline{r}) = \frac{-jk}{4\pi} \frac{e^{-jkr}}{r} \underline{a}_r \times \underline{F}(\theta,\phi) \, . \qquad (2.18)$$

$\underline{F}(\theta,\phi)$ represents the angular distribution of the radiation and is in general a complex vector.

From (2.17) and (2.18) the conclusion is drawn that

$$Z_0\underline{H}(\underline{r}) = \underline{a}_r \times \underline{E}(\underline{r}) \, . \qquad (2.19)$$

Formula (2.19) implies that the time-average intensity of energy flow is given by $\overline{\underline{S}(\underline{r},t)} = \frac{1}{2} \, \text{Re} \, [\underline{E}(\underline{r}) \times \underline{H}(\underline{r})^*] = \frac{1}{2} Z_0^{-1} \, |\underline{E}(\underline{r})|^2 \, \underline{a}_r \, .$

So far we have not discussed the validity of the far field region approximation. In other words, we have not examined for what minimum

22

distance r_{min} the far field region approximation is applicable. The distance r_{min} is found by the condition that the error in the fase-exponent is less than $\lambda/16$. The maximum error is given by

$(D/2)^2 / 2 r_{min}$; thus we find

$$r_{min} = \frac{2D^2}{\lambda} , \qquad\qquad (2.20)$$

which is a generally accepted limit for the far field region of an aperture antenna.

Sometimes one is interested in the radiation pattern of an aperture antenna in a region between the reactive near field region and the far field region. It is named the radiating near field region [29]. The hornparaboloid possesses its broadband properties [20], [21] in this region. If one wishes to calculate the electromagnetic field in the radiating near-field region a careful treatment of (2.11) and (2.12) is needed. Especially the question, what approximations are allowed is very difficult to answer [30]. Kikkert [31] applied the following approximations:

(i) $r_0^{(1)}$ is replaced by $\underline{a}_r$

(ii) r_0 in the denominator is replaced by r

(iii) $\exp(-jkr_0)$ is approximated by $\exp -jk\left[r - r' \sin\theta \cos(\phi - \phi') + \frac{(r')^2}{2r}\right]$

Then the expressions (2.11) and (2.12) can be replaced by

$$\underline{E}(\underline{r}) = \frac{-jk}{4\pi} \frac{e^{-jkr}}{r} \underline{a}_r \times \int_{S_A} \left(\{\underline{n} \times \underline{E}(\underline{r}')\} - \right.$$

$$\left. Z_0\left[\underline{a}_r \times \{\underline{n} \times \underline{H}(\underline{r}')\}\right]\right) e^{jkr' \sin\theta \cos(\phi - \phi') - jk \frac{(r')^2}{2r}} dS , \quad (2.21)$$

$$Z_0\underline{H}(\underline{r}) = \frac{-jk}{4\pi} \frac{e^{-jkr}}{r} \underline{a}_r \times \int_{S_A} \left(Z_0\{\underline{n} \times \underline{H}(\underline{r}')\} + \right.$$

$$\left. \underline{a}_r \times \{\underline{n} \times \underline{E}(\underline{r}')\}\right) e^{jkr' \sin\theta \cos(\phi - \phi') - jk \frac{(r')^2}{2r}} dS . \quad (2.22)$$

In order to derive similar expressions as given in (2.17) and (2.18) it is necessary to replace $\underline{F}(\theta,\phi)$ by $\underline{F}(\theta,\phi,r)$. So the angular distribution of the radiation depends on the distance r. But, the relation

$$Z_o\underline{H}(\underline{r}) = \underline{a}_r \times \underline{E}(\underline{r}) \tag{2.23}$$

is still valid.

Kikkert [31] used the formulae (2.21) and (2.22) to calculate the electromagnetic field of the hornparaboloid in the radiating near-field region. The diameter of the aperture of the hornparaboloid was 10λ. He compared his calculations with the measurements of the amplitude and the phase of the electromagnetic field in this region. His conclusion is that the agreement between the measurements and the calculations is rather good, provided the distance of the point of observation to the aperture is larger than twice the diameter of the aperture. The reason why the formulae (2.21) and (2.22) are written down here is because they will greatly facilitate the discussion on broadband conical horn antennas in the following section. A rather extensive discussion of the limits of the radiating near-field region can be found in the book of Hansen [27].

The formulae (2.21) and (2.22) are not very convenient for later considerations. Therefore, the vector products are carried out (see ap – pendix A).

The following results are obtained:

$$E_\theta = \frac{jka^2}{4\pi r} e^{-jkr} \int_0^1 \int_0^{2\pi} \left[\{E_r' + Z_oH_\phi' \cos\theta\} \cos(\phi - \phi') + \right.$$

$$\left. + \{E_\phi' - Z_oH_r' \cos\theta\} \sin(\phi - \phi') \right] e^{ju\rho\cos(\phi-\phi')} e^{-jv\rho^2} \rho \, d\rho \, d\phi' \tag{2.24}$$

and

$$E_\phi = \frac{jka^2}{4\pi r} e^{-jkr} \int_0^1 \int_0^{2\pi} \left[\{E_\phi' \cos\theta - Z_oH_r'\} \cos(\phi - \phi') + \right.$$

$$\left. - \{E_r' \cos\theta + Z_oH_\phi'\} \sin(\phi - \phi') \right] e^{ju\rho\cos(\phi-\phi')} e^{-jv\rho^2} \rho \, d\rho \, d\phi' \tag{2.25}$$

with

2a : diameter of aperture,

$\rho a = r'$,

$v = \dfrac{ka^2}{2r}$, $\qquad u = k\ a\ \sin\theta$.

In these expressions the aperture fields are primed and written in circular coordinates. The unprimed radiation fields are given in spherical coordinates (Fig. 2.4). These formulae are exactly the same as for the fields in the far field region except for a factor $\exp[-jv\rho^2]$, which in this region is negligible.

2.2   Theory of frequency-independent conical horn antennas

From the expressions (2.11) and (2.12) one can see that the electromagnetic field in a point P in the radiating near-field region of an aperture consists of the contributions of spherical wavelets originating from various points in the aperture. Every wavelet arrives at a point P with a phase which is a function of the electric distance between the field point P and the aperture point Q under consideration. So this phase is a function of the frequency. Now suppose that point P
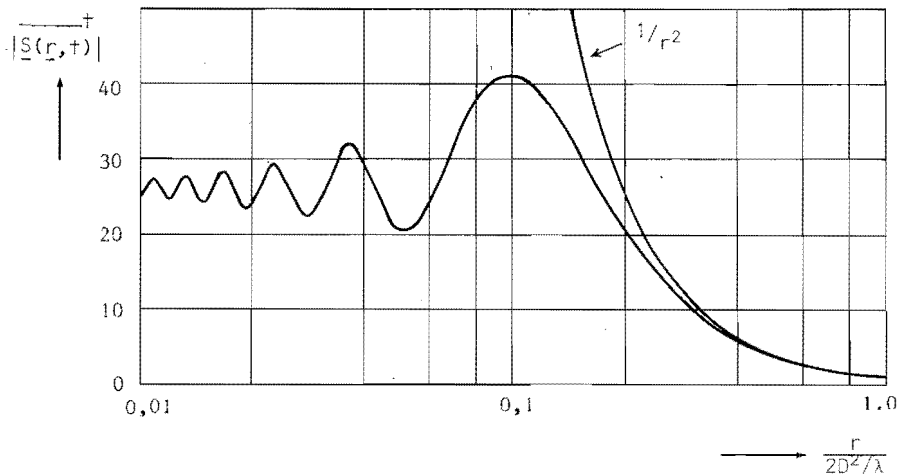

Fig. 2.5   On-axis time-average intensity of energy flow against distance to aperture. Normalised to unity at $r = 2D^2/\lambda$.

is on the axis of the aperture. Suppose further that the aperture is
an equiphase plane. Then it is easily seen that the factor $\exp[-jv\rho^2]$
in the formulae (2.24) and (2.25) takes into account the fact that the
wavelets arrive at P with a phase which is different for the various
wavelets. Hansen [32] calculated the time-average intensity of energy
flow $\overline{\underline{S}(\underline{r},t)}^t$ at P at a distance r from the aperture, in the case of a
constant-phase circular aperture and with a tapered illumination
$(1 - \rho^2)$. From his results (Fig. 2.5) it can be seen that in the radi-
ating near field region the time-average intensity of energy flow as a
function of the distance to the aperture has maxima and minima.

The maximum at distance $r = 0.2 \ D^2/\lambda$ (D is the diameter of the aper-
ture) has an interesting property. In fact, in the neighbourhood of
this point the derivative with respect to the wavelength is small in
a relatively large region. This means that we may expect that in the
neighbourhood of this point a circular aperture with tapered illumina-
tion $(1 - \rho^2)$ and constant-phase distribution has a radiation field
which, in a certain frequency band, is almost independent of the fre-
quency.

This frequency-independent property of the radiation field is restric-
ted to the near field region. However it is possible to remove the re-
gion, where this frequency-independent property occurs , to other re-
gions up to infinity. To prove this assertion we consider two circular
aperture antennas, one with a constant-phase field distribution and
amplitude distribution $\underline{E}'(\rho,\phi')$, $\underline{H}'(\rho,\phi')$, and the other with the same
amplitude distribution but with quadratic phase distribution. Thus the
fields in the aperture in the second case are given by
$\underline{E}'(\rho,\phi')[\exp -jkd\rho^2]$ and $\underline{H}'(\rho,\phi')[\exp -jkd\rho^2]$, where the quantity kd
is the phase difference between rim and centre of the aperture. Then
in each of the two cases the electromagnetic field in the radiating
near-field region is given by the formulae (2.24) and (2.25), provided
in the second case v is replaced by

$$v' = k\left(d + \frac{a^2}{2r}\right) . \tag{2.26}$$

This means that the electromagnetic field at a distance r_1 from an
aperture antenna with constant-phase distribution is the same as the

electromagnetic field of an aperture antenna with quadratic phase dis-
tribution, but now at a distance r_2 from the antenna and on condition
that

$$\frac{ka^2}{2r_1} = k\left(d + \frac{a^2}{2r_2}\right) \ . \tag{2.27}$$

The only restriction is that r_1 and r_2 are in the radiating near field
region or in the far field region. Now it is clear that with the
choice of the appropriate phase distribution it is possible to remove
the region in which an aperture antenna exhibits frequency-independent
properties, to any distance from the aperture, including infinity.
In the case calculated by Hansen the frequency-independent properties
appear at a distance $r = 0.2\ D^2/\lambda$. Thus $v = \frac{5}{4}\pi$. Suppose that we wish
to realise the same radiation pattern as in the case studied by Hansen,
but now at infinity. Then it is necessary to choose d in such a way
that $kd = \frac{5}{4}\pi$. This means that $d = \frac{5}{8}\lambda$. In the remaining part of this
study we shall consider only the far field region, except when in-
dicated otherwise.

Up till now we have suggested that a circular aperture with a quadra-
tic phase field distribution, having the property that the phase dif-
ference between rim and centre of the aperture is about half a wave-
length, has a radiation pattern which is only slightly dependent on
the frequency, at least in the forward direction. This phenomenon of-
fers the possibility to design a frequency-independent antenna, espe-
cially in the microwave region.

In fact, the theory of this section can now be applied to a conical
horn antenna. In a conical horn antenna a spherical wave can propagate
and then produces a quadratic phase field distribution across the aper-
ture provided the flare angle of the cone is small. Furthermore the
length of the horn should be chosen so large that the phase difference
between rim and centre of the aperture is approximately half a wave-
length. Next we shall prove this assertion. For that purpose let us
write down the expressions for the electromagnetic field in a conical
waveguide. (Fig. 2.6)
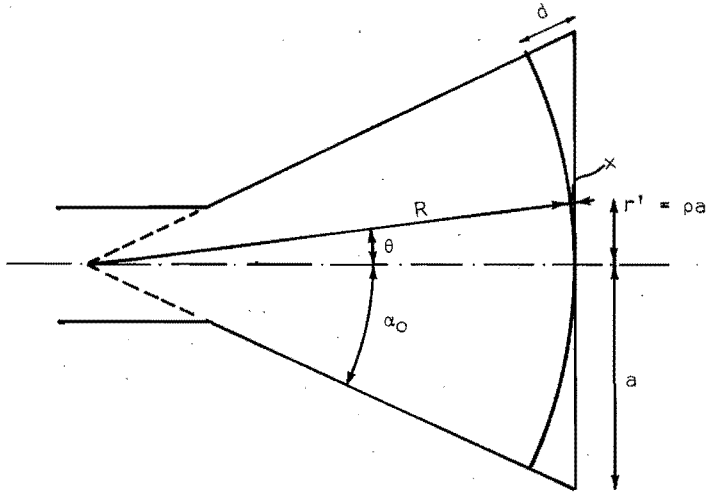
Fig. 2.6.   Conical horn antenna.

In practice the electromagnetic field in a conical horn antenna is
mostly excited by coupling the cone to a circular waveguide in which
the TE_{11}-mode propagates.
Therefore we shall assume that in the conical waveguide the $TE_{1\nu}$-mode
too, propagates. The expressions for the electromagnetic field of this
mode have the following form:

$$E_R = 0 \,,$$

$$E_\theta = -\frac{1}{R}\, h_\nu\,(kR)\,\frac{1}{\sin\theta}\, P_\nu^1\,(\cos\theta)\,\cos\phi \,,$$

$$E_\phi = \frac{1}{R}\, h_\nu\,(kR)\,\frac{d}{d\theta}\,[P_\nu^1\,(\cos\theta)]\,\sin\phi \,,$$

$$H_R = \frac{1}{j\omega\mu_0}\,\frac{\nu(\nu+1)}{R^2}\, h_\nu\,(kR)\, P_\nu^1\,(\cos\theta)\sin\phi \,,$$

$$H_\theta = \frac{1}{j\omega\mu_0}\,\frac{1}{R}\, h'_\nu\,(kR)\,\frac{d}{d\theta}\,[P_\nu^1(\cos\theta)]\,\sin\phi \,,$$

$$H_\phi = \frac{1}{j\omega\mu_0}\,\frac{1}{R}\, h'_\nu\,(kR)\,\frac{1}{\sin\theta}\, P_\nu^1(\cos\theta)\,\cos\phi \,.$$

(2.28)

The derivation of (2.28) can be found in [24] or [33]. $P_\nu^1(\cos\theta)$ is the associated Legendre function of the first kind and of the order ν. The prime in $h_\nu'(kR)$ means differentiating with respect to R. Furthermore $h_\nu(kR) = (\pi kR/2)^{\frac{1}{2}} H_{\nu+\frac{1}{2}}^{(2)}(kR)$, where $H_{\nu+\frac{1}{2}}^{(2)}$ represents a Hankel function of the second kind and of the order $\nu+\frac{1}{2}$. The choice of the Hankel function of the second kind together with the assumed time-dependence $\exp[+j\omega t]$ gives rise to a outwards propagating wave. The value of ν is determined by the condition that the tangential electrical field vanishes at the boundary $\theta = \alpha_0$.

Thus

$$\frac{d}{d\theta}\left[P_\nu^1(\cos\theta)\right]_{\theta=\alpha_0} = 0 \qquad (2.29)$$

Fradin [34] has given the value of ν for several flare angles α_0. His results are collected in Fig. 2.7.
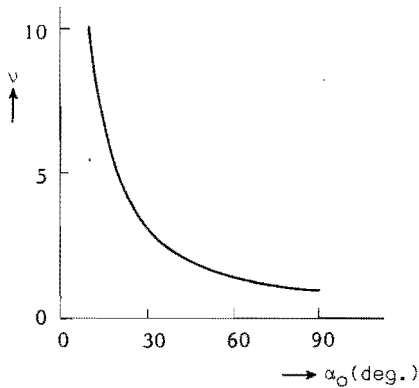
Fig. 2.7. Mode number ν against flare angle α_0.

We are now able to derive the condition under which the phase field distribution is a quadratic function of the radius.

Moreover, we shall study the condition under which the phase difference between rim and centre of the aperture is approximately half a wavelength.

From Fig. 2.6 it can be seen that

$$x = R\frac{1-\cos\theta}{\cos\theta} = \rho a \tan\tfrac{1}{2}\theta . \qquad (2.30)$$

Furthermore,

$$d = a \tan \tfrac{1}{2} \alpha_O \qquad \text{and} \tag{2.31}$$

$$x = \rho a \tan \tfrac{1}{2}\theta = \rho d \, \frac{\tan \tfrac{1}{2}\theta}{\tan \tfrac{1}{2}\alpha_O} \; . \tag{2.32}$$

Suppose that $\alpha_O \leqslant 15^O$, then $\tan \alpha_O \cong \alpha_O$ with an error of 2.5%, and the following approximation holds

$$x \cong \rho d \, \frac{\tan \theta}{\tan \alpha_O} = \rho^2 d \; . \tag{2.33}$$

So the phase field distribution is indeed a quadratic function of the radius, provided α_O is small enough, for instance, $\alpha_O \leqslant 15^O$. From Fig. 2.7 we see that in this case $\nu \gg 1$.

In order to be sure that the phase difference between centre and rim of the aperture is approximately half a wavelength, a second require- ment concerning the geometry of the cone is necessary. From Fig. 2.6 we see that

$$d = R \left(\frac{1}{\cos \alpha_O} - 1 \right) \; . \tag{2.34}$$

If we approximate $\cos \alpha_O$ by $1 - \dfrac{\alpha_O^2}{2}$, then we see that

$$d = R \, \frac{\alpha_O^2}{2} \; . \tag{2.35}$$

We know that d should be chosen in such a way that $d \cong \tfrac{1}{2}\lambda$. For the case that $\alpha_O = \pi/12$ rad, we find that $R/\lambda \cong 14,4$ and $kR \cong 90$. So the follow- ing inequality holds

$$kR \gg \nu \gg 1 \; .$$

Within this approximation we can write [33]

$$h_\nu \, (kR) \cong e^{j \, \frac{\pi}{2} \, (\nu + 1)} \, e^{-jkR} \; , \tag{2.36}$$

$$\frac{d \, h_\nu(kR)}{d \, R} \cong - \, jk \, h_\nu(kR) \; .$$

Using (2.28) and (2.36) we can prove quite easily that

$$E_\theta \cong Z_0 H_\phi \ ,$$
$$E_\phi \cong - Z_0 H_\theta \ .$$

<div align="right">(2.37)</div>

So the wave impedance is approximated by the impedance of free space.

Having specified the dimension of the horn antenna we shall compute the radiation pattern of the antenna. For this computation we use the formulae (2.24) and (2.25). In order to apply these as conveniently as possible we look for useful approximations of the aperture fields. The θ – dependence of E_ϕ and E_θ is described by the functions $\frac{dP_\nu^1 (\cos \theta)}{d\theta}$ and $\frac{1}{\sin \theta} P_\nu^1 (\cos \theta)$ respectively. These functions are difficult to deal with. However, because of the small flare angle it is possible to approximate E_ϕ and E_θ in terms of Bessel functions, which are well known. With a view to finding the approximations for E_ϕ and E_θ we note that the following relation [35] , [36] provides a basis for these approximations:

$$P_\nu^{-\mu} (\cos \theta) = \left\{(\nu + \tfrac{1}{2}) \cos \tfrac{1}{2}\theta\right\}^{-\mu} J_\mu(a) \left\{1 + 0(\sin^2 \tfrac{1}{2}\theta)\right\} \ , \quad (2.38)$$

$$(\nu \to \infty \ , \ \sin \tfrac{1}{2}\theta \to 0 \quad \text{and a finite and} \ \neq 0)$$
$$a = (2\nu + 1) \sin \tfrac{1}{2}\theta \ .$$

Because we are interested in a formula for $P_\nu^\mu (\cos \theta)$ we use the relation [35] , [36]

$$2Q_\nu^\mu (\cos \theta) \sin \pi\mu = \pi \left\{P_\nu^\mu (\cos \theta) \cos \mu\pi - \frac{\Gamma(\nu+\mu+1)}{\Gamma(\nu-\mu+1)} P_\nu^{-\mu}(\cos \theta)\right\}$$

<div align="right">(2.39)</div>

with $Q_\nu^\mu (\cos \theta)$ the associated Legendre function of the second kind and order ν. $\Gamma(x)$ is the Gamma function. Using the relation $\Gamma(1 + x) = x \Gamma(x)$ and substituting $\mu = 1$ we find

$$P_\nu^1(\cos \theta) = -\nu(\nu+1) \frac{J_1[(2\nu+1)\sin\tfrac{1}{2}\theta]}{(\nu+\tfrac{1}{2})\cos\tfrac{1}{2}\theta} \cong -\nu(\nu+1) \frac{J_1[(2\nu+1)\sin\tfrac{1}{2}\theta]}{\nu+\tfrac{1}{2}} \ .$$

<div align="right">(2.40)</div>

Now we compute

$$\frac{dP_\nu^1(\cos\theta)}{d\theta} \cong -\nu(\nu+1) \frac{J_{\frac{1}{2}}'[(2\nu+1)\sin\frac{1}{2}\theta]}{\nu+\frac{1}{2}} \times \frac{(2\nu+1)\cos\frac{1}{2}\theta}{2} \cong$$

$$- \nu(\nu+1) J_1' [(2\nu+1)\sin\frac{1}{2}\theta] . \tag{2.41}$$

After applying the boundary condition $E_\phi = 0$ we obtain

$$(2\nu+1) \sin\frac{1}{2}\alpha_o = j_{11}' , \tag{2.42}$$

j_{11}' being the first zero of $J_1'(x)$. In the region $\alpha_o \leqslant 15$ the values of ν computed from (2.42) are virtually identical with the values of Fig. 2.7. Next we wish to introduce the radius ρ in the formula for E_ϕ and E_θ and we note that

$$(2\nu+1) \sin\frac{1}{2}\theta = (2\nu+1) \sin\frac{1}{2}\alpha_o \frac{\sin\frac{1}{2}\theta}{\sin\frac{1}{2}\alpha_o} .$$

Furthermore, we see that (Fig. 2.6) $\sin\frac{1}{2}\theta \cong \frac{1}{2}\sin\theta = \rho a/2R$ and $\sin\frac{1}{2}\alpha_o \cong a/2R$.

So $(2\nu+1) \sin\frac{1}{2}\theta \cong j_{11}'\rho$ and we find

$$E_\phi = -e^{j\frac{\pi}{2}(\nu+1)} \frac{e^{-jkR}}{R} \nu(\nu+1) J_1'(j_{11}'\rho) \sin\phi . \tag{2.43}$$

A similar computation yields

$$E_\theta = e^{j\frac{\pi}{2}(\nu+1)} \frac{e^{-jkR}}{R} \nu(\nu+1) \frac{J_1(j_{11}'\rho)}{j_{11}'\rho} \cos\phi . \tag{2.44}$$

The computation of the radiation pattern of a conical horn antenna is possible by using the formulae (2.24) and (2.25). In these formulae the aperture fields are written in cylindrical components, while in (2.37), (2.43) and (2.44) spherical components are used to describe the electromagnetic field in the horn. So before the substitution of the aperture fields in the formulae (2.24) and (2.25), the following

32

transformations are necessary:

$$E_r' = E_\theta \cos \theta \cong E_\theta \ , \tag{2.45}$$

$$H_r' = H_\theta \cos \theta \cong H_\theta \ , \tag{2.46}$$

$$E_\phi' = E_\phi \ , \tag{2.47}$$

$$H_\phi' = H_\phi \ . \tag{2.48}$$

The relations (2.45) and (2.46) are valid because the flare angle of the cone is small. Expressions (2.47) and (2.48) mean a change in notation. In the derivation of (2.45) to (2.48) incl. we have neglected the space loss caused by the distance x (Fig. 2.6). For a horn with $R = 14,4 \ \lambda$ and $d \sim \frac{1}{2}\lambda$ this results in an error of about 3%. After all these preparations we find for the electromagnetic field in the aperture S_A:

$$E_r' = Z_0 H_\phi' \qquad , \qquad E_\phi' = -Z_0 H_r' \tag{2.49}$$

with

$$E_r' = f(\rho)e^{-jkd\rho^2} \cos\phi' \quad \text{and} \quad E_\phi' = g(\rho)e^{-jkd\rho^2} \sin \phi' \tag{2.50}$$

where

$$f(\rho) = A \ \frac{J_1(j_{11}'\rho)}{j_{11}'\rho}$$

and

$$g(\rho) = - A \ J_1'(j_{11}'\rho) . \tag{2.51}$$

A is a constant. In the following considerations we take $A = 1$.

In order to study the frequency-independent properties of the conical horn antenna in more detail we substitute the formulae (2.49) and (2.50) in the expressions (2.24) and (2.25). Using the relation [37]:

$$e^{ju\rho\cos(\phi-\phi')} = J_0(u\rho) + 2 \sum_{n=1}^\infty j^n J_n (u\rho) \cos n(\phi-\phi') \tag{2.52}$$

we find

$$E_\theta = \frac{jka^2}{2r} e^{-jkr} \frac{1 + \cos\theta}{2} \cos \phi \ I_E(u,v) \tag{2.53}$$

33

with

$$I_E(u,v) = \int_0^1 \left[\{f(\rho) - g(\rho)\}J_0(u\rho) - \{f(\rho)+g(\rho)\}J_2(u\rho) \right] e^{-jv\rho^2} \rho d\rho$$

and

$$E_\phi = - \frac{jka^2}{2r} e^{-jkr} \frac{1 + \cos\theta}{2} \sin\phi \; I_H(u,v) \tag{2.54}$$

with

$$I_H(u,v) = \int_0^1 \left[\{f(\rho) - g(\rho)\}J_0(u\rho) + \{f(\rho)+g(\rho)\}J_2(u\rho) \right] e^{-jv\rho^2} \rho d\rho$$

and

$$u = ka \sin\theta, \quad v = kd .$$

For further considerations it is convenient to have the following relations at our disposal:

$$\overline{\underline{S(\underline{r},t)}}^\dagger = \tfrac{1}{2}Re[\underline{E}\times\underline{H}^*] = \tfrac{1}{2}Z_0^{-1}|\underline{E}|^2\underline{a}_r = \tfrac{1}{2}Z_0^{-1}\left(|E_\theta|^2+|E_\phi|^2\right)\underline{a}_r .$$

Use has been made of (2.19). The power radiated per unit solid angle is $P(\theta,\phi) = r^2|S(\theta,\phi)|$ and is of course independent of the distance r; it is given by the expression

$$P(\theta,\phi) = \tfrac{1}{2}Z_0^{-1}\left(\frac{ka^2}{2}\right)^2 \cos^4\frac{\theta}{2} \left\{\cos^2\phi|I_E(u,v)|^2+\sin^2\phi|I_H(u,v)|^2\right\} . \tag{2.55}$$

By inspection it can be seen that $I_E(0,v) = I_H(0,v)$. Suppose that $P(\theta,\phi)$ has a maximum value for $\theta=0$. Then this value is given by

$$P(0,0) = \tfrac{1}{2}Z_0^{-1}\left(\frac{ka^2}{2}\right)^2 |I_E(0,v)|^2 . \tag{2.56}$$

The power radiation pattern $F(\theta,\phi)$ is defined by means of the following expression

$$F(\theta,\phi) = \frac{P(\theta,\phi)}{P(0,0)} . \tag{2.57}$$

From (2.55), (2.56) and (2.57) it follows immediately that

$$F(\theta,\phi) = |I_E(0,v)|^{-2}\cos^4\frac{\theta}{2} \left\{\cos^2\phi|I_E(u,v)|^2+\sin^2\phi|I_H(u,v)|^2\right\}. \tag{2.58}$$

Next we define the power radiation pattern in the E-plane and in the H-plane ($\phi = 0$ and $\phi = \frac{\pi}{2}$ respectively).
The power radiation pattern in the E-plane becomes

$$F_E(\theta) = F(\theta,0) = \left| \; I_E(0,v) \; \right|^{-2} \; \left| \; I_E(u,v) \; \right|^2 \; \cos^4 \frac{\theta}{2} \; ,$$

$$F_E(\theta) \equiv f_E(u,v) \; \cos^4 \frac{\theta}{2} \; . \tag{2.59}$$

For the power radiation pattern in the H-plane we find

$$F_H(\theta) = F(\theta,\tfrac{\pi}{2}) = \left| \; I_H(0,v) \; \right|^{-2} \; \left| \; I_H(u,v) \; \right|^2 \; \cos^4 \frac{\theta}{2} \; ,$$

$$F_H(\theta) \equiv f_H(u,v) \; \cos^4 \frac{\theta}{2} \; . \tag{2.60}$$

The functions $f_E(u,v)$ and $f_H(u,v)$ are defined by the relations (2.59) and (2.60) respectively.

Let us now return to the conical horn antenna and its frequency-independent properties. That the antenna indeed possesses these properties appears most clearly by studying the power radiation pattern F_H in the H-plane and the power radiation pattern F_E in the E-plane. The functions F_H and F_E depend on θ and on the quantities u and v. These quantities contain the dimensions d and a. If d and a are given, then the flareangle α_0 can be found by means of equation (2.31). To be sure that the results of the following calculations are applicable as generally as possible, it is preferable to study the functions $f_H(u,v)$ and $f_E(u,v)$. This is a resonable procedure because we are dealing with antennas which have a rather large aperture. This means that a large part of the energy is concentrated around the axis of the antenna. Thus the factor $\cos^4\frac{\theta}{2}$ represents only a minor correction.

Substitution of the expressions (2.51) in the formulae for $f_E(u,v)$ and $f_H(u,v)$ gives

$$f_E(u,v) = \left| \frac{\displaystyle\int_0^1 \left\{ J_0(j'_{11}\rho) \, J_0(u\rho) - J_2(j'_{11}\rho)J_2(u\rho) \right\} e^{-jv\rho^2} \rho\,d\rho}{\displaystyle\int_0^1 J_0(j'_{11}\rho)e^{-jv\rho^2} \rho\,d\rho} \right|^2 \tag{2.61}$$

and

$$f_H(u,v) = \left| \frac{\displaystyle\int_0^1 \left\{ J_0(j'_{11}\rho) \, J_0(u\rho) + J_2(j'_{11}\rho)J_2(u\rho) \right\} e^{-jv\rho^2} \rho\,d\rho}{\displaystyle\int_0^1 J_0(j'_{11}\rho)e^{-jv\rho^2} \rho\,d\rho} \right|^2 \cdot \tag{2.62}$$

In the derivation of (2.61) and (2.62) the following recurrence relations of the Bessel function have been used

$$J_m'(z) = \frac{m}{z} J_m(z) - J_{m+1}(z) ,$$

$$J_m'(z) = -\frac{m}{z} J_m(z) + J_{m-1}(z) . \tag{2.63}$$

For purposes of comparison we prefer to calculate the functions

$$f_E'(u,v) = 10^{10} \log f_E(u,v) ,$$

$$f_H'(u,v) = 10^{10} \log f_H(u,v) . \tag{2.64}$$
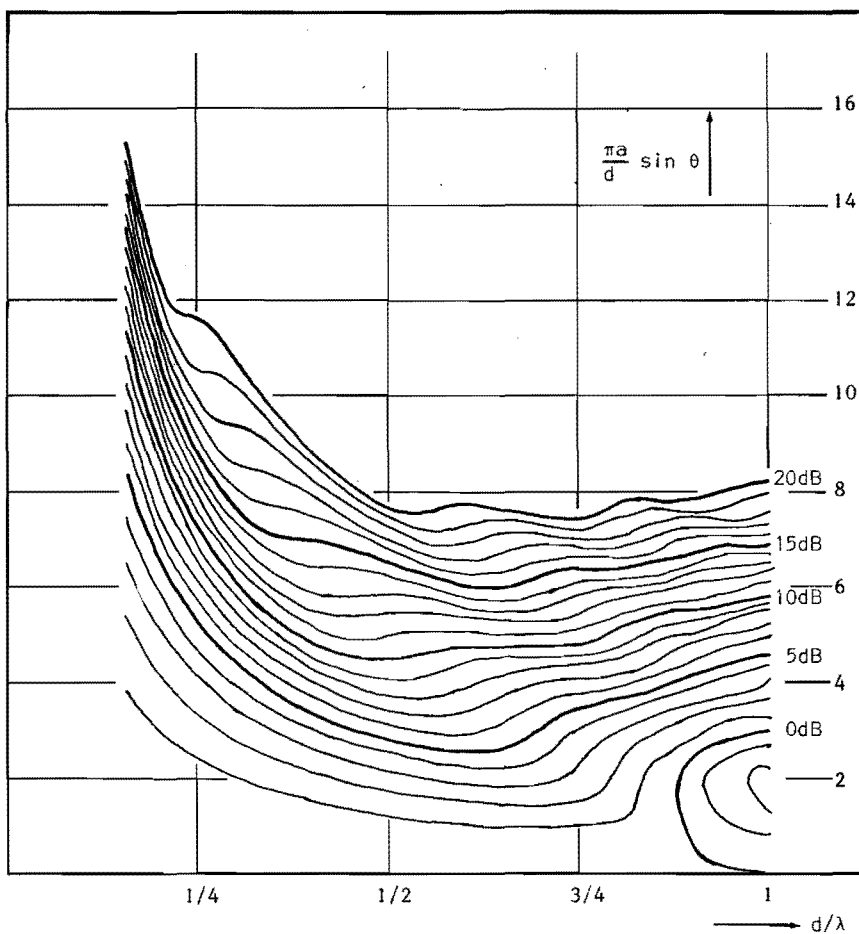

Fig. 2.8.   Beamwidth of perfectly conducting conical horn antenna with small flare angle; H-plane.

These functions have been computed with the ELX8 digital computer. With a view to getting a convenient representation of the numerical results, the following procedure has been adopted. In a rectangular coordinate system lines of constant beamwidth have been plotted. As an example, the 10-dB line in the H-plane has been found in the following manner. Take $f_H'(u,v) = 10$, prescribe the number v and find the number u, which satisfies the equation $f_H'(u,v) = 10$.

Then we plot the quantity $\frac{v}{2\pi} = \frac{d}{\lambda}$ along the abscissa. Along the ordinate we plot the quantity $\alpha = \frac{\pi u}{v} = \frac{\pi \, a \, \sin \theta}{d}$. The results are collected in Fig. 2.8 and Fig. 2.9 for the H-plane and the E-plane respectively. From Fig. 2.8 it can be seen that the beamwidth is indeed highly independent of frequency on condition that $3/8 < d/\lambda < 3/4$. The condition $3/8 < d/\lambda < 3/4$ implies a relative bandwidth of 1 : 2. Especially the 10-dB beamwidth is nearly constant in the frequency region where $3/8 < d/\lambda < 3/4$. The 5-dB beamwidth and the 20-dB beamwidth are somewhat more dependent on the frequency. If the dimensions of a conical horn antenna are given, then the value of d is fixed. Suppose that this antenna is used in a frequency band so that $d/\lambda < 1/4$. Then the aperture is approximately an equiphase plane and the classical theory of horn antennas can be applied. This theory predicts that the beamwidth is larger according as the frequency is lower. This fact can also be observed in Fig. 2.8.

Let us now choose λ in such a way that d/λ varies from $\frac{1}{2}$ to 1. This gives also rise to a relative bandwidth 1 : 2. However, the picture is now different. For the value of d/λ given by $1/2 < d/\lambda < 3/4$ the beamwidth is still constant as a function of frequency. For the values of d/λ between 3/4 and 1 the beamwidth increases as d/λ increases. Besides the phenomenon of the splitting of the beam is observed for $7/8 < d/\lambda < 1$. This means that the function $f_H'(u,v)$ does not have its maximum value for $\theta = 0$, but for two other values of θ on either side of the direction $\theta = 0$. So there are two values of θ for which the function $f_H(u,v)$ has a value which is, for instance, 1 dB higher than the value of $f_H(u,v)$ for $\theta = 0$. Fig. 2.8a shows the main lobe of a radiation pattern with beamsplitting.
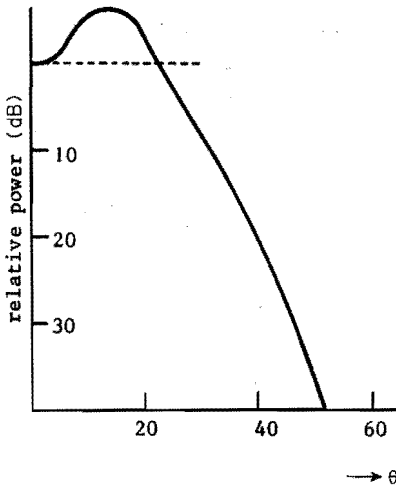
Fig. 2.8ᵃ. Illustration of beamsplitting.

A glance at Fig.2.9 shows immediately that the beamwidth in the E-plane
is more dependent on frequency. Furthermore, we see that the beamwidth
in the H-plane and in the E-plane is different for the same frequency.
This means that the power radiation pattern is asymmetric with respect
to the angle ϕ. We also observe that sometimes the beamwidth is not
uniquely defined, since the radiation pattern does not decrease mono-
tonously with increasing θ. This phenomenon is illustrated in Fig.2.9a.

Moreover we observed that the splitting of the beam takes place at a
lower frequency. In spite of these imperfections we can say that a co-
nical horn antenna with a quadratic phase distribution exhibits indeed
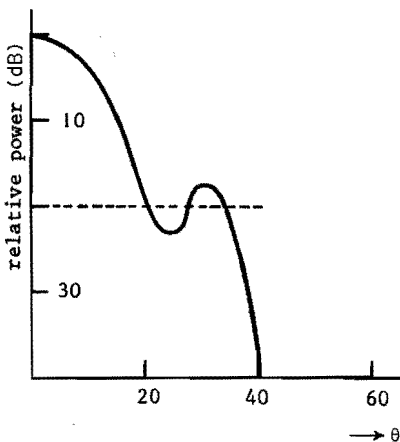frequency-independent properties.

Fig. 2.9ᵃ. Illustration of a power
radiation pattern in which the
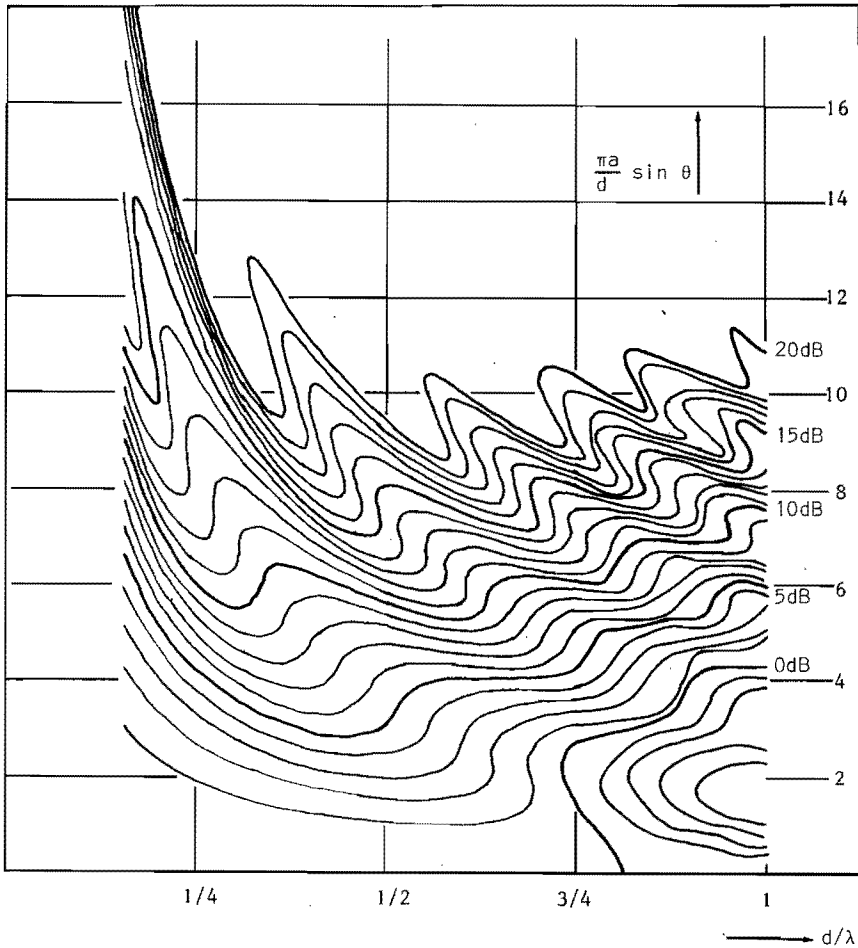power decreases non-monotonously.

38

Fig. 2.9.   Beamwidth of perfectly conducting conical horn antenna with
            small flare angle; E-plane.

The sidelobes in the E-plane are caused by the fact that E_r' is rather
large at the rim $r' = a$. To prove this assertion we have computed the
power radiation pattern of an aperture with a field distribution given
by (2.49) and (2.50) and with $g(\rho) = -f(\rho) = -J_1'(j_{11}'\rho)$. Now we are
sure that E_r' is zero at the rim $r' = a$. The results of this computation
show that indeed the sidelobes have disappeared. We also have computed
the power radiation pattern of an aperture with a field distribution
given by (2.49) and (2.50) and $g(\rho) = -f(\rho) = -J_1(j_{11}'\rho)$. We know that

$J_1(0) = 0$ and $J_1'(j_{11}') = 0.58$. So we should expect that high sidelobes exist in the power radiation pattern. A computation confirmed this expectation.

In the final part of this section we shall study the gain of such a horn antenna. The definition of the gain function $G(\theta \, \phi)$ is given by the relation

$$G(\theta,\phi) = \frac{P(\theta,\phi)}{\frac{1}{4\pi}P_+} \, , \tag{2.65}$$

where P_+ represents the power radiated by the antenna. P_+ can be found by effecting an integration of Poynting's vector over the aperture S_A of the antenna. Using the relations (2.49) and (2.50) we find

$$P_+ = \int_0^a \int_0^{2\pi} \tfrac{1}{2}\mathrm{Re}[\underline{E}\times\underline{H}^*]r'dr'd\phi' = \tfrac{1}{2}Z_0^{-1}\int_0^a \int_0^{2\pi} [\,|E_r'|^2+|E_\phi'|^2]r'dr'd\phi' =$$

$$\tfrac{1}{2}Z_0^{-1}\pi\,a^2\int_0^1 \{\,|f(\rho)|^2 + |g(\rho)|^2\} \, \rho d\rho \ . \tag{2.66}$$

Suppose that $P(\theta,\phi)$ has a maximum value for θ_0, ϕ_0. Then the gain G of the antenna is defined by $G = G(\theta_0,\phi_0)$. Next we restrict ourselves to the case that $\theta_0 = 0$. Then we find for the gain

$$G = \frac{|\ ka \int_0^1 \{f(\rho) - g(\rho)\}\ e^{-jv\rho^2}\ \rho d\rho\ |^2}{\int_0^1 \{\,|f(\rho)|^2+|g(\rho)|^2\}\rho d\rho} \ . \tag{2.67}$$

In the derivation of (2.67) use has been made of (2.56). The integral in the denominator of (2.67) is calculated in the following way. Substituting the expression (2.51) in this integral and replacing $j_{11}'\rho$ by x and A by 1 gives

$$\left(1/j_{11}'\right)^2 \int_0^{j_{11}'} \left[\left\{\frac{J_1(x)}{x}\right\}^2 + \left\{J_1'(x)\right\}^2\right] x dx \ .$$

This integral can be transformed to the next two after using (2.63)

$$\left(1/j_{11}'\right)^2 \int_0^{j_{11}'} J_0^2(x)\ x dx - 2\left(1/j_{11}'\right)^2 \int_0^{j_{11}'} J_1'(x)\ J_1(x)\ dx \ .$$

40

For the first integral we find [38]

$$\int_0^{j'_{11}} x\, J_0^2(x)\, dx = \frac{(j'_{11})^2}{2} \left[\left\{ J_0'(j'_{11}) \right\}^2 + \left\{ J_0(j'_{11}) \right\}^2 \right] =$$

$$\frac{(j'_{11})^2}{2} \left[\left\{ J_1(j'_{11}) \right\}^2 + \frac{1}{(j'_{11})^2} \left\{ J_1(j'_{11}) \right\}^2 \right] .$$

The second integral

$$-2\left(1/j'_{11} \right)^2 \int_0^{j'_{11}} J_1'(x)\, J_1(x)\, dx = -\left(\frac{1}{j'_{11}} \right)^2 \left\{ J_1(j'_{11}) \right\}^2$$

For the gain G we then find

$$G = \frac{2(ka)^2}{\left\{ J_1(j'_{11}) \right\}^2 \left\{ 1 - (1/j'_{11})^2 \right\}} \left| \int_\alpha^1 J_0(j'_{11}\rho)\, e^{-jv\rho^2}\, \rho d\rho \right|^2 . \tag{2.68}$$

This formula can be written in the somewhat more simple form

$$G = C(ka)^2\, A(v) \quad \text{with } C = 8.38 \text{ and} \tag{2.69}$$

$$A(v) = \left| \int_0^1 J_0(j'_{11}\rho)\, e^{-jv\rho^2}\, \rho d\rho \right|^2 .$$

The gain of an antenna is mostly expressed in decibels. Therefore we study the quantity $g = 10^{10}\log G$ and we find that

$$g = 20^{10}\log \frac{2\pi a}{\lambda} - L(v) \tag{2.70}$$

where

$$L(v) = -10^{10}\log A(v) - 9.23 .$$

The function $L(v)$ has been plotted in Fig. 2.10.

The gain of a conical horn antenna can now be found from formula (2.70) and Fig. 2.10, provided the conditions, under which the formulae (2.50) and (2.51) are derived, are fulfilled. These conditions are: $\alpha_0 \leq 15^0$ and $kR \gg 1$. From equation (2.70) and Fig. 2.10 we conclude that a maximum gain for prescribed diameter 2a and fixed frequency is
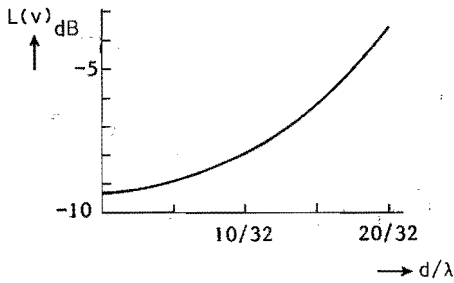
Fig. 2.10. The function $L(v)$ against d/λ.

obtained if $d = 0$; this implies that the aperture is an equiphase plane. So the slant length $l = R+d$ (Fig. 2.6) should be infinite long. This raises the question of how to obtain a maximum gain for prescribed parameters, for instance, the slant length l. Let us now consider a conical horn antenna with fixed slant length l. The dimensions of the antenna are completely determined if we also choose the dia — meter $2a$. Formula (2.70) suggests that for a fixed frequency a large gain can be realised if we choose $2a$ large. However, this gives also rise to a large value of d/λ and thus to a large value of $L(v)$. So there seems to be an optimum value of the gain for prescribed slant length l and fixed frequency. Let us try to find the condition for which this optimum gain is obtained for fixed slant length and frequency.

From Fig. 2.6 it can be derived that

$$d/\lambda \cong (a/\lambda)^2 \bigg/ (2l/\lambda, \text{provided } \alpha_o \leqslant 150 .$$

(2.71)

Then

$$g = 10^{10} \log C + 10^{10} \log \frac{4\pi l}{\lambda} + 10^{10} \log v \, A(v) .$$

(2.72)

So the gain has a maximum value if $10^{10} \log v \, A(v)$ has a maximum value. The function $10^{10} \log v \, (A)v$ has been plotted in Fig. 2.11.

The maximum value of the gain occurs if $d/\lambda = 25/64$. And in that case we find for the gain

$$g = 20^{10} \log \frac{2\pi a}{\lambda} - 2,86 \quad [\text{dB}] .$$
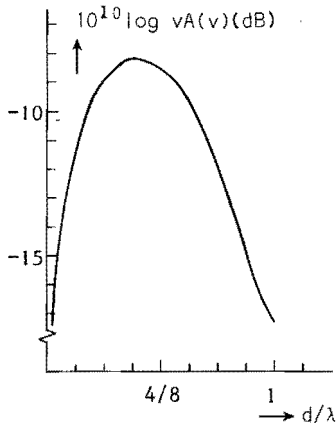
(2.73)

42

Fig. 2.11. Maximum gain for fixed slant length and fixed frequency.

It should be noted that the results given in the formulae (2.70) and (2.73) can also be found in [39]. However, no derivation of the results is given there and a reference is lacking also. To the best of the autor's knowledge Gray and Schelkunoff were the first to calculate the gain of a conical horn antenna. They did not publish the results of their calculations, but these can be found in a paper by King [40]. In this paper it is pointed out that optimum gain for fixed axial length R can be obtained if $d/\lambda = 0,3$. It is very easy to prove that the expression (2.71) is also valid if we replace l by the axial length R, provided $d \ll R$, which implies that the horn antenna should be long. So with our theory it may be expected that maximum gain for fixed axial length occurs when we choose $d/\lambda = 25/64$. It should be noted that the exact value of d/λ for which the function $10^{10} \log vA(v)$ has a maximum can not be found accurately. From Fig. 2.11 we observed that the choice $d/\lambda = 0.3$ gives rise to a difference in gain of 0.2 dB compared with the choice $d/\lambda = 25/64$. Recently Hamid [41] reported a good agreement between the calculations of Gray and Schelkunoff and his own calculations of the gain of a conical horn antenna. He reported a difference of $\pm$ 0.09 dB between the gain calculated by him and the results of King. The calculations of Hamid are based on the geometrical theory of diffraction of J.B. Keller.

It is also possible to choose a fixed value of the angle α_0 and a fixed frequency and to adjust the length of the horn antenna in such a way that a maximum gain is obtained. If α_0 is constant, then a/d is con-

43

stant, as can be derived from (2.31). The expression (2.69) can be
written in a somewhat other form

$$G = \left(\frac{a}{d}\right)^2 C v^2 A(v) .$$ (2.74)
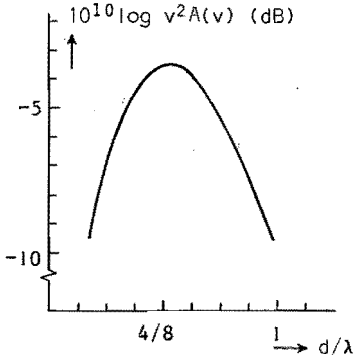
$10^{10}\log v^2 A(v)$ (dB)

Fig. 2.12. Maximum gain for fixed
flare angle and fixed frequency.

The quantity $10^{10}\log v^2 A(v)$ has been plotted in Fig. 2.12. Now we see
that the gain has a maximum if $d = 0.53$ λ and this value of d deter-
mines the value of 2a.

Suppose that the dimensions of the horn antenna are specified, then
equation (2.74) can be used for finding the frequency for which the
gain has a maximum. Again we find that $d = 0.53$ λ, where d is a fixed
quantity. In conclusion we may say that frequency independence of the
gain occurs in the same frequency region where the beamwidth is fre-
quency-independent. Obviously, the requirement for minimum frequency-
dependence of the beamwidth is the same as for maximum gain, as was
also to be expected from Fig. 2.5.

44

2.3   Experimental investigation of the power radiation pattern of a
       frequency-independent conical horn antenna with a small flare
       angle.

The main conclusion of the preceding section is that a conical horn an-
tenna possesses a power radiation pattern which under certain conditi-
ons is independent of frequency, especially in the H-plane. Besides,it
is obvious that Fig. 2.8 and Fig. 2.9 together can be used as a design
chart. However, in the derivation of the results plotted in the two
diagrams mentioned above some approximations have been made. These ap-
proximations restrict the usefulness of Fig. 2.8 and Fig. 2.9 somewhat.
In this section we shall first investigate the limits of the useful-
ness of these two diagrams. In the latter part of this section we shall
describe experiments that confirm the theoretical predictions.

Suppose that we wish to design a conical horn antenna with a power ra-
diation pattern independent of the frequency in a relative frequency
band of 1 : 2. From Fig. 2.9 we see that we have to choose $d/\lambda < 3/4$
in order to prevent the main lobe of the pattern from splitting. On
the other hand we must choose $d/\lambda > 3/8$ in order to be sure that the
desired frequency band is obtained. Fig. 2.8 shows that the choice
$3/8 < d/\lambda < 3/4$ indeed gives rise to a power radiation pattern, which
is independent of the frequency, although some broadening of the beam
occurs at the lower end of the desired frequency band. Fig. 2.9 shows
us that the pattern in the E-plane will vary somewhat more with frequen-
cy.

In the preceding section we have assumed that $\alpha_0 \leq 15^\circ$. This imposes a
restriction with respect to the power radiation pattern which can be
realised with antennas of the type that we are discussing. Let us in-
vestigate this question in more detail. From this preceding section we
know that

$$d = a \tan \tfrac{1}{2} \alpha_0 \quad \text{or} \tag{2.31}$$

$$\frac{d}{a} \cong \frac{\alpha_0}{2} . \tag{2.75}$$

So $\dfrac{d}{a} < \dfrac{1}{2} \dfrac{\pi}{12}$ and $\dfrac{\pi a}{d} > 24.$

From Fig. 2.8 we see that $\frac{\pi a}{d} \sin \theta_{10,H} = 4.8$, where $2 \theta_{10,H}$ denotes the 10 dB beamwidth in the H-plane.
Thus

$$\sin \theta_{10,H} < \frac{4.8}{24} = 0.2 \quad \text{and}$$

$$\theta_{10,H} < 12^{\circ} \,. \tag{2.76}$$

In a similar way we find for the 20 dB beamwidth in the H-plane

$$\theta_{20,H} < 19^{\circ}. \tag{2.77}$$

A comparison of Fig. 2.8 with Fig. 2.9 shows that the beamwidth in the E-plane is somewhat larger than in the H-plane.

The theory developed so far can be used only for the design of broad-band conical horn antennas with a rather narrow beam. These antennas are very suitable as feeds in cassegrain antennas, where the feeds il-luminate a rather small subreflector. More details concerning casse-grain antennas are given in [42]. In practice the 10-dB beamwidth or the 20-dB beamwidth of the feed is specified and it is the task of the designer of the feed to meet the required specification. This can be done by using the following formulae
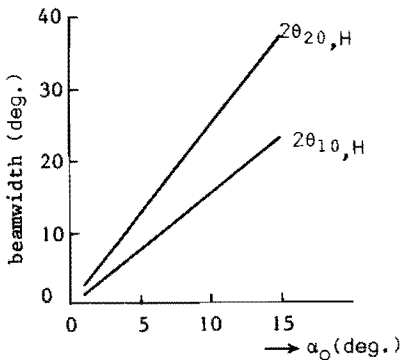

Fig. 2.13. 10-dB beamwidth and 20-dB beamwidth in H-plane of frequency-independent conical horn antenna with small flare angle against flare angle α_o.

$$\frac{\pi a}{d} \sin \theta_{10,H} = 4.8 \qquad \frac{\pi a}{d} \sin \theta_{20,H} = 7.7 \ . \qquad (2.78)$$

Using (2.78) and the relation

$$d = a \tan \tfrac{1}{2} \alpha_o \qquad (2.31)$$

we have calculated the curves of Fig. 2.13, which gives the flare angle α_o for prescribed beamwidth in the H-plane. By means of the relation

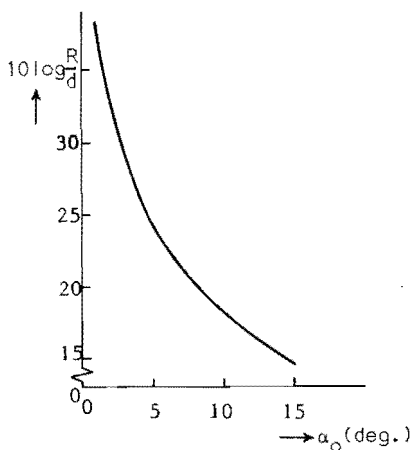$$R/d = \frac{2}{\alpha_o{}^2} \qquad (2.35)$$

Fig. 2.14.   Length of frequency-independent conical horn antenna with small flare angle against flare angle.

we can find R/d. The results are given in Fig. 2.14 and show that large values of R/d are necessary if the flare angle α_o becomes small. This is the case if we try to design an antenna with a power radiation pattern with a rather narrow beam. Up till now we have not found the values of α_o and R/d. The dimensions of the conical horn antenna are completely specified if the value of d is known. The value of d depends on the frequency band for which the antenna will be used. From the first part of the section we know that the value of d/λ is between 3/8 and 3/4. Suppose that the lowest frequency for which the antenna will

47

be used is given by f_1, then $\lambda_1 = c/f_1$ and

$$d = \frac{3}{8} \lambda_1. \qquad (2.79)$$

Summerising we may formulate the design procedure as follows. Choose the 10-dB beamwidth in the H-plane. From Fig. 2.13 the 20-dB beamwidth and the angle α_0 are found. Now Fig. 2.14 gives the value of R/d. The choice of d depends on the desired frequency band, in which the antenna will be used. If d is known, R can be found and this completes the design.

In order to verify the theory developed in this study we have compared the measured power radiation pattern of a conical horn antenna with the theoretical power radiation pattern. The measurements have been carried out in the frequency band between 7 GHz and 14 GHz. The dimensions of the horn antenna are given in Fig. 2.15. They are not exactly equal to the dimensions obtained from the design procedure of the first part of this section. The reason for the discrepancy is that this horn antenna was already available before the theory, described in the present study, was developed.

In fact, some preliminary measurements with the horn have already been described [4]. Suppose that f_1 = 7 GHz. Then from (2.79) it follows that d = 16.1 mm. This value differs only slightly from the actual value of 17.4 mm. So the antenna can be used for an experimental verification of the theory.
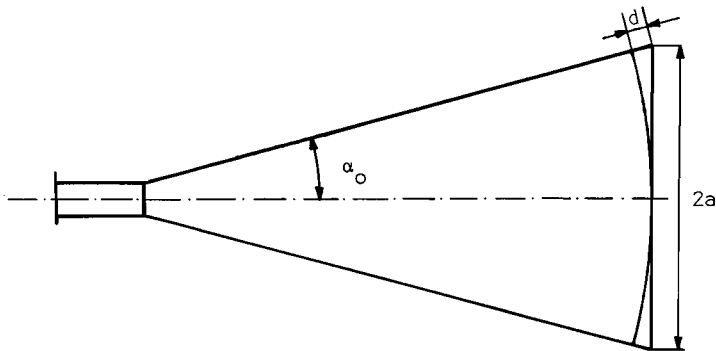

Fig. 2.15. Illustration of frequency-independent conical horn antenna.
2a = 264mm; d = 17,4mm; α_0 = 15°.

The $TE_{1\nu}$-mode in the horn is launched by coupling the cone to a circular waveguide in which the TE_{11}-mode propagates. The diameter of the waveguide is 28 mm . In order to investigate, whether the dominant mode can propagate through the waveguide for frequencies between 7 GHz and 14 GHz without exciting higher modes, we have composed a table with the cut-off frequencies f_c of several modes which can possible be excited.
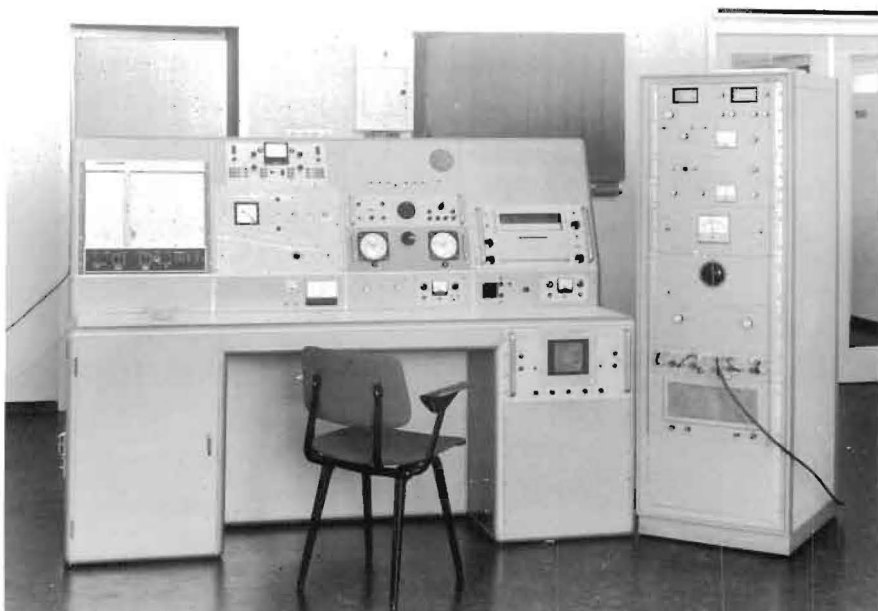
Table I

mode	f_c[GHz]
TE_{11}	6.281
TM_{01}	8.206
TE_{21}	10.420
TM_{11}	13.075
TE_{01}	13.075
TM_{21}	17.520

The table gives rise to the following considerations:

(i) the circular waveguide can be used for frequencies aboven 6.281 GHz. However, it is advisable to choose the lowest frequency somewhat above 6.281 GHz, to be sure that the losses are low. Moreover, the connection between the generator and the transmitting antenna at the test range consists of a normal X-band waveguide with a cut-off frequency of 6.557 GHz. So it was decided to start the measurements at 7 GHz,

(ii) There are several modes with a cut-off frequency between 7 GHz and 14 GHz. So in principle these modes can be excited if there are discontinuities in the waveguide. A discontinuity is the connection between the waveguide and the cone. For physical reasons we may say that only modes with the same ϕ'-dependence as the TE_{11}-mode can be excited. So it must be expected that the TM_{11}-mode will be excited in the frequency band from 13.075 GHz to 14 GHz,
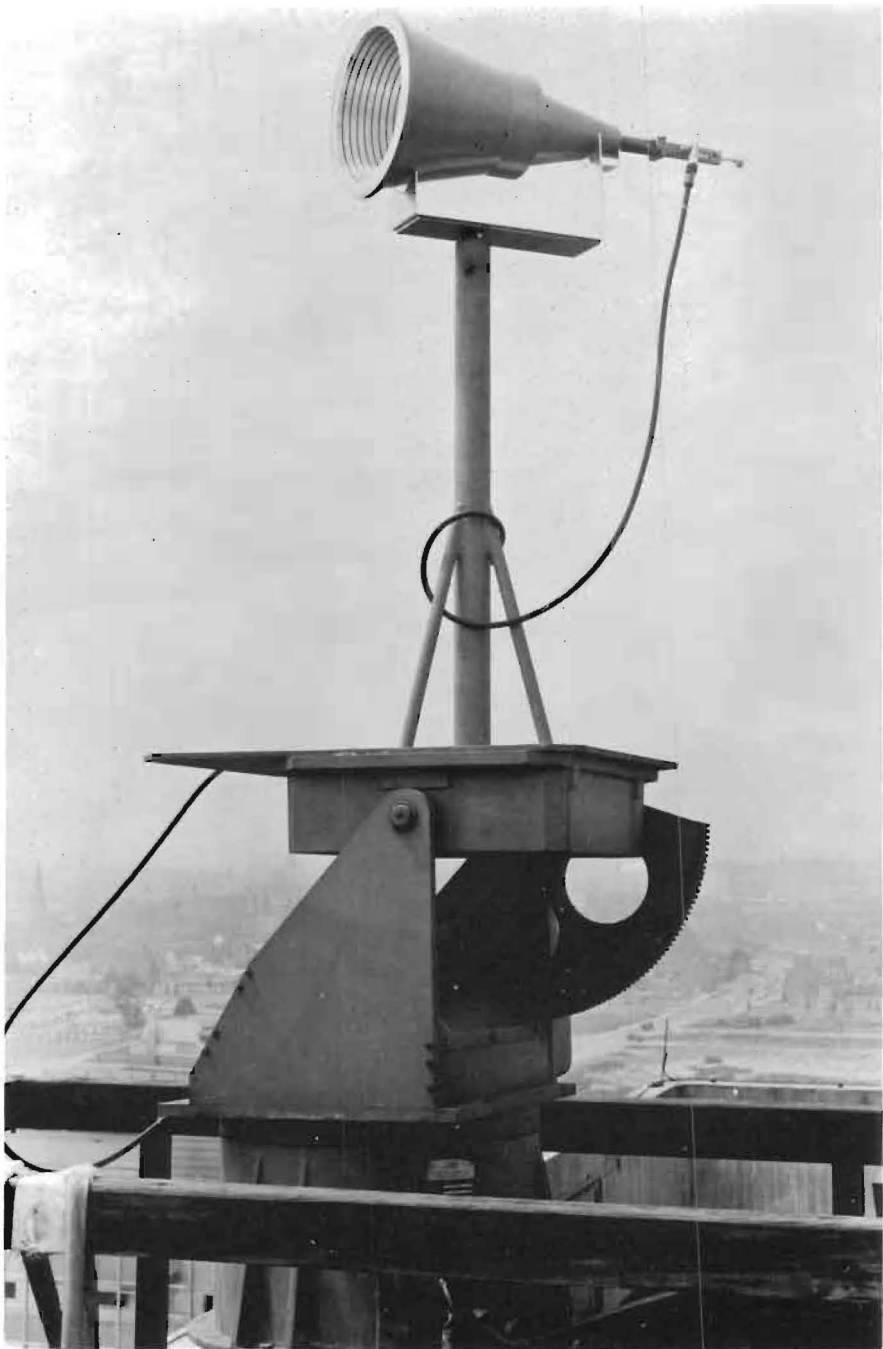
Photograph 2.　Equipment for the measurement of the radiation pattern of antennas. (Scientific-Atlanta instruments).

Photograph 1.　Conical horn antenna under test on the turntable.

(iii) If there is a good agreement between the computed and the mea-
sured power radiation pattern in the frequency band from 13.075
GHz to 14 GHz, then we may draw the conclusion that the influ-
ence of higher modes, excited at the waveguide-cone transition,
is negligible as far as the radiation pattern is concerned.

For the measurement of the power radiation pattern use has been made
of an antenna test range of 180 m. length. The antenna under test is
used as a receiving antenna and is mounted on a turntable. The antenna
under test rotates while a plane wave is incident upon it. The plane
wave is produced by a transmitting antenna situated at a distance of
180 m. from the turntable. So the far field region condition (2.20) is
satisfied. The transmitting antenna is a paraboloid reflector type with
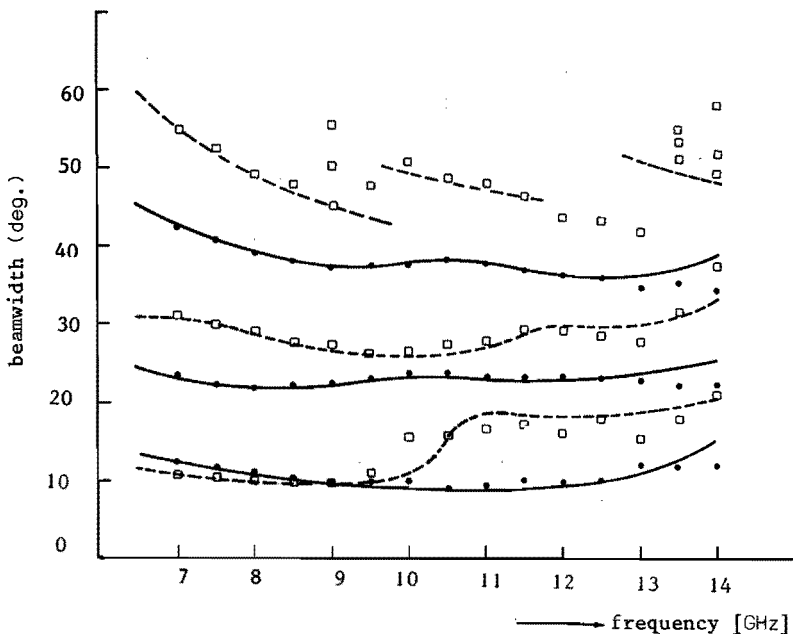a diameter of 1.20 m.

Fig. 2.16. Beamwidth of conical horn antenna of Fig. 2.15 against frequency.
———, theoretical, H-plane,
----, theoretical, E-plane,
• , experimental,H-plane,
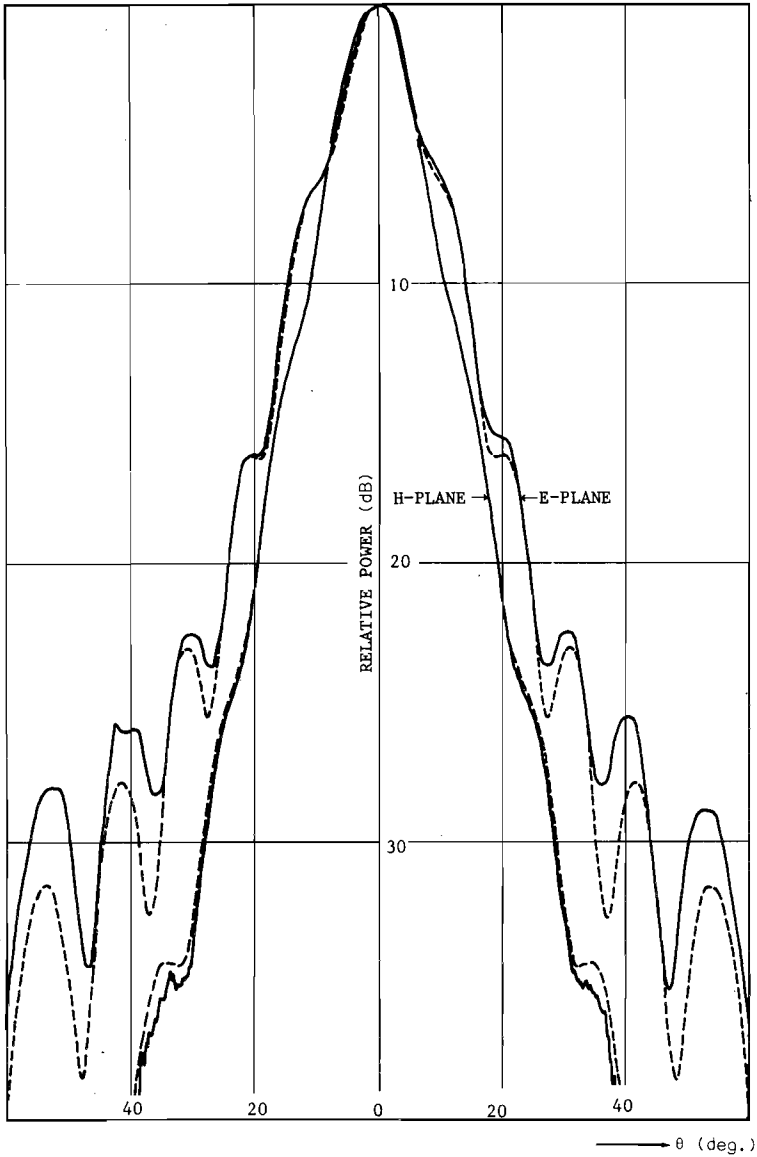□ , experimental,E-plane.

Fig. 2.17. Power radiation pattern of the conical horn antenna of Fig. 2.15
at 8 GHz.

.---, theoretical, H-plane and E-plane,

——, experimental,H-plane,

——, experimental,E-plane.

In photo 1 an antenna under test is mounted on the turntable. On the right hand side of photo 2 the receiver used in the measurements is shown. The right part of the console contains the recording equipment and some instruments for operating the turntable. A more comprehensive description of this type of measurements can be found in [43] and [44], where many references are also given.

With the equipment described above we have measured the power radiation pattern of the antenna of Fig. 2.15 as a function of frequency. The results of the measurements have been collected in Fig. 2.16 together with theoretical results, and they show good agreement. It should be noted that beamsplitting is observed for frequencies between 13 GHz and 14 GHz. Furthermore it was impossible to sketch the 20 dB line between 13 GHz and 14 GHz owing to the capricious behaviour of the sidelobes.

For purposes of illustration the complete power radiation pattern in the H-plane and the E-plane has been included for the frequencies 8GHz, 13 GHz and 14 GHz and are shown in Fig. 2.17, Fig. 2.17a and Fig. 2.17b respectively. The agreement between theoretical en experimental results is good for 8 GHz. In Fig. 2.17a we observe that the theoretically predicted beamsplitting in the E-plane does not occur in the experimentical results. In Fig. 2.17b we have shifted both the theoretical and the experimental power radiation pattern in the E-plane about 2 dB with respect to the H-plane patterns. This was done to keep the curves within the frame of the diagram. In fact, the value of the maxima of $f_H(0,v)$ and $f_E(0,v)$ are equal as can be seen from (2.59) and (2.60). From Fig. 2.17b we concluded that at 14 GHz beamsplitting in the E-plane occurs indeed. Another conclusion is that the agreement between theoretical and experimental results is not so good at this frequency. Probably this is caused by the excitation of the TM_{11}-mode. Finally, we have measured the V.S.W.R. of the antenna as a function of the frequency. We found that the V.S.W.R. was less than 1.15 in the frequency range between 7 GHz and 14 GHz.

In conclusion we may say that conical horn antennas with a bandwidth of 1 : 2 can be designed as described in this section and the agreement between theoretical predictions and experimental results is resonably good. The bandwidth is restricted by the occurrence of the beamsplitting of the pattern and the excitation of higher modes at the transition from

54

waveguide to cone. In cases where beamsplitting presents no difficulties, a larger bandwidth can be obtained. However, in that case it is necessary to improve the bandwidth of the waveguide, which is coupled to the conical horn antenna.

Fig. 2.17[a]. Power radiation pattern of the conical horn antenna of Fig. 2.15 at 13 GHz.

        —·—·—, theoretical, H-plane,

        - - - -, theoretical, E-plane,

        ———, experimental,H-plane,
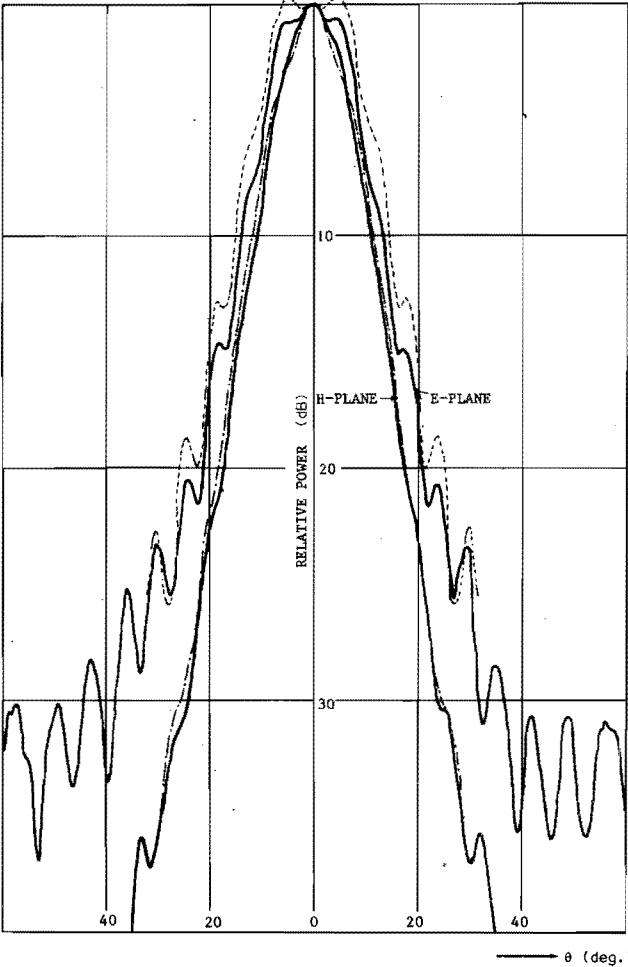
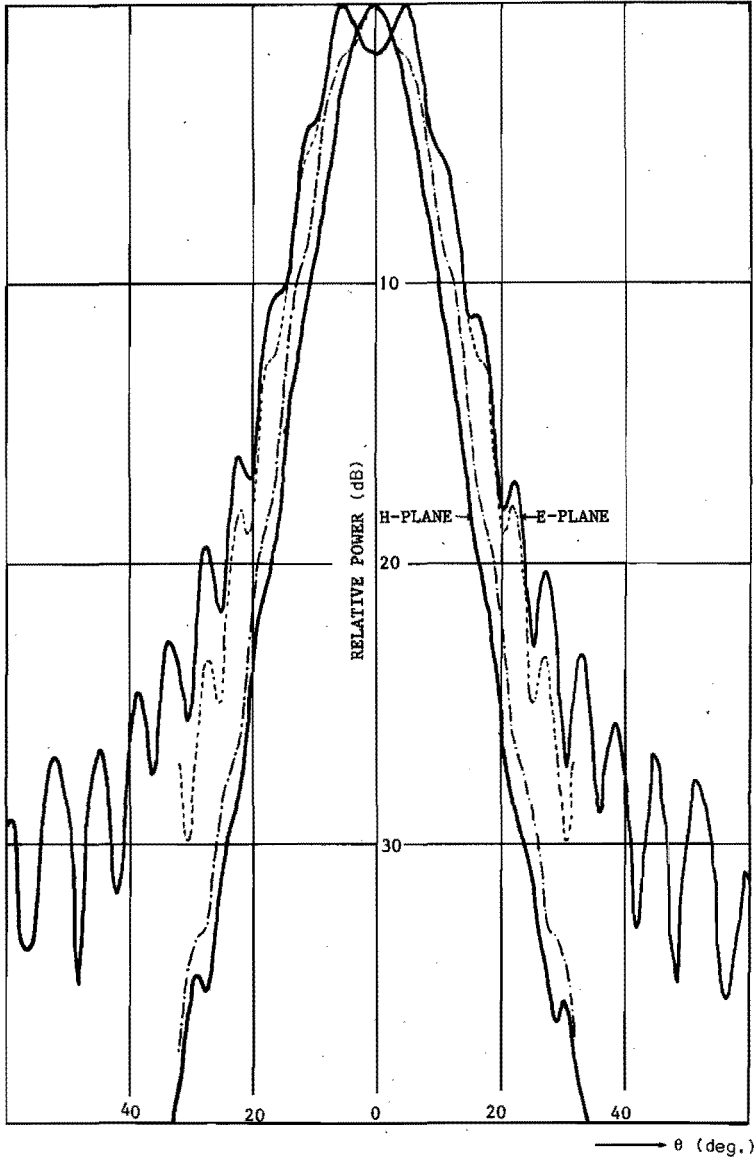   ———, experimental,E-plane.

Fig. 2.17^b. Power radiation pattern of the conical horn antenna of Fig. 2.15
at 14 GHz.

            , theoretical, H-plane,

            , theoretical, E-plane,

            , experimental,H-plane,

            , experimental,E-plane.

2.4 Theory of the equiphase surfaces of a frequency-independent conical horn antenna with a small flare angle.

In the preceding two sections it was found both theoretically and experimentally that the conical horn antenna has a power radiation pattern which is independent of frequency in a relative frequency band 1 : 2, provided the dimensions of the horn are chosen correctly. From Fig.2.13 we draw the conclusion that the 20 dB beamwidth of this type of antenna is less than 20°. So this antenna is very suitable as a feed in a cassegrain antenna. A cassegrain antenna consists of a large paraboloid reflector and a small hyperboloid reflector (Fig. 2.18).
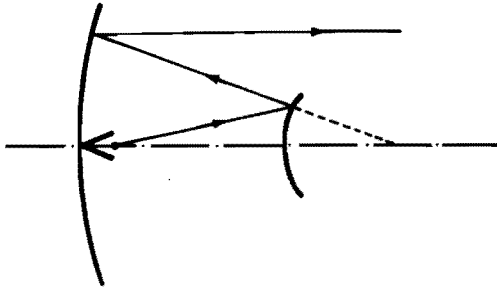

Fig. 2.18. Diagram of cassegrain antenna.

The feed illuminates the hyperboloid reflector. This implies that the beamwidth of the power radiation pattern of the feed should be narrow.

The theory of the cassegrain antenna starts with the assumption that the equiphase planes of the feed are spherical, at least in the vicinity of the hyperboloid reflector. This assumption allows the designer of a cassegrain antenna to treat the feed as a point source, located at the so called phase centre. It is important that the position of the phase centre is independent of the frequency in the same frequency band where the beamwidth is constant. In fact, a change in the position of the phase centre disturbs the phase distribution over the paraboloid reflector and this gives rise to a reduction of the gain of the cassegrain antenna [45].

So it is important to study the equiphase surfaces of the conical horn antenna with frequency-independent power radiation pattern. To start this study we repeat the formulae (2.53) and (2.54), which give the electric field in the far field region

$$E_\theta = \frac{jka^2}{2r} e^{-jkr} \frac{1 + \cos\theta}{2} \cos\phi \, I_E(u,v) \, , \tag{2.53}$$

$$E_\phi = -\frac{jka^2}{2r} e^{-jkr} \frac{1 + \cos\theta}{2} \sin\phi \, I_H(u,v) \, . \tag{2.54}$$

The functions $I_H(u,v)$ and $I_E(u,v)$ are both complex for all values of u and v except $v = 0$. So $I_H(u,0)$ and $I_E(u,0)$ are real functions. In case $v = 0$ we are dealing with an aperture S_A (Fig.2.3) with a constant phase field distribution. An open circular waveguide is an example of such an aperture. The equiphase surfaces are now given by $r = $ constant. This implies that the equiphase surfaces are spheres and the phase centre coincides with the centre of the aperture S_A.

If the functions $I_H(u,v)$ and $I_E(u,v)$ are complex, then we may write

$$I_H(u,v) = \left| I_H(u,v) \right| e^{j[\psi_H(u,v)]} \tag{2.80}$$

and

$$I_E(u,v) = \left| I_E(u,v) \right| e^{j[\psi_E(u,v)]} \tag{2.81}$$

and $\psi_H(u,v) - \psi_H(0,v)$ describes the phase variations in the H-plane with respect to the point $u = 0$, along a circle with radius r. The function $\psi_E(u,v) - \psi_E(0,v)$ has the same meaning, but now in the E-plane. The conclusion that can be drawn now is that the sphere with radius r is not an equiphase surface. In this case, too, the equiphase surfaces may be spheres, but the centre of the spheres does not coincide with the origin of the coordinate system. However, this is only possible if the functions $\psi_H(u,v)$ and $\psi_E(u,v)$ are identical. If the functions $\psi_H(u,v)$ and $\psi_E(u,v)$ differ, we may conclude that the centre of curvature of the equiphase lines in the H-plane is not the same point as the centre of curvature of the equiphase lines in the E-plane. We shall now speak about the phase centre in the H-plane and the phase centre in the E-plane respectively. We shall now show that the above situation occurs in the conical horn antennas, the properties of which are described in this study. To study the position of the two phase centres in more detail the functions

58

Fig. 2.19.

Phase variations in the H-plane along a circle with large radius r against $\frac{\pi a}{d}$ sin θ for several values of d/λ. The centre of the circle coincides with the centre of the aperture of the conical horn antenna.
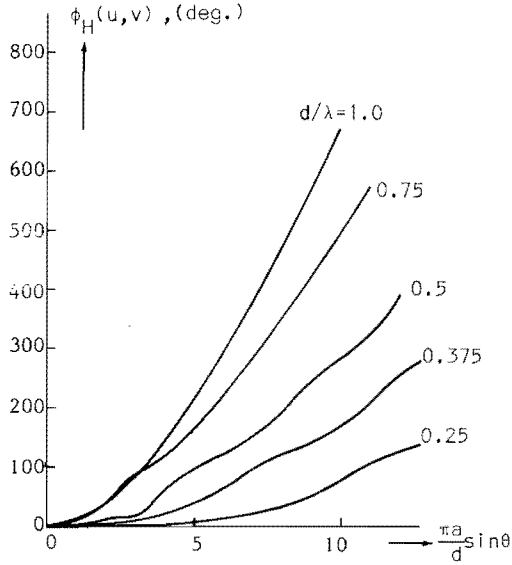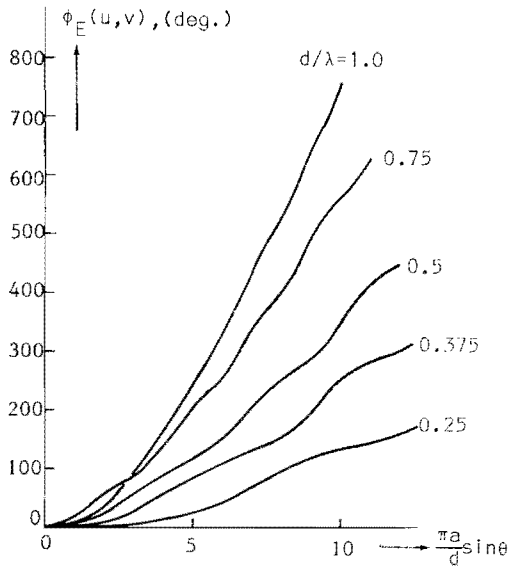

Fig. 2.20.

Phase variations in the E-plane along a circle with large radius r against $\frac{\pi a}{d}$ sin θ for several values of d/λ. The centre of the circle coincides with the centre of the aperture of the conical horn antenna.
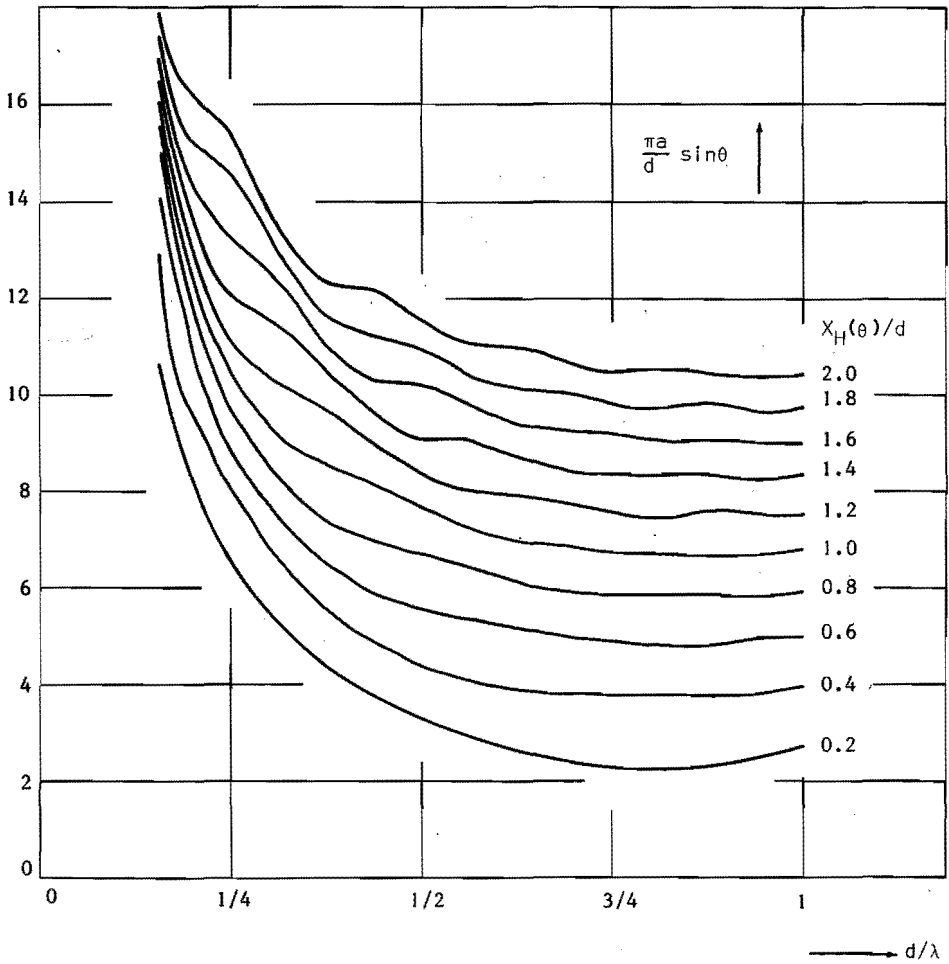
Fig. 2.21. Curves of constant $X_H(\theta)/d$-value against d/λ for a conical horn antenna with small flare angle.

$$\phi_H(u,v) = \frac{360}{2\pi} [\psi_H(u,v) - \psi_H(0,v)]$$

and

$$\phi_E(u,v) = \frac{360}{2\pi} [\psi_E(u,v) - \psi_E(0,v)]$$

(2.82)

have been computed for several values of u and v. In Fig. 2.19 and Fig. 2.20 we have plotted $\phi_H(u,v)$ and $\phi_E(u,v)$ respectively as function of $\alpha = u/v = \frac{\pi a}{d} \sin \theta$ for some values of d/λ. In Fig. 2.19 we have plotted $\phi_H(u,v)$ only for values of $\frac{\pi a}{d} \sin \theta$ which are within the 20 dB points,

60
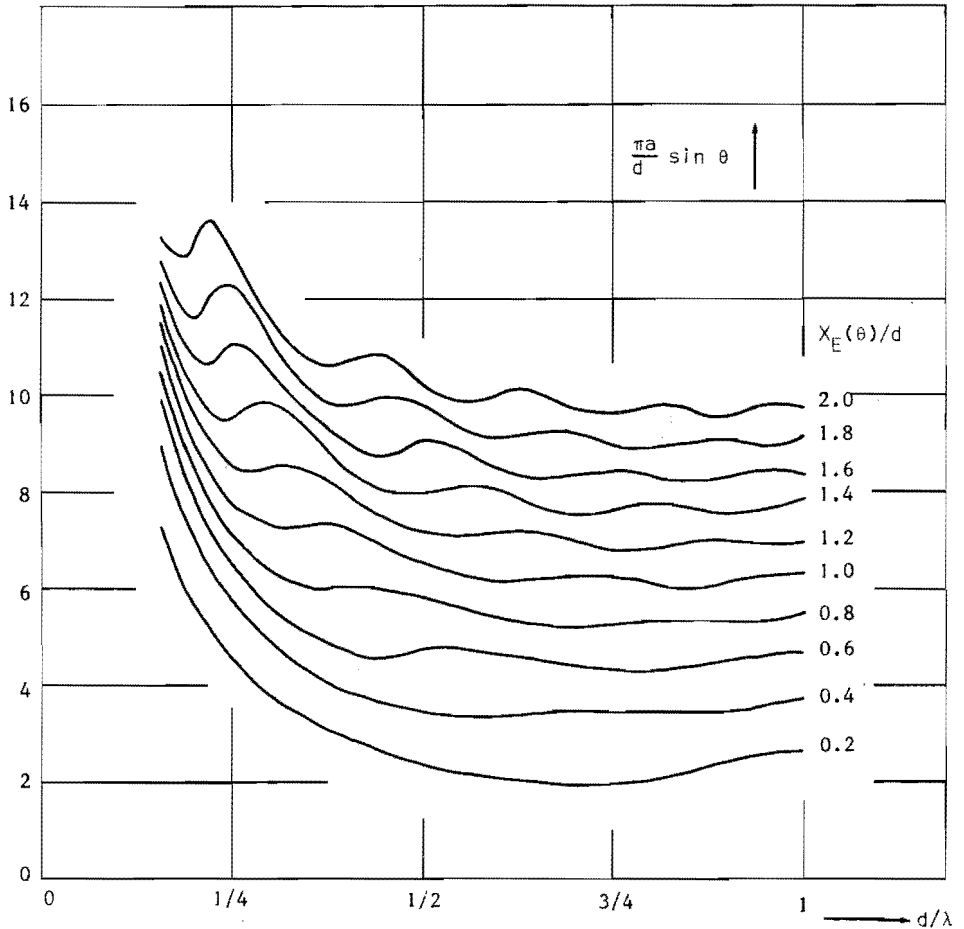
Fig. 2.22. Curves of constant $x_E(\theta)/d$-value against d/λ for a conical horn antenna with small flare angle.

This can be verified by comparing Fig. 2.19 with Fig. 2.8. The same policy has been followed with respect to Fig. 2.20. With these curves it is possible to find the equiphase lines in the H-plane and the E-plane. In Fig. 2.23 a diagram of a conical horn is given and it is supposed that point P is in the far field region of the antenna.

If the circle with radius r and centre 0 is known, then the equiphase line through P can be constructed, because $x_H(\theta) = \dfrac{\lambda}{360} \, \phi_H(u,v)$. The

Fig. 2.23. Horn antenna and equiphase line PQ in far field region.

same procedure can be adopted for finding the equiphase line through P
in the E-plane. In the latter case $x_E(\theta) = \frac{\lambda}{360} \phi_E(u,v)$. From the fact
that the functions $\phi_H(u,v)$ and $\phi_E(u,v)$ are positive we conclude that
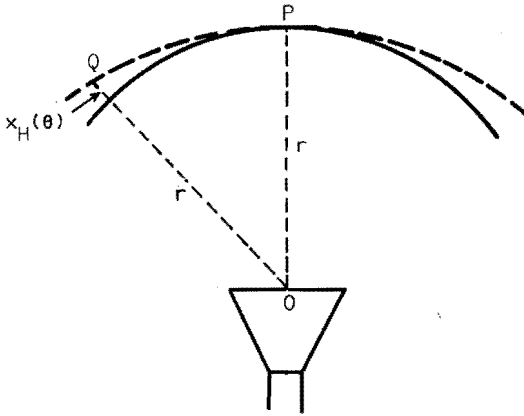the two centres of curvature are shifted into the horn.

Now that we are able to find the equiphase lines in the H-plane and the
E-plane, there remain two questions to be solved. First we have to in-
vestigate whether the equiphase lines in the H-plane and the E-plane
are circles or not. In the second place we have to investigate the
frequency dependence of the equiphase lines. We prefer to investigate
first the second question. For this purpose we have composed a diagram
(Fig. 2.21), which gives lines of constant $x_H(\theta)/d$ as a function of
d/λ.

In Fig. 2.22 the same information has been gathered for the E-plane.
From these two diagrams we conclude that the equiphase lines in the
H-plane and in the E-plane are indeed independent of frequency in the
range $\frac{1}{2} < \frac{d}{\lambda} < 1$. In the range $3/8 < d/\lambda < \frac{1}{2}$ the equiphase lines are
slightly dependent on the frequency. Suppose that the antennas under
discussion is used as a feed in a reflector antenna, then the phase
efficiency [4] of this reflector antenna can be found using the dia-
grams Fig. 2.21 and Fig. 2.22.

For the investigation concerning the question whether the equiphase lines
are circles we adopt the following procedure. Fig. 2.24 shows a circle
with radius r and an equiphase line in the H-plane through P. Suppose

this equiphase line is a circle with centre 0. Then we compute the distance p between 0 and 0' from the phase variations $x_H(\theta)$. If the equiphase line is a circle then p does not depend on the angle θ.
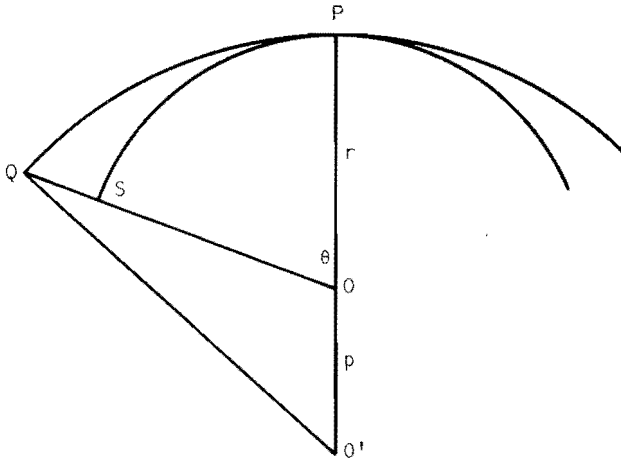
Fig. 2.24. Geometrical figure for calculating the phase centre of a horn antenna.

Let $0'Q = r + p$ and $QS = x_H(\theta)$.
Applying the cosine rule we find

$$(r + p)^2 = p^2 + \left\{r + x_H(\theta)\right\}^2 + 2p\left\{r + x_H(\theta)\right\}\cos\theta,$$

which gives

$$p = \frac{x_H(\theta)\left\{x_H(\theta) + 2r\right\}}{2r(1-\cos\theta) - 2x_H(\theta)\cos\theta} \quad . \tag{2.83}$$

Expression (2.83) simplifies if r is very large and $\theta \neq 0$. In that case we may write, except for $\theta = 0$,

$$p = \frac{x_H(\theta)}{1 - \cos\theta} \quad . \tag{2.84}$$

Using the definition of $x_H(\theta)$ and substituting the first expression of (2.82) gives

$$\left(\frac{p}{d}\right)_H = \frac{1}{2\pi} \frac{\psi_H(u,v) - \psi_H(0,v)}{1 - \cos\theta} \frac{\lambda}{d} \quad . \tag{2.85}$$

63

In a similar way we find for the E-plane

$$\left(\frac{p}{d}\right)_E = \frac{1}{2\pi} \frac{\psi_E(u,v) - \psi_E(0,v)}{1 - \cos\theta} \frac{\lambda}{d} \quad . \tag{2.86}$$

The functions $\left(\frac{p}{d}\right)_H$ and $\left(\frac{p}{d}\right)_E$ have been calculated as a function of θ for the antenna of Fig. 2.15. These calculations have been performed for three values of d/λ. The results of the computations are gathered in Fig. 2.25 and Fig. 2.26. From these diagrams we may conclude that no phase centre in H-plane or E-plane exists.
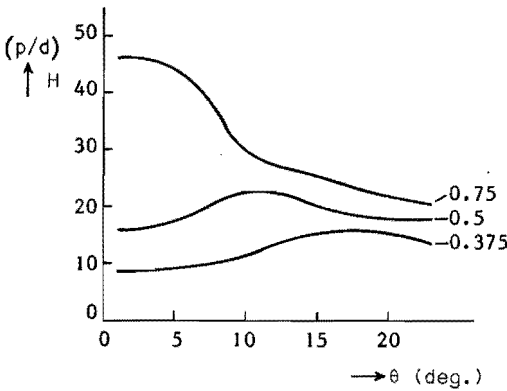

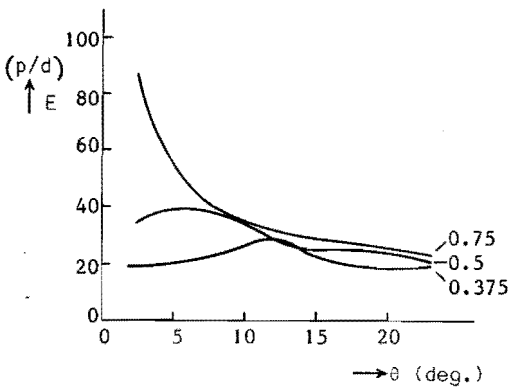Fig. 2.25. Location of phase centre of conical horn antenna in H-plane for some values of d/λ.

Fig. 2.26. Location of phase centre of conical horn antenna in E-plane for some values of d/λ.

64

However, on closer examination we see that for small values of d/λ the equiphase lines in the H-plane and the E-plane are approximately circles, at least in the vicinity of the direction $\theta = 0$. For large values of d/λ the equiphase lines are not circles. This phenomenon has an influence on the phase efficiency as a function of frequency. In order to investigate this effect it is advisable to use the diagrams in Fig. 2.21 and Fig. 2.22. However, it should be noted that this investigation can be carried out only if the dimensions of the reflector antenna are known. As we are studying the properties of the feed only, it is clear that this investigation is outside the scope of the present study.

From the previous discussion we have concluded that Fig. 2.21 and Fig. 2.22 are important for the practical use of the broadband feeds, the properties of which are described in the present study. Therefore there is need for an experimental verification of the theoretical results of this section. These experiments will be described in the next section.

2.5   Experimental investigation of the phase radiation pattern of a frequency-independent conical horn antenna with a small flare angle.

From the preceding section we have learned that the frequency-independent antennas which are the subject of the present study, have no phase centre. The second conclusion was that the phase efficiency of a paraboloid reflector antenna, illuminated by a frequency-independent conical horn antenna, can be determined using Fig. 2.21 and Fig. 2.22. So there is need for an experimental confirmation of the theoretical results of Fig. 2.21 and Fig. 2.22. Unfortunately, Fig. 2.21 and Fig. 2.22 are not suitable for a direct experimental confirmation, because the results of phase measurements are given in terms of degrees, while in Fig. 2.21 and Fig. 2.22 the information concerning the phase radiation pattern is gathered in terms of distances. However, the diagrams of Figs. 2.21 and 2.22 are derived from the same numerical results as those of Figs. 2.19 and 2.20. The only difference is that in Figs.2.21 and 2.22 more information has been collected than in Figs. 2.19 and 2.20, which are only given for the purpose of reference. To obtain an

experimental confirmation of the numerical results which are used for composing Figs. 2.21 and 2.22 it is sufficient to measure the quantities $\phi_H(u,v)$ and $\phi_E(u,v)$. Therefore, it was decided to measure these quantities as a function of θ for some values of d/λ.

In principle, it is possible to carry out these measurements with two probes. One probe has a fixed position P (Fig. 2.24) with respect to the antenna under test. The other is moving along an arc of a circle PS. Connecting these two probes to a phase-measuring circuit we obtain the quantities $\phi_H(u,v)$, $\phi_E(u,v)$ respectively, as a function of θ. However, this method is not very convenient for the following reason. The distance r (Fig. 2.24) should be so long that the probes are in the far field region of the antenna under test. This requirement imposes a restruction on the distance r, which is given by

$$r \geqslant \frac{2D^2}{\lambda} \, , \qquad\qquad\qquad (2.20)$$

D being the diameter of the antenna under test. For an antenna with $D = 10\lambda$, we find $r \geq 200\lambda$. To measure the phase variations $\phi_H(u,v)$ and $\phi_E(u,v)$ with an accuracy of, for instance, $2\pi/72$ rad, it is necessary to be sure that the distance r is constant within $\lambda/72$, which obviously offers mechanical problems. The $\lambda/72$ criterion has been chosen because the accuracy of the phase measuring circuit is approximately 5°. Even if we choose a less stringent criterion than $\lambda/72$, for instance, $\lambda/16$, the method proposed above gives mechanical problems.

A better method of measuring $\phi_H(u,v)$ and $\phi_E(u,v)$ is the following. The antenna under test rotates around the point O, which coincides with the centre of the aperture of the antenna under test. At the same time a plane wave is incident upon the antenna along P O. This plane wave is produced by a transmitting antenna in P. The reference signal is coupled out from the transmission line between the generator and the transmitting antenna (Fig. 2.27).
It can be proved that the phase variations, which are measured, if the antenna under test rotates around an axis through O, are indeed equal to $\phi_H(u,v)$ and $\phi_E(u,v)$ respectively. The proof of this assertion can not be given by means of the well-known reciprocity theorem of antennas. This theorem states that the ratio of the gain function of an antenna used as a transmitting antenna and the effective receiving cross-

1: generator
2: transmitting antenna
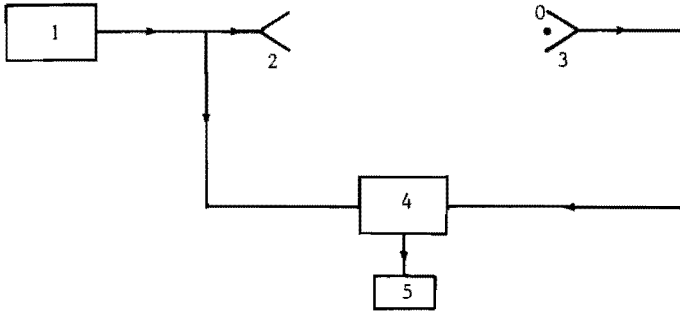
3: antenna under test
4: phase measuring circuit
5: recorder

Fig. 2.27. Diagram of the measuring system for the measurement of phase
variations.

section of the antenna, when the antenna is used as a receiving anten-
na is the same for all antennas. So this theorem is formulated in terms
of energy, and consequently it cannot be used for proving the above
assertion, which is concerned with measuring of phase-differences.How-
ever, the proof of the above assertion can be derived from a recent
paper of De Hoop [46]. The details of the proof are found in appen-
dix B.

The accuracy of the measuring method proposed above is chiefly deter-
mined by the accuracy with which the axis of rotation coincides with
the aperture.To be sure that thisis indeedthe case, the following
method has been adopted. Suppose that an open circular waveguide is
mounted on the turntable in such a way that the aperture of this radi-
ator coincides with the axis of rotation. Then we know from the prece-
ding section and from the paper of De Hoop [46] that the phase varia -
tion is zero if the waveguide rotates. We shall use this criterion to
determine whether the axis of rotation lies within the aperture of the
conical horn antenna. Therefore, the antenna is mounted on the turn-
table and a thin metal plate is connected to the antenna. The plate
coincides with the aperture of the antenna. In the centre of the plate
is a hole, which acts as the aperture of a circular waveguide. The dia-

67

meter of the hole is 28 mm. and the thickness of the plate is 1 mm. The details of the system are given in Fig. 2.28.
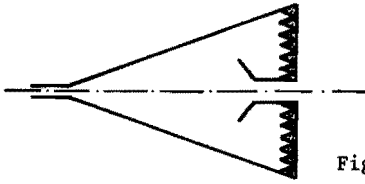

Fig. 2.28. Conical horn antenna with plate.

The precise position of the antenna with respect to the turntable is found by mounting the antenna on the turntable in such a way that the measured phase variation is zero if the antenna rotates. Next, the plate is removed and the measurement of the phase variation is repeated. In this case the quantities $\phi_H(u,v)$ and $\phi_E(u,v)$ respectively are measured. In Fig. 2.29 an example of the results of these two measurements has been plotted. The measurements have been carried out for the an - tenna of Fig. 2.15 and for the frequency 8.6 GHz.

The method of measuring described above has been used to measure the quantities $\phi_H(u,v)$ and $\phi_E(u,v)$ for several frequencies. The measurements have been performed for the antenna of Fig. 2.15. An anechoic chamber, designed by Emerson and Cuming, was used. The distance r between the transmitting antenna and the antenna under test was 4.8m. So the distance requirement (2.20) is satisfied for frequencies below 10 GHz . However, for frequencies above 10 GHz the requirement (2.20) is not satiesfied. For frequencies below 15 GHz the requirement

$$r \geqslant \frac{D^2}{\lambda} \tag{2.87}$$

can be satisfied . So it is to be expected that the results of the measurements for frequencies above 10 GHz deviate somewhat from the theoretical predictions.

Photograph 3 shows a picture of the antenna mounted on the turntable in the anechoic chamber. Photograph 4 shows the same picture, but now with the plate connected to the antenna. Finally we report that the receiver of photograph 2 is used as the phase measuring circuit.

68
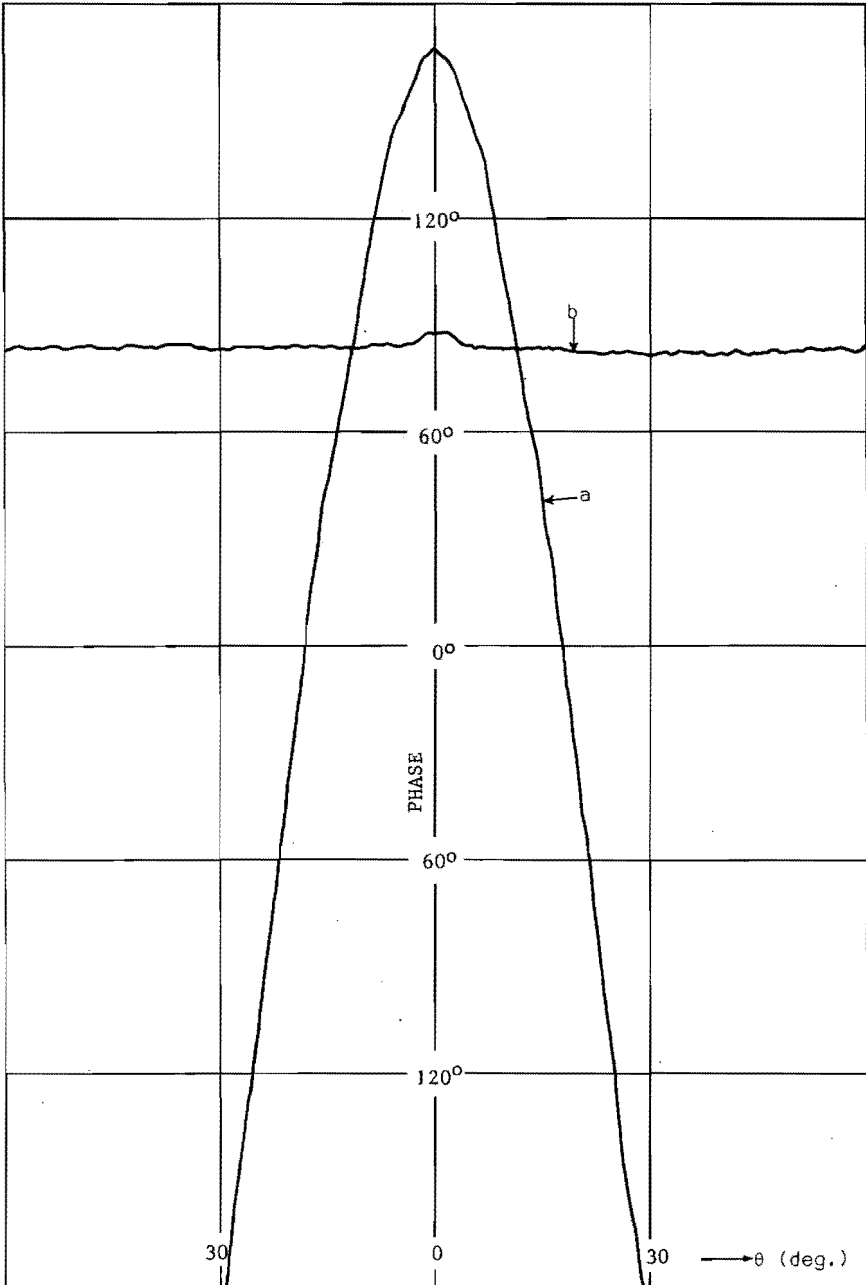
Fig. 2.29. Measured phase variations in H-plane at 8.6 GHz.
        a: antenna of Fig. 2.15,
        b: antenna of Fig. 2.15 with plate.
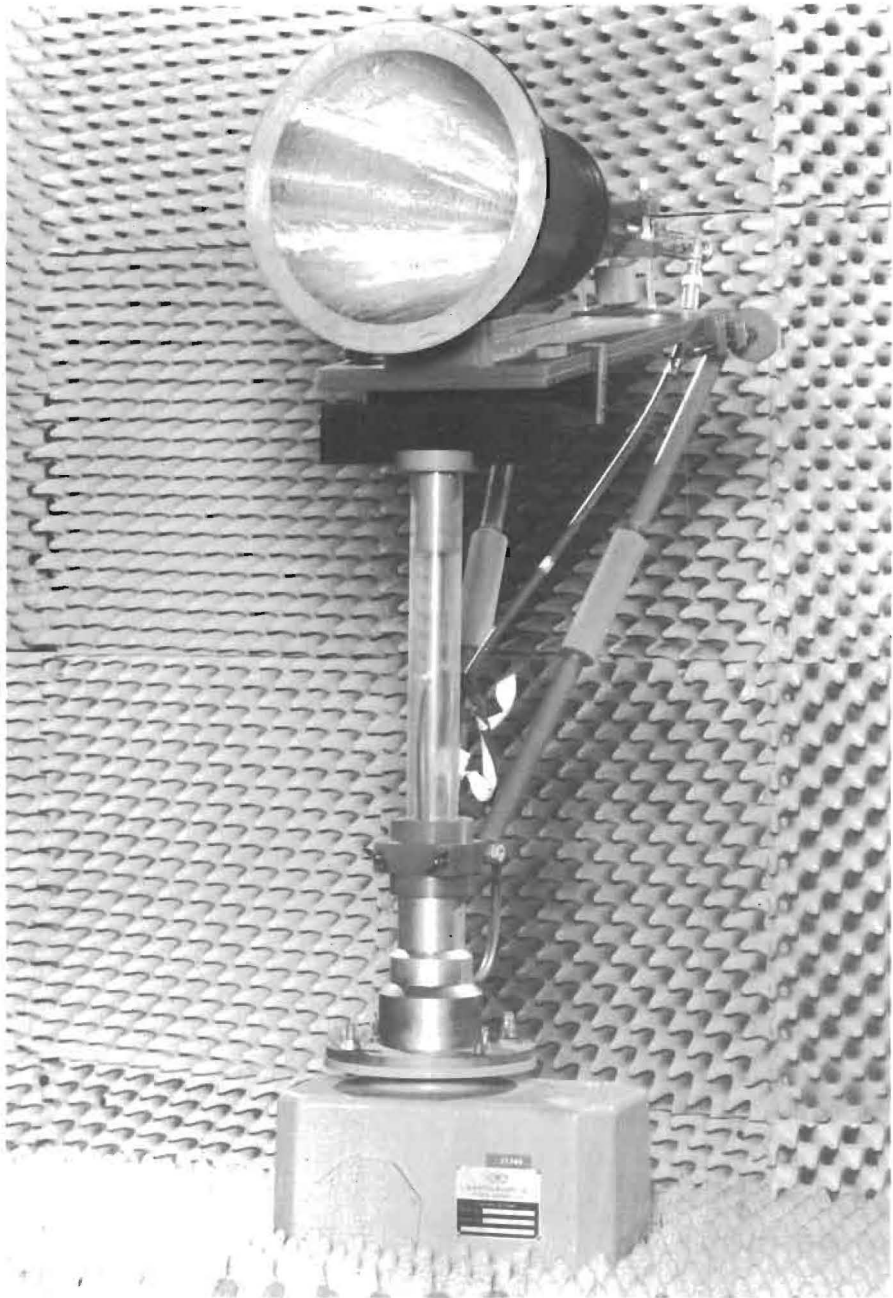
Photograph 3. Conical horn antenna of Fig. 2.15 mounted on a turntable in the anechoic chamber.
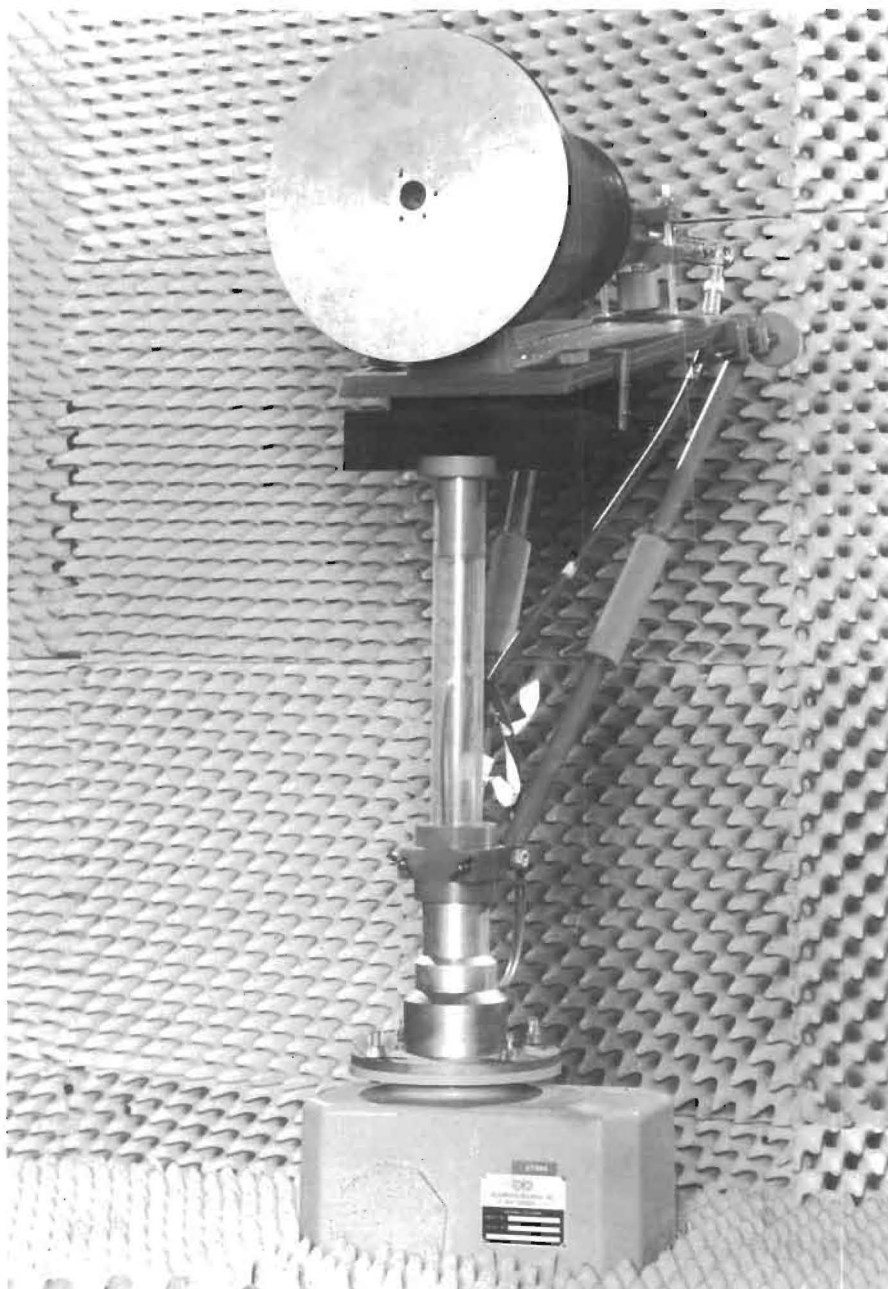
Photograph 4.   Conical horn antenna of Fig. 2.15 with plate mounted on a
turntable in the anechoic chamber.
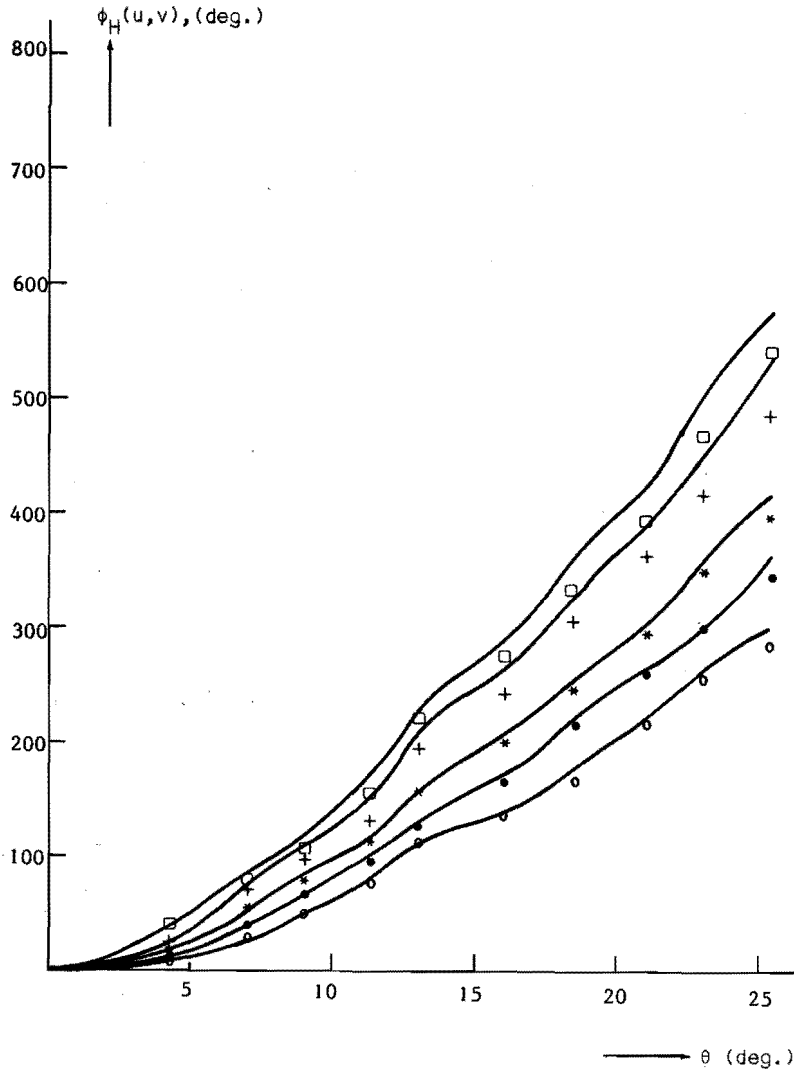
Fig. 2.30 Measured phase variations in H-plane of the antenna of Fig. 2.15
————, theoretical.

o $\frac{d}{\lambda}$ = 0.5000,   + $\frac{d}{\lambda}$ = 0.7500,

• $\frac{d}{\lambda}$ = 0.5625,   □ $\frac{d}{\lambda}$ = 0.8125.
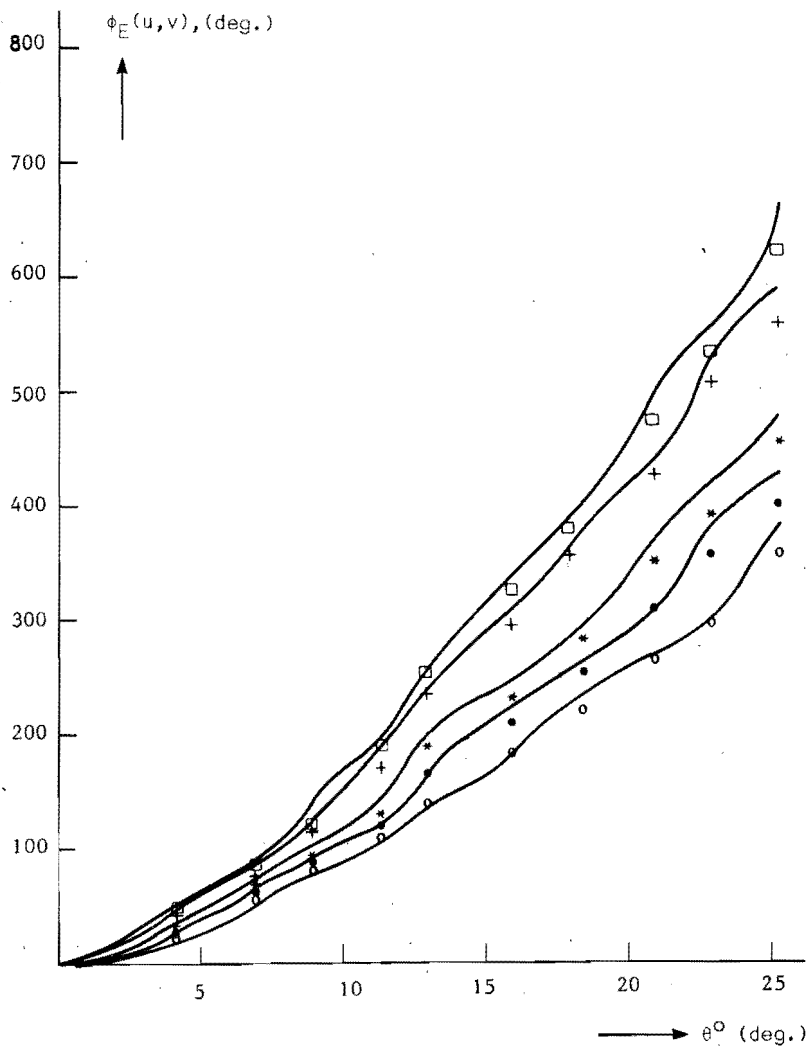
* $\frac{d}{\lambda}$ = 0.6250,

Fig. 2.31. Measured phase variations in E-plane of the antenna of Fig. 2.15
————, theoretical.

o $\frac{d}{\lambda}$ = 0.5000,   + $\frac{d}{\lambda}$ = 0.7500,

• $\frac{d}{\lambda}$ = 0.5625,   □ $\frac{d}{\lambda}$ = 0.8125.

* $\frac{d}{\lambda}$ = 0.6250,

The results of the measurements are collected in Fig. 2.30 and Fig. 2.31 for the H-plane and the E-plane respectively. Tabel II can be used for converting the d/λ values into frequencies.

Table II

d/λ	f [GHz]
0.5000	8.6
0.5625	9.7
0.6250	10.8
0.7500	12.9
0.8125	14.0

This table has been composed assuming that d = 17,4mm. From Fig. 2.30 and Fig. 2.31 the following conclusions and comments may be formulated:

(i)   the agreement between experimental results and theoretical pre-
        dictions is rather good for frequencies below 10.8 GHz,especially
        in the H-plane. In fact, the maximum deviation between theory and
        experimental results was less than 25°. The experimental results
        are slightly smaller than the theoretical predictions. An expla-
        nation of this deviation has not been found;

(ii)   the discrepancy between experimental and theoretical results at
        14 GHz might be caused by the excitation of the TM_{11}-mode;

(iii) the discrepancy between experimental and theoretical results at
        the higher frequencies might be also caused by the fact that the
        distance requirement (2.20) is not satisfied for frequencies
        above 10 GHz.

In conclusion we may say that the agreement between experimental re-
sults and theoretical predictions is rather good. So the diagrams of
Fig. 2.21 and Fig. 2.22 can indeed be used for determining the phase
efficiency of a paraboloid reflector antenna, illuminated by a fre-
quency-independent conical horn antenna.

CHAPTER 3

CONICAL HORN ANTENNAS WITH SYMMETRICAL RADIATION PATTERN

3.1 Circular aperture with a symmetrical radiation pattern.

In the sections 2.2 and 2.3 we have seen that the radiation pattern of
a conical horn antenna is not symmetrical with respect to the antenna-
axis. A second phenomenon that was observed is that there exist rather
high sidelobes in the E-plane. This implies that the conical horn an -
tenna of Fig. 2.15 is not very suitable as a feed in a cassegrain an -
tenna, as drawn schematically in Fig. 3.1. In order to prove this as -
sertion we have computed the fraction of the total energy which is ra-
diated within the cone angle θ for various values of θ.
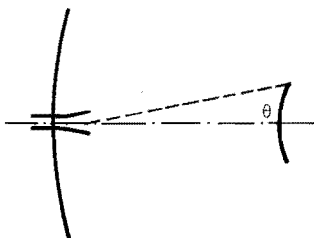
Fig. 3.1.   Diagram of cassegrain antenna.

The calculations have been performed for the frequency 8 GHz. The re -
sults are collected in Fig. 3.2. Together with Fig. 2.17 we may formu-
late the following conclusions. If the system is designed in such a way
that in the H-plane the edge illumination at the subreflector is 10 dB,
then only 63% of the energy is intercepted by the subreflector. If we
apply an edge illumination of 15 dB then 88% of the energy is inter -
cepted by the reflector. Finally we see that 91% of the energy will
reach the subreflector if the edge illumination is 20 dB.

This unfavourable situation is, of course, caused by the high sidelobes
in the E-plane. Therefore it would be desirable if a conical horn an-
tenna could be designed with a symmetrical radiation pattern which,for
instance, is identical with the radiation pattern in the H-plane of

75

Fig. 3.2   Fraction of the energy radiated within a cone-angle θ against θ.
           Antenna of Fig. 2.15.

the antenna of Fig. 2.15. Moreover, we recall that a feed for a para-
bolic reflector for radio-astronomical investigations should possess
a symmetrical radiation pattern as well. This is of importance if one
wishes to study the polarisation characteristics of radio sources. In
case of antennas for radio-astronomical investigations, however the
feed is placed at the focus of the paraboloid. Therefore, in this case,
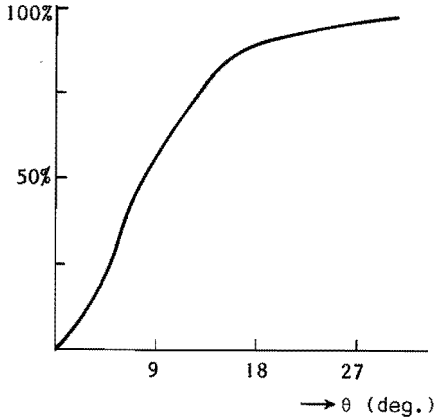a feed with a beamwidth larger than that of the antenna of Fig. 2.15
should be applied. So we see that it is necessary to have at our dis-
posal a theory concerning feeds with symmetrical radiation patterns.
In the remaining part of this section we shall develop a theory of
symmetrical radiation patterns of circular apertures. In the following
considerations use will be made of a special class of solutions of
Maxwell's equations. These solutions were discovered by Rumsey [47].

To introduce these solutions we observe that, if the equations
$\mathrm{curl}\ \underline{E}(\underline{r}) = -\,j\omega\mu_0\,\underline{H}(\underline{r})$ and $\mathrm{curl}\ \underline{H}(\underline{r}) = j\omega\varepsilon_0\,\underline{E}(\underline{r})$ possess   solutions
of the type $\underline{E}(\underline{r}) = C\underline{H}(\underline{r})$, then $C = \pm\,jZ_0$.

Substitution of the relation $\underline{E}(\underline{r}) = C\,\underline{H}(\underline{r})$ in each of the two Maxwell
equations shows immediately that $C = \pm\,jZ_0$. We shall denote these two
types of solution by $\underline{E}_\alpha(\underline{r})$ and $\underline{E}_\beta(\underline{r})$:

$$\underline{E}_\alpha(\underline{r}) = jZ_0\underline{H}_\alpha(\underline{r}) \quad \text{and} \quad \underline{E}_\beta(\underline{r}) = -\,jZ_0\underline{H}_\beta(\underline{r}) \tag{3.1}$$

It is very interesting to study Poynting's vector of this type of elec-

76

tromagnetic field. We find

$$\underline{S}_\alpha(\underline{r}) = \text{Re}(\underline{E}_\alpha(\underline{r})e^{j\omega t}) \times \text{Re}(\underline{H}_\alpha(\underline{r})e^{j\omega t}) = Z_o \underline{H}_{\alpha r} \times \underline{H}_{\alpha i} =$$

$$-\frac{1}{2j} Z_o \underline{H}_\alpha \times \underline{H}_\alpha^*. \qquad (3.2)$$

In expression (3.2) we have assumed that $\underline{H}_\alpha = \underline{H}_{\alpha r} + j \underline{H}_{\alpha i}$; so $\underline{H}_{\alpha r}$ and $\underline{H}_{\alpha i}$ represent the real and imaginary part of $\underline{H}_\alpha$. The asterisk denotes complex conjugate.

For the other solution we find

$$\underline{S}_\beta(\underline{r}) = -Z_o \underline{H}_{\beta r} \times \underline{H}_{\beta i} = -\frac{1}{2j} Z_o \underline{H}_\beta^* \times \underline{H}_\beta. \qquad (3.3)$$

We notice that S_α and S_β have the remarkable property that they are in-dependent of time.

The types of electromagnetic field as discussed above were first studied by Rumsey. Some other properties of these fields, which are not relevant to the present considerations, can be found in [47]. Especially elementary sources which generate the electromagnetic fields (3.1) is given. It is possible to find other sources of the electromagnetic fields (3.1). Therefore the following lemma has been formulated.
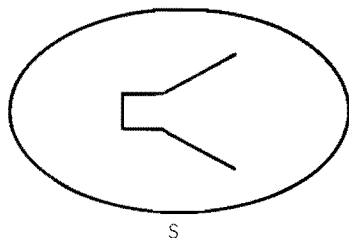
Fig. 3.3.   Antenna within closed surface S.

Lemma 1.

If the electric and magnetic fields on a closed surface S are related by the relation $\underline{E}(\underline{r}') = \pm jZ_o \underline{H}(\underline{r}')$ (Fig. 3.3), then the electric and magnetic fields in a point P are also related by $\underline{E}(\underline{r}) = \pm jZ_o \underline{H}(\underline{r})$.

Proof.   Substitution of $\underline{E}(\underline{r}') = \pm jZ_o \underline{H}(\underline{r}')$ in the expressions (2.4) and (2.5) immediately gives the result

$$\underline{E}(\underline{r}) = \pm jZ_o \underline{H}(\underline{r}).$$ (3.4)

In the next lemma we formulate a property of the radiation field of an antenna with aperture S_A (Fig. 2.2) and we assume that the tangential electric field and the tangential magnetic field are zero on the surface S_C.

Lemma 2.

If the electric and magnetic fields in an aperture S_A satisfy the relation $\underline{E}_\alpha(\underline{r}') = + jZ_o \underline{H}_\alpha(\underline{r}')$, then the electromagnetic field in the far field region is circularly polarised in every point. The sense of polarisation is counter-clockwise with respect to the direction of propagation.

Proof. From expression (2.19) we know that $\underline{a}_r \times \underline{E}_\alpha(\underline{r}) = Z_o \underline{H}_\alpha(\underline{r})$. Lemma 1 gives the relation $\underline{E}_\alpha(\underline{r}) = jZ_o \underline{H}_\alpha(\underline{r})$.

So $j\{\underline{a}_r \times \underline{E}_\alpha(\underline{r})\} = jZ_o \underline{H}_\alpha(\underline{r}) = \underline{E}_\alpha(\underline{r})$ and

$j \underline{a}_r \times \{E_{\alpha\theta} \underline{a}_\theta + E_{\alpha\phi} \underline{a}_\phi\} = E_{\alpha\theta} \underline{a}_\theta + E_{\alpha\phi} \underline{a}_\phi.$

And we see that

$$E_{\alpha\theta} = -j E_{\alpha\phi}$$ (3.5)

for every value θ and ϕ.

A similar property can be formulated for the electromagnetic field given by $E_\beta = -jZ_o H_\beta$.

If the electric and magnetic fields in the aperture S_A satisfy the relation $\underline{E}_\beta(\underline{r}') = -jZ_o \underline{H}_\beta(\underline{r}')$, then the electromagnetic field in the far field region is circularly polarised in every point. The sense of polarisation is clockwise with respect to the direction of propagation. The components of the electric field in the far field region are related by

$$E_{\beta\theta} = + j E_{\beta\phi}$$ (3.6)

In the following lemmas we shall restrict ourselves to a circular aperture S_A as defined in Fig. 2.4. Furthermore we assume a quadratic phase distribution across the aperture S_A.

Lemma 3

Let the electromagnetic fields in the aperture S_A be given by

$$\underline{E}_\alpha(\underline{r}') = + j\, Z_o \underline{H}_\alpha(\underline{r}') \quad \text{and}$$

$$\underline{E}_\alpha(\underline{r}') = \underline{e}_{\alpha 1}(r')\, e^{jn\phi'} \quad \text{with}$$

$$\underline{e}_{\alpha 1}(r') = \left\{ f_{\alpha 1}(r')\, \underline{a}_{r'} + g_{\alpha 1}(r')\, \underline{a}_{\phi'} \right\} e^{-jv\left(\frac{r}{a}\right)^2}; \tag{3.7}$$

$\underline{a}_{r'}$ and $\underline{a}_{\phi'}$ are the unit vectors in the circular aperture S_A.

Then the electromagnetic field in the far field region is given by:

$$E_{\alpha 1\theta} = -j\, E_{\alpha 1\phi} = F_{\alpha 1}(r,\theta)\, e^{jn\phi} \quad \text{with}$$

$$F_{\alpha 1}(r,\theta) = j^{n-1}\, \frac{jka^2}{4r}\, e^{-jkr} \times$$

$$\int_0^1 \left[\left\{ f_{\alpha 1}(\rho) - j\, g_{\alpha 1}(\rho)\, \cos\theta \right\} \times \left\{ J_{n-1}(u\rho) - J_{n+1}(u\rho) \right\} \right.$$
$$\left. -j\left\{ g_{\alpha 1}(\rho) + jf_{\alpha 1}(\rho)\, \cos\theta \right\}\left\{ J_{n-1}(u\rho) + J_{n+1}(u\rho) \right\} \right] e^{-jv\rho^2}\rho\, d\rho. \tag{3.8}$$

Proof.   From the substitution of the relations given in (3.7) in the expression (2.24) and using the relations

$$\int_0^{2\pi} e^{jn\phi'}\cos(\phi-\phi')e^{ju\rho\,\cos(\phi-\phi')}d\phi' = \pi j^{n-1}e^{jn\phi}\left\{ J_{n-1}(u\rho)-J_{n+1}(u\rho) \right\}$$

$$\int_0^{2\pi} e^{jn\phi'}\sin(\phi-\phi')e^{ju\rho\,\cos(\phi-\phi')}d\phi' = -j\pi j^{n-1}e^{jn\phi}\left\{ J_{n-1}(u\rho)+J_{n+1}(u\rho) \right\} \tag{3.9}$$

the result (3.8) follows immediately.

Although the next three lemmas are quite similar to lemma 3, we shall formulate them rather extensively. This method of working offers the opportunity to define all the quantities needed in the following argumentation.

Lemma 4.

Let the electromagnetic field in the aperture S_A be given by

$$\underline{E}_\alpha(\underline{r}') = jZ_0 \, \underline{H}_\alpha(\underline{r}') \qquad \text{and}$$

$$\underline{E}_\alpha(\underline{r}') = \underline{e}_{\alpha 2}(r') \, e^{-jn\phi'} \qquad \text{with} \tag{3.10}$$

$$\underline{e}_{\alpha 2}(r') = \left\{ f_{\alpha 2}(r') \, \underline{a}_{r'} + g_{\alpha 2}(r') \, \underline{a}_{\phi'} \right\} e^{-jv\left(\frac{r'}{a}\right)^2}.$$

Then the electromagnetic field in the far field region is given by

$$E_{\alpha 2\theta} = -j \, E_{\alpha 2\phi} = F_{\alpha 2}(r,\theta) \, e^{-jn\phi} \qquad \text{with}$$

$$F_{\alpha 2}(r,\theta) = j^{n-1} \, \frac{jka^2}{4r} \, e^{-jkr} \times$$

$$\int_0^1 \left[\left\{ f_{\alpha 2}(\rho) - j \, g_{\alpha 2}(\rho) \cos\theta \right\} \times \left\{ J_{n-1}(u\rho) - J_{n+1}(u\rho) \right\} \right.$$

$$\left. + j \left\{ g_{\alpha 2}(\rho) + j \, f_{\alpha 2}(\rho) \cos\theta \right\} \left\{ \left(J_{n-1}(u\rho) + J_{n+1}(u\rho) \right) \right\} \right] e^{-jv\rho^2} \rho \, d\rho. \tag{3.11}$$

Proof. From the substitution of the relations given in (3.10) in the expression (2.24) and using the relations

$$\int_0^{2\pi} e^{-jn\phi'} \cos(\phi-\phi') e^{ju\rho \cos(\phi-\phi')} d\phi' = \pi \, j^{n-1} e^{-jn\phi} \left\{ J_{n-1}(u\rho) - J_{n+1}(u\rho) \right\}$$

$$\int_0^{2\pi} e^{-jn\phi'} \sin(\phi-\phi') e^{ju\rho \cos(\phi-\phi')} d\phi' = j\pi \, j^{n-1} e^{-jn\phi} \left\{ J_{n-1}(u\rho) + J_{n+1}(u\rho) \right\} \tag{3.12}$$

the result (3.11) follows immediately.

The next two lemmas are given without proof.

Lemma 5.

Let the electromagnetic fields in the aperture S_A be given by

$$\underline{E}_\beta(\underline{r}') = - \, jZ_0 \underline{H}_\beta(\underline{r}') \qquad \text{and}$$

$$\underline{E}_\beta(\underline{r}') = \underline{e}_{\beta 1}(r') \, e^{jn\phi'} \qquad \text{with} \tag{3.13}$$

$$\underline{e}_{\beta 1}(r') = \left\{ f_{\beta 1}(r') \, \underline{a}_{r'} + g_{\beta 1}(r') \, \underline{a}_{\phi'} \right\} e^{-jv\left(\frac{r'}{a}\right)^2}.$$

Then the electromagnetic field in the far field region is given by

$$E_{\beta 1\theta} = j\,E_{\beta 1\phi} = F_{\beta 1}(r,\theta)\,e^{jn\phi} \quad \text{with}$$

$$F_{\beta 1}(r,\theta) = j^{n-1}\,\frac{jka^2}{4r}\,e^{-jkr}\int_0^1 \left[\{f_{\beta 1}(\rho)+jg_{\beta 1}(\rho)\cos\theta\}\{J_{n-1}(u\rho)-J_{n+1}(u\rho)\}\right.$$

$$\left.-j\{g_{\beta 1}(\rho)-jf_{\beta 1}(\rho)\cos\theta\}\{J_{n-1}(u\rho)+J_{n+1}(u\rho)\}\right]\,e^{-jv\rho^2}\rho\,d\rho. \qquad (3.14)$$

Lemma 6.

Let the electromagnetic fields in the aperture S_A be given by

$$\underline{E}_\beta(\underline{r}') = -j\,Z_o\underline{H}_\beta(\underline{r}') \qquad \text{and}$$

$$\underline{E}_\beta(\underline{r}') = \underline{e}_{\beta 2}(r')\,e^{-jn\phi'} \quad \text{with} \qquad (3.15)$$

$$\underline{e}_{\beta 2}(r') = \left\{f_{\beta 2}(r')\,\underline{a}_{r'} + g_{\beta 2}(r')\,\underline{a}_{\phi'}\right\}\,e^{-jv\left(\frac{r}{a}\right)^2}.$$

Then the electromagnetic field in the far field region is represented
by

$$E_{\beta 2\theta} = +jE_{\beta 2\phi} = F_{\beta 2}(r,\theta)\,e^{-jn\phi}$$

$$F_{\beta 2}(r,\theta) = j^{n-1}\,\frac{jka^2}{4r}\,e^{-jkr}\int_0^1 \left[\{f_{\beta 2}(\rho)+jg_{\beta 2}(\rho)\cos\theta\}\{J_{n-1}(u\rho)-J_{n+1}(u\rho)\}\right.$$

$$\left.+j\{g_{\beta 2}(\rho)-jf_{\beta 2}(\rho)\cos\theta\}\{J_{n-1}(u\rho)+J_{n+1}(u\rho)\}\right]\,e^{-jv\rho^2}\rho\,d\rho\,. \qquad (3.16)$$

Next we formulate a property of the power radiation pattern of an aperture S_A with aperture fields as specified in lemma 3.

Let the electromagnetic fields in the aperture S_A be given by

$$\underline{E}_\alpha(\underline{r}') = j\,Z_o\underline{H}_\alpha(\underline{r}') \quad \text{and}$$

$$\underline{E}_\alpha(\underline{r}') = \underline{e}_{\alpha 1}(r')\,e^{jn\phi'}. \qquad (3.7)$$

Then in the far field region Poynting's vector is

$$\underline{S}(\underline{r}) = Z_o^{-1}\,|F_{\alpha 1}(r,\theta)|^2\,\underline{a}_r\,. \qquad (3.17)$$

From the lemmas 2 and 3 we know that

$$Z_0 \underline{H}_\alpha(\underline{r}) = -j\, \underline{E}_\alpha(\underline{r}) = -j\, (\underline{a}_\theta + j\, \underline{a}_\phi)\, F_{\alpha 1}(r,\theta)\, e^{jn\phi}.$$

Applying formula (3.2) we find

$$\underline{S}(\underline{r}) = Z_0\, \frac{1}{2j}\, \left(\underline{H}_\alpha^* \times \underline{H}_\alpha\right) =$$

$$Z_0^{-1}\, \frac{1}{2j}\, |F_{\alpha 1}(r,\theta)|^2\, \{(\underline{a}_\theta - j\underline{a}_\phi) \times (\underline{a}_\theta + j\, \underline{a}_\phi)\} =$$

$$Z_0^{-1}\, |F_{\alpha 1}(r,\theta)|^2 \underline{a}_r.$$

So we see that the aperture fields as specified in (3.7) give rise to a radiation field with the property that the power radiation pattern is symmetrical with respect to the antenna-axis. This is not a remarkable property, because it can be proved that a circular aperture with an electromagnetic field of the type $e^{+jn\phi'}$ gives rise to a symmetrical power radiation pattern. The precise form of the power radiation pattern depends of course on the vector function $\underline{e}_{\alpha 1}(r')$.

However, one general property of the function $F_{\alpha 1}(r,\theta)$ can be derived quite easily. Using the property of the Bessel function that $J_n(0) = 0$ with the exception that $J_0(0) = 1$, we see that $F_{\alpha 1}(r,\theta)$ is zero for $\theta = 0$ if $n \neq 1$. Therefore we conclude that especially the case $n = 1$ is of practical importance. It should be noted, however, that antennas with a radiation pattern which has a zero in the forward direction are sometimes used for autotracking purposes [48], [49]. But the study of these antennas is beyond the scope of the present study.

Finally, it is obvious that the aperture fields of the lemmas 4,5 and 6 give rise to symmetrical power radiation patterns as well.

So far we have formulated properties of radiation fields which are circularly polarised in every point, and we have introduced aperture fields which can generate them. With these types of electromagnetic field one can compose also radiation fields with a symmetrical power radiation pattern, but which are linearly polarised. In fact, it is well-known that a linearly polarised plane wave can be decomposed into two circularly polarised plane waves, one of them with clockwise polarisation, the other with counter-clockwise polarisation. On the other

82

hand, one can find a linearly polarised plane wave as a superposition of two circularly polarised plane waves, one of them with clockwise polarisation, the other with counter-clockwise polarisation. We shall use this idea to construct radiation fields which are linearly polarised and possess symmetrical power radiation patterns. Moreover, we shall derive the aperture fields, which can generate them.

Theorem 1.

A superposition of the radiation fields as specified in the lemmas 3 and 6 produces a radiation field which is linearly polarised, provided we choose

$$f_{\alpha 1}(r') = f_{\beta 2}(r') \text{ and}$$

$$g_{\alpha 1}(r') = -g_{\beta 2}(r').$$

Moreover, the power radiation pattern is symmetrical with respect to the antenna – axis. The aperture fields which can generate this electromagnetic field are represented by

$$E'_r = 2f_{\alpha 1}(\rho) \cos n\phi' \ e^{-jv\rho^2},$$

$$E'_\phi = 2j \ g_{\alpha 1}(\rho) \sin n\phi' \ e^{-jv\rho^2},$$

$$Z_o H'_r = 2f_{\alpha 1}(\rho) \sin n\phi' \ e^{-jv\rho^2}, \qquad (3.18)$$

$$Z_o H'_\phi = -2j \ g_{\alpha 1}(\rho) \cos n\phi' \ e^{-jv\rho^2} \text{ with}$$

$$\rho = r'/a .$$

Proof.   From the lemmas 3 and 6 we know that

$$E_{\alpha 1\theta} = e^{jn\phi} F_{\alpha 1}(r,\theta) \quad \text{and} \quad E_{\alpha 1\phi} = jE_{\alpha 1\theta}.$$

$$E_{\beta 2\theta} = e^{-jn\phi} F_{\beta 2}(r,\theta) \quad \text{and} \quad E_{\beta 2\phi} = -jE_{\beta 2\theta}.$$

With the choice $f_{\alpha 1}(r') = f_{\beta 2}(r')$ and $g_{\alpha 1}(r') = -g_{\beta 2}(r')$ we see that $F_{\alpha 1}(r,\theta) = F_{\beta 2}(r,\theta)$.

The sum of the two fields is now given by

$$E_\theta = E_{\alpha 1\theta} + E_{\beta 2\theta} = 2F_{\alpha 1}(r,\theta) \cos n\phi \quad \text{and}$$

$$E_\phi = E_{\alpha 1\phi} + E_{\beta 2\phi} = -2F_{\alpha 1}(r,\theta) \sin n\phi. \qquad (3.19)$$

So the phase-difference between the two components of the electric field is 0 or π, which means that the electromagnetic field is linearly polarised.

The magnetic field can be found from (3.19) with the relation

$$Z_o \underline{H}(\underline{r}) = \underline{a}_r \times \underline{E}(\underline{r}).\qquad(2.19)$$

Then we find for the time-average of Poynting's vector

$$\overline{\underline{S(\underline{r},t)}}^\dagger = \tfrac{1}{2}\mathrm{Re}\left(\underline{E} \times \underline{H}^*\right) = \tfrac{1}{2}Z_o^{-1}\left(|E_\theta|^2 + |E_\phi|^2\right)\underline{a}_r = 2Z_o^{-1}\,|F_{\alpha 1}(r,\theta)|^2 \underline{a}_r,$$

which is independent of the angle ϕ. Thus the power radiation pattern is symmetrical with respect to the antenna-axis. The aperture fields, which give rise to the radiation field as specified in (3.19), can be found by summing up the aperture fields as specified in lemma 3 and 6. We then find

$$E_r' = \left\{ f_{\alpha 1}(\rho)e^{+jn\phi'} + f_{\beta 2}(\rho)e^{-jn\phi'}\right\}e^{-jv\rho^2} = 2f_{\alpha 1}(\rho)\cos n\phi'\,e^{-jv\rho^2},$$

$$E_\phi' = \left\{ g_{\alpha 1}(\rho)e^{+jn\phi'} + g_{\beta 2}(\rho)e^{-jn\phi'}\right\}e^{-jv\rho^2} = 2j\dot{g}_{\alpha 1}(\rho)\sin n\phi'\,e^{-jv\rho^2},$$

$$Z_oH_r' = \left\{ -jf_{\alpha 1}(\rho)e^{+jn\phi'} + jf_{\beta 2}(\rho)e^{-jn\phi'}\right\}e^{-jv\rho^2} = 2f_{\alpha 1}(\rho)\sin n\phi'\,e^{-jv\rho^2},$$

$$Z_oH_\phi' = \left\{ -jg_{\alpha 1}(\rho)e^{+jn\phi'} + jg_{\beta 2}(\rho)e^{-jn\phi'}\right\}e^{-jv\rho^2} = -2jg_{\alpha 1}(\rho)\cos n\phi'e^{-jv\rho^2}.$$

which completes the proof.

From the electromagnetic fields as discussed in lemma 3 and 6 we can find a radiation field similar to the one of theorem 1. The only difference is that we have to assume

$$f_{\alpha 1}(r') = -f_{\beta 2}(r') \qquad g_{\alpha 1}(r') = g_{\beta 2}(r').$$

However, on closer examination we see that these fields are the same as those of theorem 1, apart from a rotation in ϕ (and ϕ') over $\frac{\pi}{2n}$.

Combining the electromagnetic fields of lemma 4 and 5 we can formulate a theorem similar to theorem 1. We shall state it without proof.

Theorem 2.

Superposition of the radiation fields as specified in lemma 4 and 5 produces a radiation field which is linearly polarised, provided we choose

$$f_{\alpha 2}(r') = f_{\beta 1}(r') \text{ and}$$

$$g_{\alpha 2}(r') = -g_{\beta 1}(r') \; .$$

Moreover, the power radiation pattern is symmetrical with respect to the antenna-axis. The aperture fields, which generate this electromagnetic field are given by

$$E'_r = 2 \, f_{\alpha 2}(\rho) \cos n\phi' \; e^{-j\nu\rho^2},$$

$$E'_\phi = -2jg_{\alpha 2}(\rho) \sin n\phi' \; e^{-j\nu\rho^2},$$

$$Z_o H'_r = -2 \, f_{\alpha 2}(\rho) \sin n\phi' \; e^{-j\nu\rho^2},$$ (3.20)

$$Z_o H'_\phi = -2jg_{\alpha 2}(\rho) \cos n\phi' \; e^{-j\nu\rho^2}.$$

It should be noted that the aperture fields of (3.18) and (3.20) are indeed of a different type. So, in general, they will give rise to a different power radiation pattern in the two cases.
The choice

$$f_{\alpha 2}(r') = - f_{\beta 1}(r') \quad \text{and}$$

$$g_{\alpha 2}(r') = g_{\beta 1}(r')$$

leads to a symmetrical power radiation pattern as well. However, this pattern is the same as specified in theorem 2, apart from a rotation over ϕ (and ϕ') of $\dfrac{\pi}{2n}$.

At this point of the considerations it is useful to return to the beginning of this section. There we have stated that there is a need for symmetrical power radiation patterns, which are of the same form as, for instance, the H-plane pattern of the antenna of Fig. 2.15. Up till now we have only developed a theory of symmetrical power radiation patterns. These patterns are the same form as the H-plane pattern of the antenna of Fig. 2.15 provided the corresponding functions $\underline{e}_{\alpha 1,2}$ and $\underline{e}_{\beta 1,2}$ can be found. So the question is now to find a structure, for instance a circular waveguide, which guides waves of the type as

discussed in the theorems 1 and 2. This problem will be discussed in
the sections 3.2 and 3.4. In section 3.3 we shall investigate the
power radiation patterns in more detail.

3.2 Propagation_of_waves_in_a_circular_cylindrical_waveguide_with anisotropic_boundary.

In the formulae (3.18) and (3.20) we have specified the electromagnetic
fields in a circular aperture, which produce a symmetrical radiation
pattern. The next task is to investigate , how these aperture fields
can be generated. Because we are dealing with a circular aperture it
is but natural to try to generate these electromagnetic fields in a
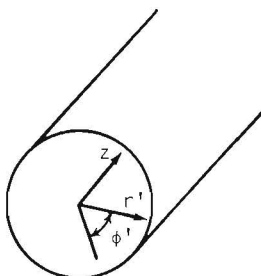circular waveguide (Fig. 3.4).

Fig. 3.4.   Circular waveguide.

Therefore we investigate whether modes with a transverse electric
field and a transverse magnetic field as specified in (3.18) and
(3.20) with v = 0 can exist in a circular waveguide with a perfectly
conducting boundary. We know that in such a waveguide the tangential
electric field is zero at the boundary. But then the normal component
of the magnetic field is also zero [50]. The expressions (3.18) and
(3.20) prescribe that in that case the normal component of the elec-
trical field should be zero as well, provided n ≠ 0. Using [50] again
we see that the tangential component of the magnetic field is also zero
at the boundary. This implies that there are no currents in the wave-
guide wall. So it is impossible to generate the electromagnetic fields

of (3.18) and (3.20) in a circular waveguide with a perfectly conducting
boundary, even if we use a sum of TE-modes and TM-modes instead of one
mode.

Suppose that we wish to design a circular waveguide in which modes can
exist with a transverse electric field and a transverse magnetic field
as specified in (3.18) and (3.20) with $v = 0$. From the divergence
equations we derive that these modes have E_z' and H_z' components, which
in general are unequal zero. Next we shall prove that these modes can
exist in a circular waveguide with a very special anisotropic boundary.
This boundary is characterized by the conditions

$$E_z' = Z_z H_\phi'$$

$$E_\phi' = Z_\phi H_z' .$$

(3.21)

We assume that the real parts of Z_z and Z_ϕ are zero. In that case we
are sure that the time-average power flow in the radial direction is
zero.

So $Z_z = j X_z$ and

$$Z_\phi = j X_\phi ,$$

(3.22)

X_ϕ and X_z are the circumferential and longitudinal surface reactances
respectively. The question of the realisation of this surface reactance
will be discussed in one of the forthcoming sections. The electromag-
netic field in a waveguide with an anisotropic boundary, defined by the
equations (3.21) and (3.22), is the sum of a TE field and a TM field,
because there exist an H_z' and an E_z' at the boundary. This type of field
is called a hybrid field.

Suppose that the TE field has a generating function [51]

$$\psi_1(r',\phi',z) = A_1 J_n(k_c r') \sin n\phi' e^{-\gamma z},$$

(3.23)

the TM field being generated by

$$\psi_2(r',\phi',z) = A_2 J_n(k_c r') \cos n\phi' e^{-\gamma z},$$

(3.24)

with $k_c^2 = k^2 + \gamma^2$.

Then we can derive the components of the electromagnetic field of a
TE field by means of the following expressions [52]

$$E'_r = -\frac{1}{r'} \frac{\partial \psi_1}{\partial \phi'}, \qquad H'_r = \frac{1}{j\omega\mu_o} \frac{\partial^2 \psi_1}{\partial r' \partial z},$$

$$E'_\phi = \frac{\partial \psi_1}{\partial r'}, \qquad H'_\phi = \frac{1}{j\omega\mu_o} \frac{1}{r'} \frac{\partial^2 \psi_1}{\partial \phi' \partial z}, \qquad (3.25)$$

$$E'_z = 0, \qquad H'_z = \frac{1}{j\omega\mu_o} \left(\frac{\partial^2}{\partial z^2} + k^2 \right) \psi_1.$$

For a TM field we find

$$E'_r = \frac{1}{j\omega\varepsilon_o} \frac{\partial^2 \psi_2}{\partial r' \partial z}, \qquad H'_r = \frac{1}{r'} \frac{\partial \psi_2}{\partial \phi'},$$

$$E'_\phi = \frac{1}{j\omega\varepsilon_o} \frac{1}{r'} \frac{\partial^2 \psi_2}{\partial \phi' \partial z}, \qquad H'_\phi = -\frac{\partial \psi_2}{\partial r'}, \qquad (3.26)$$

$$E'_z = \frac{1}{j\omega\varepsilon_o} \left(\frac{\partial^2}{\partial z^2} + k^2 \right) \psi_2, \qquad H'_z = 0.$$

Then we find for the electromagnetic field in the waveguide

$$E'_r = \left\{ \frac{-n}{r'} A_1 J_n(k_c r') - \frac{\gamma}{j\omega\varepsilon_o} A_2 J'_n(k_c r') (k^2 + \gamma^2)^{\frac{1}{2}} \right\} \cos n\phi', \qquad (3.27)$$

$$E'_\phi = \left\{ A_1 J'_n(k_c r') (k^2 + \gamma^2)^{\frac{1}{2}} + \frac{\gamma}{j\omega\varepsilon_o} A_2 \frac{n}{r'} J_n(k_c r') \right\} \sin n\phi', \qquad (3.28)$$

$$Z_o H'_r = \left\{ \frac{-\gamma}{jk} A_1 J'_n(k_c r') (k^2 + \gamma^2)^{\frac{1}{2}} - Z_o A_2 \frac{n}{r'} J_n(k_c r') \right\} \sin n\phi', \qquad (3.29)$$

$$Z_o H'_\phi = \left\{ \frac{-\gamma}{jk} A_1 \frac{n}{r'} J_n(k_c r') - Z_o A_2 J'_n(k_c r') (k^2 + \gamma^2)^{\frac{1}{2}} \right\} \cos n\phi', \qquad (3.30)$$

$$E'_z = \frac{\gamma^2 + k^2}{j\omega\varepsilon_o} A_2 J_n(k_c r') \cos n\phi', \qquad (3.31)$$

$$H'_z = \frac{\gamma^2 + k^2}{j\omega\mu_o} A_1 J_n(k_c r') \sin n\phi'. \qquad (3.32)$$

The prime in $J'_n(k_c r')$ means differentiating with respect to $k_c r'$. In the expressions (3.27) to (3.32) incl. we have omitted the common factor $e^{-\gamma z}$.

By inspection it may be shown that these expressions are of the same type as (3.18) provided

$$A_1 = Z_o A_2. \qquad (3.33)$$

The choice

$$A_1 = -Z_o A_2 \qquad (3.34)$$

88

gives rise to expressions which are the same as specified in (3.20).
Obviously, the relations (3.33) and (3.34) yield a restriction for the
value of Z_ϕ and Z_z. This restriction may be found by applying the
boundary conditions (3.21).
We find

$$\frac{k^2+\gamma^2}{j\omega\varepsilon_o} A_2 J_n(k_c a) = Z_z \left\{ \frac{-\gamma}{j\omega\mu_o} \frac{n}{a} A_1 J_n(k_c a) - A_2 J_n'(k_c a) (k^2+\gamma^2)^{\frac{1}{2}} \right\} \quad (3.35)$$

and

$$Z_\phi \frac{k^2+\gamma^2}{j\omega\mu_o} A_1 J_n(k_c a) = A_1 J_n'(k_c a) (k^2+\gamma^2)^{\frac{1}{2}} + \frac{\gamma}{j\omega\varepsilon_o} \frac{n}{a} A_2 J_n(k_c a), \quad (3.36)$$

a being the radius of the waveguide. Substitution of $A_1 = \pm Z_o A_2$ in
(3.35) and (3.36) gives

$$Z_z Z_\phi + Z_o^2 = 0. \quad (3.37)$$

This relation has been derived also in [15] using a completely diffe-
rent approach.

For the case $A_1 = Z_o A_2$ we derive the dispersion equation from (3.36).
The result is

$$\left\{ Z_\phi \frac{(k^2+\gamma^2)^{\frac{1}{2}}}{j\omega\mu_o} - \frac{\gamma}{jk} \frac{n}{k_c a} + \frac{n}{k_c a} \right\} J_n(k_c a) = J_{n-1}(k_c a) , \quad (3.38)$$

where use has been made of the second recurrence relation of (2.63). In
case $A_1 = -Z_o A_2$ we find

$$\left\{ Z_\phi \frac{(k^2+\gamma^2)^{\frac{1}{2}}}{j\omega\mu_o} + \frac{\gamma}{jk} \frac{n}{k_c a} + \frac{n}{k_c a} \right\} J_n(k_c a) = J_{n-1}(k_c a). \quad (3.39)$$

In the preceding section we have pointed out that the case $n = 1$ is of
practical significance. Therefore, we shall restrict ourselves in the
following considerations to the case $n = 1$. In the section 3.4 we shall
discuss how a circular waveguide with the boundary conditions as spe-
cified in (3.21) can be realised. We shall then see that a physical
realisation is possible for the case $Z_\phi = 0$ and $Z_z = \infty$. So in the re-
maining part of this section we shall assume that $Z_\phi = 0$ and $Z_z = \infty$,
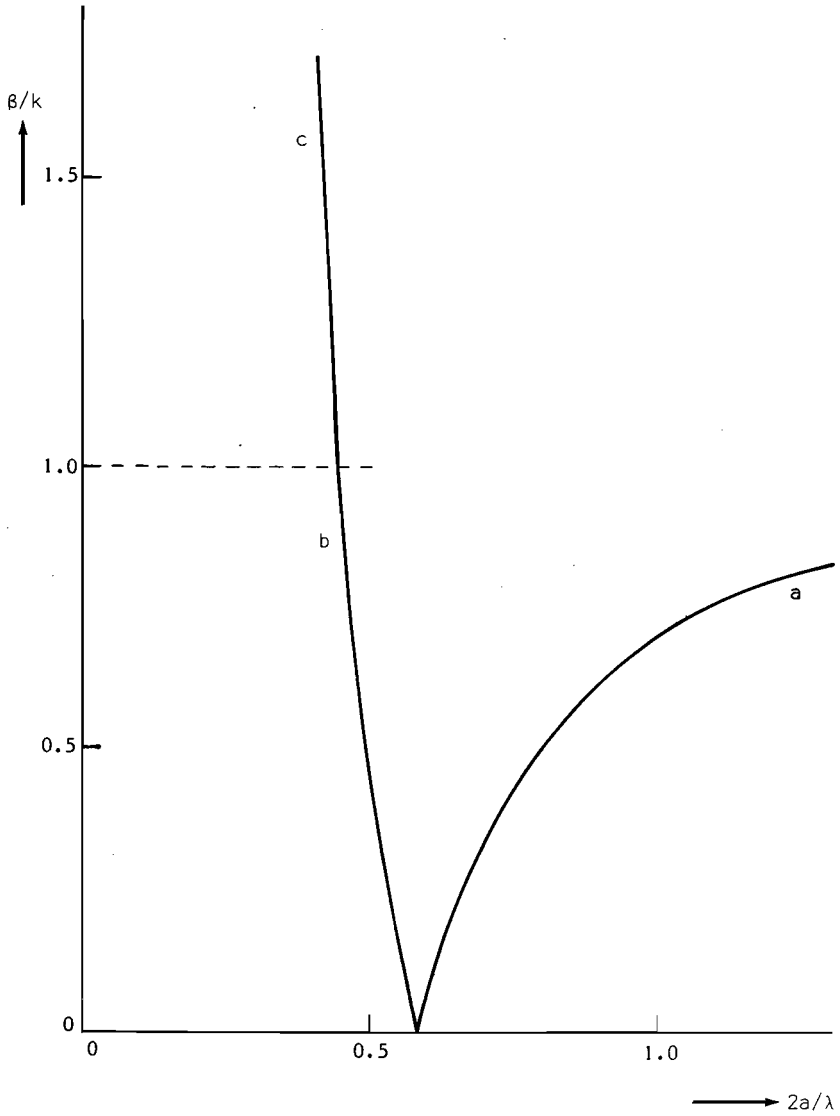which is in agreement with (3.37). Now the dispersion equations reduce
to the form

Fig. 3.5. β/k against $2a/\lambda$ for circular waveguide with anisotropic boundary:

a: $HE_{11}^{(1)}$-mode,

b: fast $HE_{11}^{(2)}$-mode,

c: slow $HE_{11}^{(2)}$-mode.

90

$$\left(1 \pm \frac{\gamma}{jk}\right) \frac{1}{k_c a} J_1(k_c a) = J_0(k_c a) . \qquad (3.40)$$

For a propagating mode we have $\gamma = j\beta$. The dispersion equation (3.40) gives the value of β/k for a prescribed value of ka.

Let us now consider the solutions of equation (3.40). The $\beta/k-$ versus $2a/\lambda$ curve of this equation has been plotted in Fig. 3.5.
We see that the curve has two branches with one common point. The branch marked with the symbol a is related to the solution with $A_1 = Z_0 A_2$ wheras the other branch, marked b is related to the solution with $A_1 = -Z_0 A_2$. We shall call the mode associated with the branch a the $HE_{11}^{(1)}$-mode. The other mode is the $HE_{11}^{(2)}$-mode.

The common point can be found by putting $\beta/k = 0$ in equation (3.40). The result is

$$\frac{1}{ka} J_1(ka) = J_0(ka) \text{ or}$$

$$\qquad\qquad (3.41)$$

$$J_1'(ka) = 0$$

The first root of this equation is ka = 1.841 or $2a/\lambda = 0.58$. The condition (3.41) is exactly the same as the one which gives the cut-off frequency of the TE_{11}-mode in a perfectly conducting waveguide with radius a. The second root of (3.41) is ka = 5.331 or $2a/\lambda = 1.69$ and gives the cut-off frequency of a higher hybrid mode.

Let us now investigate the transverse electric field of the $HE_{11}^{(1)}$-mode. For this mode we have $A_1 = Z_0 A_2$ and the components E_r' and E_ϕ' can be found in the following way.

$$E_r' = - A_2 Z_0 (k^2-\beta^2)^{\frac{1}{2}} \left\{ \frac{1}{k_c r'} J_1(k_c r') + \frac{\beta}{k} J_1'(k_c r') \right\} \cos \phi'$$

$$= - \tfrac{1}{2} A_2 Z_0 (k^2-\beta^2)^{\frac{1}{2}} \left[\{ J_0(k_c r')+J_2(k_c r') \} + \frac{\beta}{k} \{ J_0(k_c r')-J_2(k_c r') \} \right] \cos\phi'$$

$$= - \tfrac{1}{2} A_2 Z_0 (k^2-\beta^2)^{\frac{1}{2}} \left\{ \left(1 + \frac{\beta}{k}\right) J_0(k_c r') + \left(1 - \frac{\beta}{k}\right) J_2(k_c r') \right\} \cos \phi'$$

$$\equiv - \tfrac{1}{2} A_2 Z_0 (k^2-\beta^2)^{\frac{1}{2}} \left(1 + \frac{\beta}{k}\right) f_1(k_c r') \cos \phi'. \qquad (3.42)$$

91

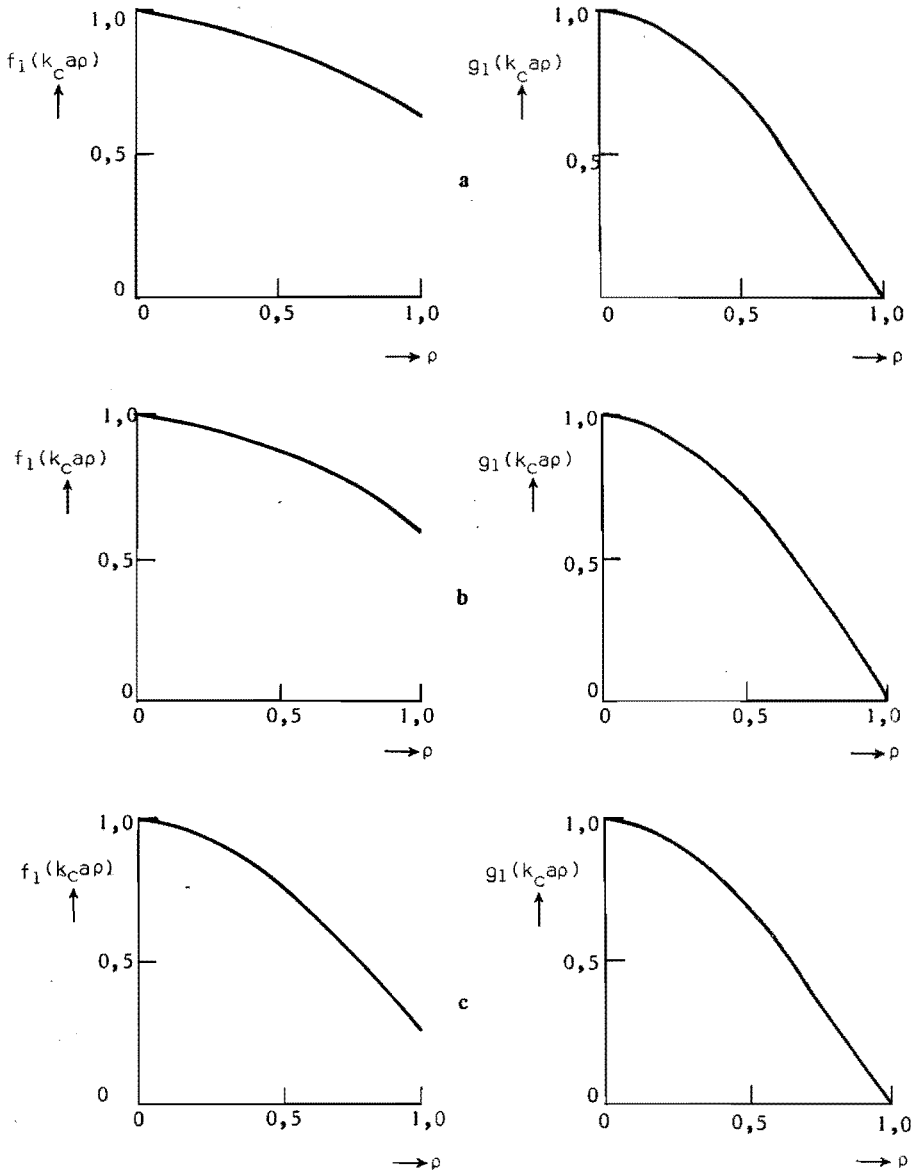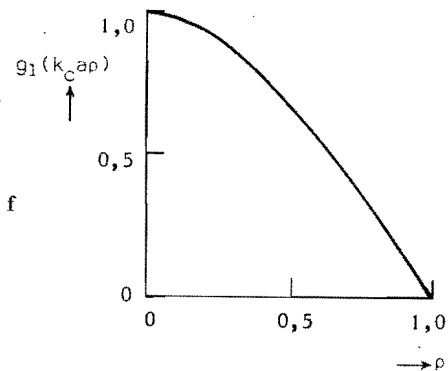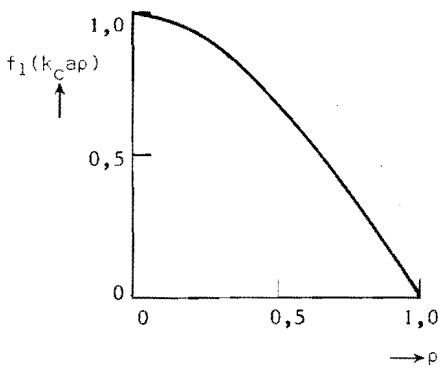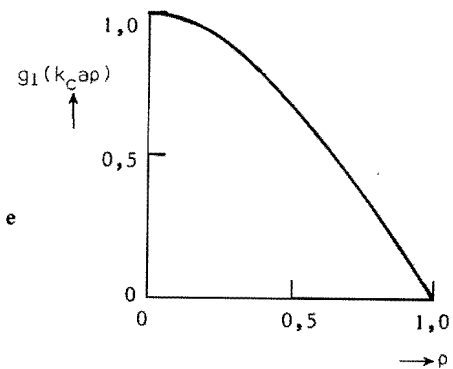Fig. 3.6.   The functions $f_1(k_c a\rho)$ and $g_1(k_c a\rho)$ against ρ.

a: TE_{11}-mode of perfectly conducting waveguide.
$HE_{11}^{(1)}$-mode,

b: $2a/\lambda = 0.6$;   c: $\dfrac{2a}{\lambda} = 0.8$;

$$\mathbf{d}: \frac{2a}{\lambda} = 1.0$$

$$\mathbf{e}: 2a/\lambda = 1.4; \quad \mathbf{f}: 2a/\lambda = 1.8.$$

93
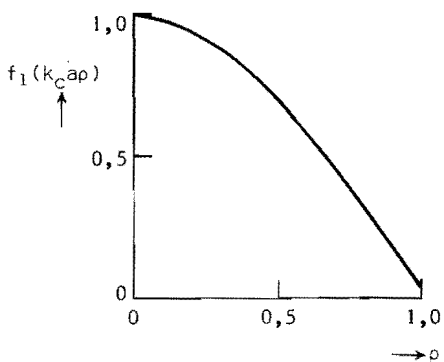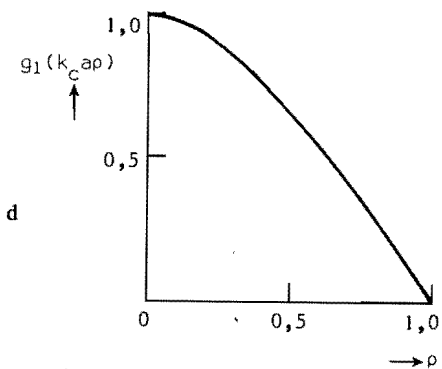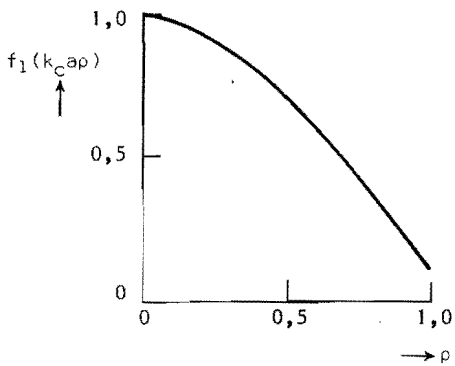
In (3.42) use has been made of the formulae (2.63).
In a similar way we find

$$E'_\phi = \tfrac{1}{2} A_2 Z_0 (k^2-\beta^2)^{\tfrac{1}{2}} \left\{ \left(1 + \tfrac{\beta}{k}\right) J_0(k_c r') - \left(1 - \tfrac{\beta}{k}\right) J_2(k_c r') \right\} \sin \phi'$$

$$\equiv \tfrac{1}{2} A_2 Z_0 (k^2-\beta^2)^{\tfrac{1}{2}} \left(1 + \tfrac{\beta}{k}\right) g_1(k_c r') \sin \phi'. \qquad (3.43)$$

The functions $f_1(k_c r')$ and $g_1(k_c r')$ are plotted in Fig.3.6 for several
values of $2a/\lambda$. In Fig.3.6a we have plotted the corresponding functions
of the TE_{11}-mode in a perfectly conducting waveguide. From these figures
two conclusions can be drawn.

(i) For increasing values of $2a/\lambda$ we observe that the function $g_1(k_c r')$
undergoes only a minor change, whereas the function $f_1(k_c r')$
changes drastically.

(ii) For a frequency at which $2a/\lambda = 0.6$ we see that the components of
the electromagnetic field of the $HE_{11}^{(1)}$-mode are virtually the same
as of the TE_{11}-mode.

Fig. 3.7.
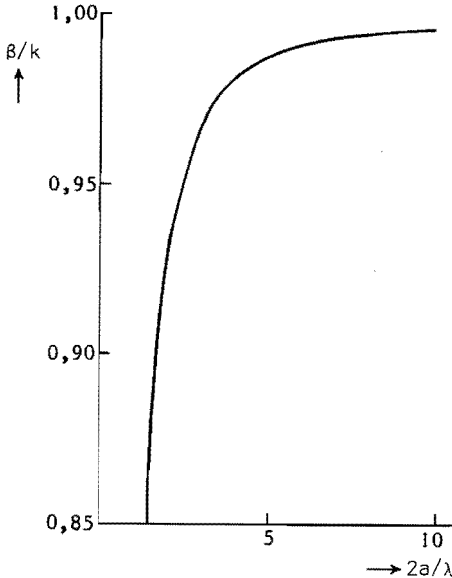β/k against $2a/\lambda$ for $HE_{11}^{(1)}$-mode.
Large values of $2a/\lambda$.

From conclusion (i) we see that the value of E'_r at the boundary $r' = a$
decreases for increasing values of $2a/\lambda$. In chapter 2 we have seen that

94

the high sidelobes in the E-plane radiation pattern of a conical horn antenna are caused by the fact that the value of E_r' is rather large at the boundary $r' = a$. So the conical horn antenna with the special ani- sotropic boundary discussed in this section gives us the possibility to improve the sidelobe behaviour in the E-plane.

We shall discuss this phenomenon in more detail in section 3.6. Then we shall also use Fig. 3.7.

From equation (3.27) to (3.30) incl. and the relation (3.33) we may conclude that the electric field lines of the $HE_{11}^{(1)}$-mode are of the same form as the magnetic field lines apart from a rotation in ϕ' of 90°. From conclusion (ii) we know that the electrical field lines of the $HE_{11}^{(1)}$- mode are virtually of the same form as those of the TE_{11}-mode in a per- fectly conducting waveguide, at least for $2a/\lambda = 0.6$. So it is now pos- sible to sketch the field lines of the $HE_{11}^{(1)}$-mode for $2a/\lambda = 0.6$. This has been done in Fig. 3.8, where also a sketch of the field lines of the TE_{11}-mode is given.

a

b
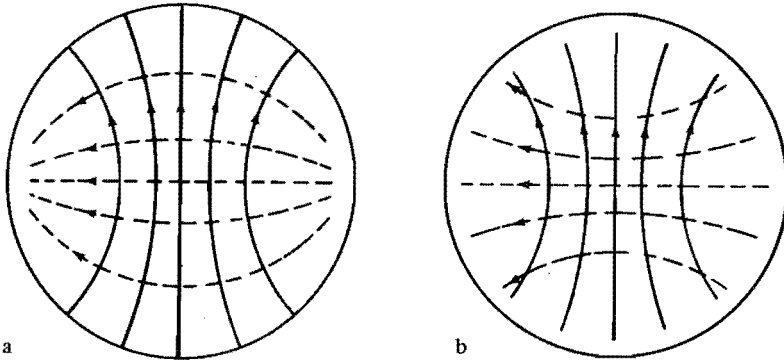
Fig. 3.8. Transverse electric field lines and transverse magnetic field lines.
        a : TE_{11}-mode,
        b : $HE_{11}^{(1)}$-mode for $2a/\lambda = 0.6$.

It is now possible to make some qualitative remarks about the problem of generating the $HE_{11}^{(1)}$-mode. Let us couple a perfectly conducting wave- guide with radius a, in which the TE_{11}-mode propagates, to a waveguide with the same radius but with boundary conditions as specified in (3.21) and with $Z_z = \infty$ and $Z_\phi = 0$. (See Fig. 3.9).

z=0

| 1   2

2a   TE₁₁   HE₁₁⁽¹⁾

Fig. 3.9. Transition from perfectly conducting waveguide to waveguide with anisotropic boundary.

Then we are sure that $2a/\lambda > 0.58$. This implies that the $HE_{11}^{(2)}$-mode will not be excited in waveguide 2. Then remains the question whether the $HE_{11}^{(1)}$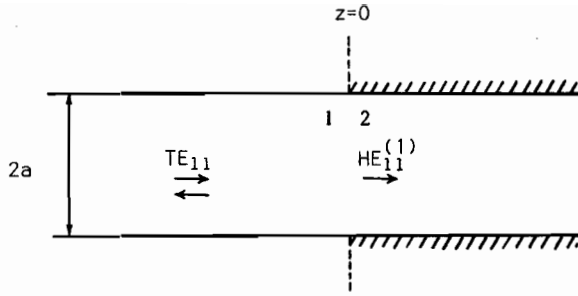-mode will be excited in waveguide 2. If the components of the electromagnetic field of the $HE_{11}^{(1)}$-mode depend on the coordinates of the waveguide in a similar way as in the case of the TE_{11}-mode, then we may expect that only a minor part of the energy will be reflected. From Fig. 3.8 we conclude that this condition is satisfied and it seems that the excitation of the $HE_{11}^{(1)}$-mode offers no important difficulties.

For the sake of completeness we have calculated the transverse electric field of the $HE_{11}^{(2)}$-mode as well.
For this mode we have $A_1 = - Z_o A_2$.

$$E_r' = \tfrac{1}{2} A_2 Z_o (k^2 - \beta^2)^{\frac{1}{2}} \left\{ \left(1 - \tfrac{\beta}{k}\right) J_o(k_c r') + \left(1 + \tfrac{\beta}{k}\right) J_2(k_c r') \right\} \cos \phi'$$

$$\equiv \tfrac{1}{2} A_2 Z_o (k^2 - \beta^2)^{\frac{1}{2}} \left(1 - \tfrac{\beta}{k}\right) f_2(k_c r') \cos \phi'. \tag{3.44}$$

$$E_\phi' = -\tfrac{1}{2} A_2 Z_o (k^2 - \beta^2)^{\frac{1}{2}} \left\{ \left(1 - \tfrac{\beta}{k}\right) J_o(k_c r') - \left(1 + \tfrac{\beta}{k}\right) J_2(k_c r') \right\} \sin \phi'$$

$$\equiv -\tfrac{1}{2} A_2 Z_o (k^2 - \beta^2)^{\frac{1}{2}} \left(1 - \tfrac{\beta}{k}\right) g_2(k_c r') \sin \phi'. \tag{3.45}$$

The functions $f_2(k_c r')$ and $g_2(k_c r')$ are calculated for three values of $2a/\lambda$. The results are plotted in Fig. 3.10 and show us that for $2a/\lambda = 0.55$ the components of the electromagnetic field of the $HE_{11}^{(2)}$-mode are quite similar to those of the electromagnetic field of the TE_{11}-mode in a perfectly conducting waveguide. However, if β/k approaches the value one, the picture changes completely. Now we see that the function

96
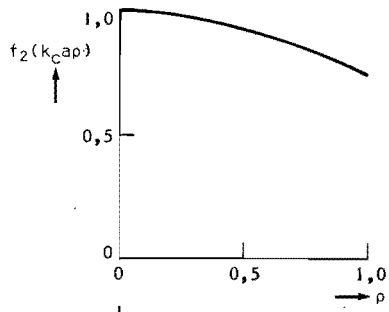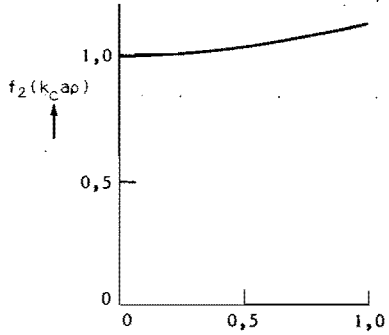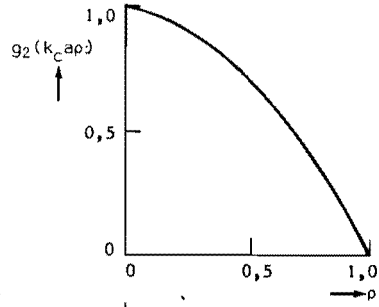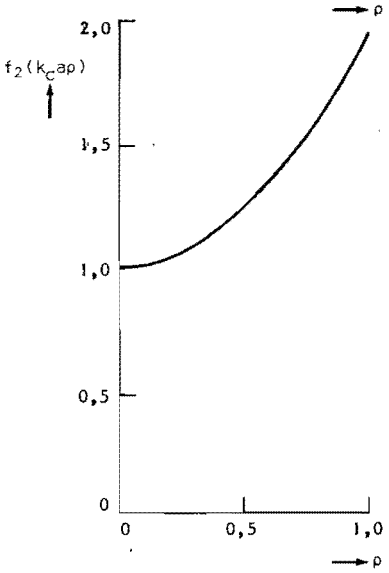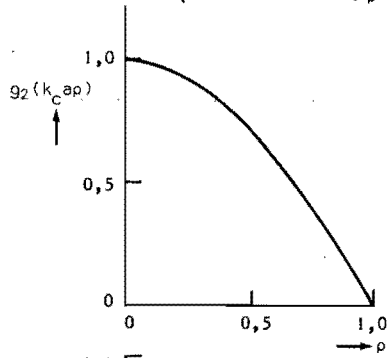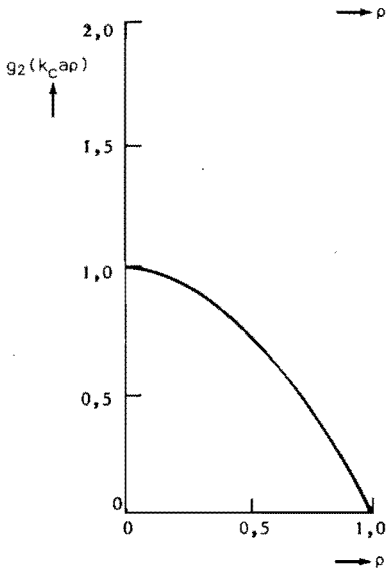
Fig. 3.10. The functions $f_2(k_c a\rho)$ and $g_2(k_c a\rho)$ against ρ.

      a : $2a/\lambda = 0.55$,

      b : $2a/\lambda = 0.50$,

      c : $2a/\lambda = 0.45$.

$f_2(k_cr')$ is larger in the neigbourhood of the boundary, whereas the function $g_2(k_cr')$ is zero at the boundary. So this mode is not suitable for antenna applications.

Branch b of Fig. 3.5 suggests that slow waves can exist if $2a/\lambda < 0.44$. Therefore we shall investigate the occurence of these waves in more detail.

Now the generating function of the TE field is given by

$$\psi_3(r',\phi',z) = A_3 \, I_n(\Gamma_c r') \, \sin n\phi' \, e^{-\gamma z}, \qquad (3.46)$$

whereas the TM field has the generating function

$$\psi_4(r',\phi',z) = A_4 \, I_n(\Gamma_c r') \, \cos n\phi' \, e^{-\gamma z}. \qquad (3.47)$$

I_n is the modified Bessel function [53] and $\Gamma_c^2 = -(k^2 + \gamma^2)$. Then the components of the electromagnetic field are

$$E_r' = \Gamma_c \left\{ \frac{-n}{\Gamma_c r'} A_3 I_n(\Gamma_c r') - \frac{\gamma}{j\omega\varepsilon_o} A_4 I_n'(\Gamma_c r') \right\} \cos n\phi', \qquad (3.48)$$

$$E_\phi' = \Gamma_c \left\{ A_3 I_n'(\Gamma_c r') + \frac{\gamma}{j\omega\varepsilon_o} A_4 \frac{n}{\Gamma_c r'} I_n(\Gamma_c r') \right\} \sin n\phi', \qquad (3.49)$$

$$Z_o H_r' = \Gamma_c \left\{ \frac{-\gamma}{jk} A_3 I_n'(\Gamma_c r') - Z_o A_4 \frac{n}{\Gamma_c r'} I_n(\Gamma_c r') \right\} \sin n\phi', \qquad (3.50)$$

$$Z_o H_\phi' = \Gamma_c \left\{ \frac{-\gamma}{jk} \frac{n}{\Gamma_c r'} A_3 I_n(\Gamma_c r') - Z_o A_4 I_n'(\Gamma_c r') \right\} \cos n\phi', \qquad (3.51)$$

$$E_z = \frac{k^2 + \gamma^2}{j\omega\varepsilon_o} A_4 \, I_n(\Gamma_c r') \, \cos n\phi', \qquad (3.52)$$

$$H_z = \frac{k^2 + \gamma^2}{j\omega\varepsilon_o} A_3 \, I_n(\Gamma_c r') \, \sin n\phi'. \qquad (3.53)$$

In the expressions (3.48) to (3.53) incl. we have omitted the factor $e^{-\gamma z}$. Also in this case we find that the condition

$$A_3 = Z_o A_4 \qquad (3.54)$$

gives rise to an electromagnetic field as specified in (3.18). Electromagnetic fields of the type of (3.20) can be found by substitution of

$$A_3 = -Z_o A_4 \qquad (3.55)$$

In both cases we find again that

$$Z_z \, Z_\phi + Z_O^2 = 0. \tag{3.37}$$

If we restrict ourselves to the special case $Z_\phi = 0$ and $Z_z = \infty$ we derive for the dispersion equation

$$\left(1 \pm \frac{\gamma}{jk}\right) \frac{n}{\Gamma_c a} \, I_n(\Gamma_c a) = I_{n-1}(\Gamma_c a). \tag{3.56}$$

The – sign corresponds to the solution with the condition (3.54) and the + sign refers to that with the condition (3.55).
In the special case $n = 1$ these equations reduce to

$$\left(1 \pm \frac{\beta}{k}\right) \frac{1}{\Gamma_c a} \, I_1(\Gamma_c a) = I_O(\Gamma_c a). \tag{3.57}$$

From the fact that the functions $I_1(\Gamma_c a)$ and $I_O(\Gamma_c a)$ are positive [53] and β/k is greater than one we see that the equation with the – sign has no solution at all. The solution of the other equation is plotted as branche c in Fig. 3.5. Comparing branch b and branch c of Fig. 3.5 we see that branch c is the continuation of branch b of Fig. 3.5, and we observe that there exists a continuous transition from the fast to the slow waves. Therefore, it is reasonable to assume that the electromagnetic field of this mode is similar to that plotted in Fig. 3.10. In order to verify this assumption we have calculated the transverse electric field of the slow $HE_{11}^{(2)}$-mode.
The next two expressions serve as a starting-point

$$E_r' = \tfrac{1}{2}\Gamma_c \, A_4 Z_O \cos\phi' \left\{ \left(1 - \frac{\beta}{k}\right) I_O(\Gamma_c r') - \left(1 + \frac{\beta}{k}\right) I_2(\Gamma_c r') \right\}$$

$$\equiv \tfrac{1}{2}\Gamma_c \, A_4 Z_O \left(1 - \frac{\beta}{k}\right) f_3(\Gamma_c r') \cos\phi', \tag{3.58}$$

$$E_\phi' = -\tfrac{1}{2}\Gamma_c \, A_4 Z_O \sin\phi' \left\{ \left(1 - \frac{\beta}{k}\right) I_O(\Gamma_c r') + \left(1 + \frac{\beta}{k}\right) I_2(\Gamma_c r') \right\}$$

$$\equiv -\tfrac{1}{2}\Gamma_c \, A_4 Z_O \left(1 - \frac{\beta}{k}\right) g_3(\Gamma_c r') \sin\phi'. \tag{3.59}$$

Use has been made of the recurrence relations [53]

$$\frac{2\gamma}{z} \, I_\gamma(z) = I_{\gamma-1}(z) - I_{\gamma+1}(z),$$

$$2 \, I_\gamma'(z) = I_{\gamma-1}(z) + I_{\gamma+1}(z). \tag{3.60}$$
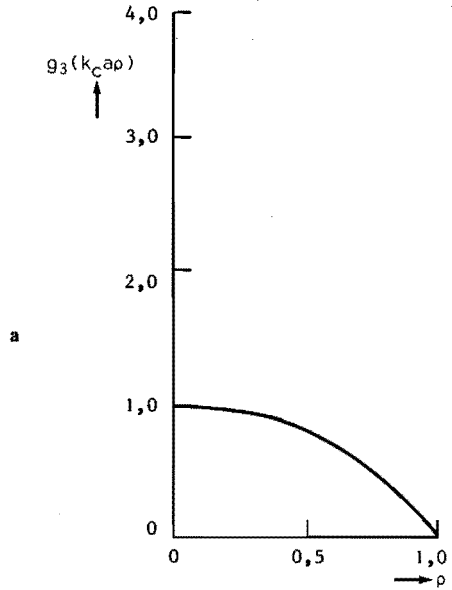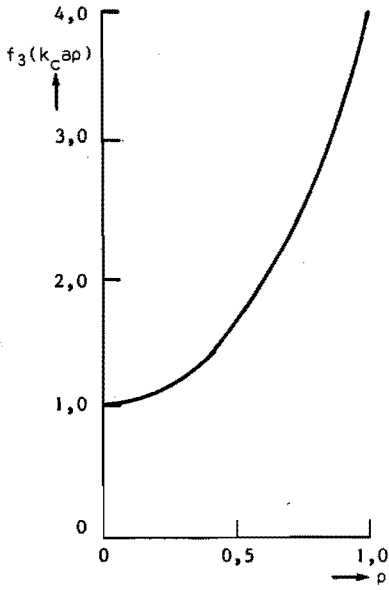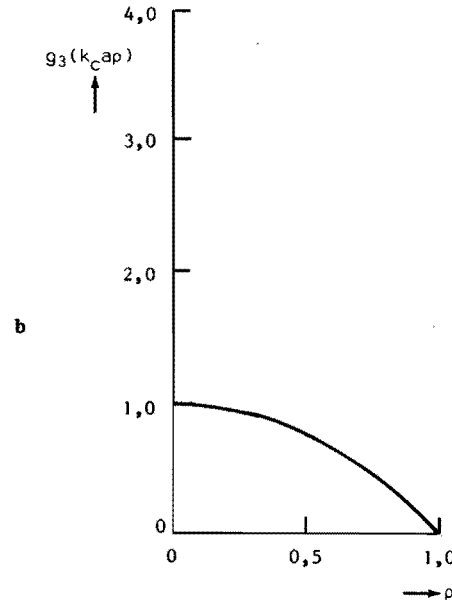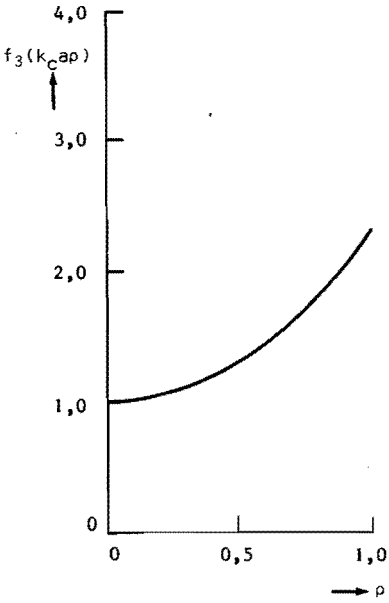
Fig. 3.11.   The functions $f_3(k_c a\rho)$ and $g_3(k_c a\rho)$ against ρ.

a : $2a/\lambda$ = 0.41,

b : $2a/\lambda$ = 0.44.

In Fig. 3.11 we have plotted two typical examples, namely for $2a/\lambda = 0.41$
and $2a/\lambda = 0.44$.

Observing Fig. 3.10 and Fig. 3.11 we conclude that neither the fast nor
the slow $HE_{11}^{(2)}$-mode is suitable for antenna applications. Moreover this
mode can only exist if $2a/\lambda < 0.58$. The properties of the $HE_{11}^{(1)}$-mode,
however, indicate that this mode can be used for antenna applications
and that the excitation of the mode is not a serious problem. In the
next section we shall investigate the radiation pattern of an open cir-
cular waveguide with aperture fields equal to the transverse electro-
magnetic fields of the $HE_{11}^{(1)}$-mode.

3.3   Power radiation pattern of an open circular waveguide with ani-
sotropic boundary.

One of the results of section 3.2 is that the $HE_{11}^{(1)}$-mode has the inte-
resting property that the component E_r' has only a small value at the
boundary of the waveguide, provided the frequency is not too close to
the cut-off frequency. This implies that the radiation pattern of an
open waveguide which supports this mode, will have lower sidelobes
than in the corresponding case of the TE_{11}-mode in a perfectly conduc-
ting waveguide. Therefore, it is interesting to calculate the radiation
pattern of an open circular waveguide with an anisotropic boundary. We
start by writing down the aperture fields in the following form:

$$E_r' = -\tfrac{1}{2} A_2 Z_O (k^2 - \beta^2)^{\frac{1}{2}} f(k_c r') \cos \phi', \tag{3.61}$$

$$E_\phi' = \tfrac{1}{2} A_2 Z_O (k^2 - \beta^2)^{\frac{1}{2}} g(k_c r') \sin \phi', \tag{3.62}$$

$$Z_O H_r' = -\tfrac{1}{2} A_2 Z_O (k^2 - \beta^2)^{\frac{1}{2}} f(k_c r') \sin \phi', \tag{3.63}$$

$$Z_O H_\phi' = -\tfrac{1}{2} A_2 Z_O (k^2 - \beta^2)^{\frac{1}{2}} g(k_c r') \cos \phi', \tag{3.64}$$

with

$$f(k_c r') = \left(1 + \frac{\beta}{k}\right) J_0(k_c r') + \left(1 - \frac{\beta}{k}\right) J_2(k_c r'), \tag{3.65}$$

$$g(k_c r') = \left(1 + \frac{\beta}{k}\right) J_0(k_c r') - \left(1 - \frac{\beta}{k}\right) J_2(k_c r'), \tag{3.66}$$

and

$$k_c = (k^2 - \beta^2)^{\frac{1}{2}}.$$

Moreover, we assume that the aperture is an equiphase plane; so $v = 0$.
Substitution of the expressions (3.61) to (3.64) incl. in the formulae
(2.24) and (2.25), and using the relations:

$$\int_0^{2\pi} \cos\phi'\cos(\phi-\phi')e^{ju\rho\cos(\phi-\phi')}d\phi' = \pi\cos\phi\{J_0(u\rho) - J_2(u\rho)\} \quad , \quad (3.67)$$

$$\int_0^{2\pi} \sin\phi'\sin(\phi-\phi')e^{ju\rho\cos(\phi-\phi')}d\phi' = -\pi\cos\phi\{J_0(u\rho) + J_2(u\rho)\} \quad , \quad (3.68)$$

$$\int_0^{2\pi} \sin\phi'\cos(\phi-\phi')e^{ju\rho\cos(\phi-\phi')}d\phi' = \pi\sin\phi\{J_0(u\rho) - J_2(u\rho)\} \quad , \quad (3.69)$$

$$\int_0^{2\pi} \cos\phi'\sin(\phi-\phi')e^{ju\rho\cos(\phi-\phi')}d\phi' = \pi\sin\phi\{J_0(u\rho) + J_2(u\rho)\} \quad , \quad (3.70)$$

which can be derived quite easily from the formulae (3.9) and (3.12),
we find

$$E_\theta = -\tfrac{1}{2} A_2 Z_0 (k^2-\beta^2)^{\frac{1}{2}} \frac{jka^2}{4r} e^{-jkr} \cos\phi \times$$

$$\int_0^1 \{F(\rho a_1,\theta) J_0(u\rho) - G(\rho a_1,\theta) J_2(u\rho)\} \rho d\rho, \quad (3.71)$$

$$E_\phi = \tfrac{1}{2} A_2 Z_0 (k^2-\beta^2)^{\frac{1}{2}} \frac{jka^2}{4r} e^{-jkr} \sin\phi \times$$

$$\int_0^1 \{F(\rho a_1,\theta) J_0(u\rho) - G(\rho a_1,\theta) J_2(u\rho)\} \rho d\rho \quad (3.72)$$

with

$$a_1 = k_c a.$$

The functions $F(\rho a_1,\theta)$ and $G(\rho a_1,\theta)$ are defined by the relations

$$F(\rho a_1,\theta) = \{f(\rho a_1) + g(\rho a_1)\} (1 + \cos\theta),$$

$$\quad (3.73)$$

$$G(\rho a_1,\theta) = \{f(\rho a_1) - g(\rho a_1)\} (1 - \cos\theta),$$

with

$$\rho = r'/a.$$

The expressions (3.71) and (3.72) are of the same form as (3.19). So
they describe a symmetrical power radiation pattern, as was to be ex-
pected. The expressions (3.71) and (3.72) can be written in the
following abbreviated form

$$E_\theta = -\tfrac{1}{2} A_2 Z_0 (k^2-\beta^2)^{\frac{1}{2}} \frac{jka^2}{4r} e^{-jkr} \cos\phi \; I(\theta),$$

$$E_\phi = \tfrac{1}{2} A_2 Z_0 (k^2-\beta^2)^{\frac{1}{2}} \frac{jka^2}{4r} e^{-jkr} \sin\phi \; I(\theta),$$

(3.74)

with

$$I(\theta) = 2 \int_0^1 \left\{ \left(1 + \frac{\beta}{k}\right) J_0(\rho a_1) \, J_0(u\rho) \, (1+\cos\theta) - \left(1 - \frac{\beta}{k}\right) J_2(\rho a_1) \, J_2(u\rho) \, (1-\cos\theta) \right\} \rho d\rho.$$

(3.75)

In the derivation of $I(\theta)$ use has been made of the formulae (3.65) and (3.66). Poynting's vector is given by

$$\underline{S}(r,\theta,\phi) = \tfrac{1}{2} Z_0^{-1} \left(\frac{ka^2}{4r}\right)^2 (\tfrac{1}{2} A_2 Z_0)^2 (k^2-\beta^2) \times |I(\theta)|^2 \, \underline{a}_r \, .$$

The power radiated per unit solid angle is $P(\theta,\phi) = r^2 |\underline{S}(r,\theta,\phi)|$ and the power radiation pattern is then represented by

$$F(\theta) = \left| \frac{I(\theta)}{I(0)} \right|^2$$

(3.76)

with

$$I(0) = 4 \left(1 + \frac{\beta}{k}\right) \int_0^1 J_0(\rho a_1) \, \rho d\rho$$

The function $F(\theta)$ can be written in a closed form if we use the formula [54]

$$\int_0^\rho J_n(k_1\rho) J_n(k_2\rho) \, \rho d\rho = \frac{\rho}{k_1^2-k_2^2} \left\{ k_2 J_n(k_1\rho) J_{n-1}(k_2\rho) - k_1 J_{n-1}(k_1\rho) J_n(k_2\rho) \right\}.$$

(3.77)

By means of this formula we can calculate the following integrals

$$\int_0^1 J_0(a_1\rho) \, \rho d\rho = \frac{1}{a_1} J_1(a_1).$$

(3.78)

$$\int_0^1 J_0(a_1\rho) \, J_0(u\rho) \rho d\rho = \frac{1}{a_1^2-u^2} \left\{ a_1 J_1(a_1) J_0(u) - u J_0(a_1) J_1(u) \right\}.$$

(3.79)

$$\int_0^1 J_2(a_1\rho) \, J_2(u\rho) \rho d\rho = \frac{1}{a_1^2-u^2} \left\{ u J_2(a_1) J_1(u) - a_1 J_1(a_1) J_2(u) \right\}.$$

(3.80)

For the function $F(\theta)$ we now find

$$F(\theta) = \frac{a_1}{2J_1(a_1)} \frac{1}{a_1^2-u^2} \left[(1+\cos\theta) \left\{ a_1 J_1(a_1) J_0(u) - u J_0(a_1) J_1(u) \right\} \right.$$
$$\left. + \alpha(1 - \cos\theta) \left\{ a_1 J_1(a_1) J_2(u) - u J_2(a_1) J_1(u) \right\} \right].$$
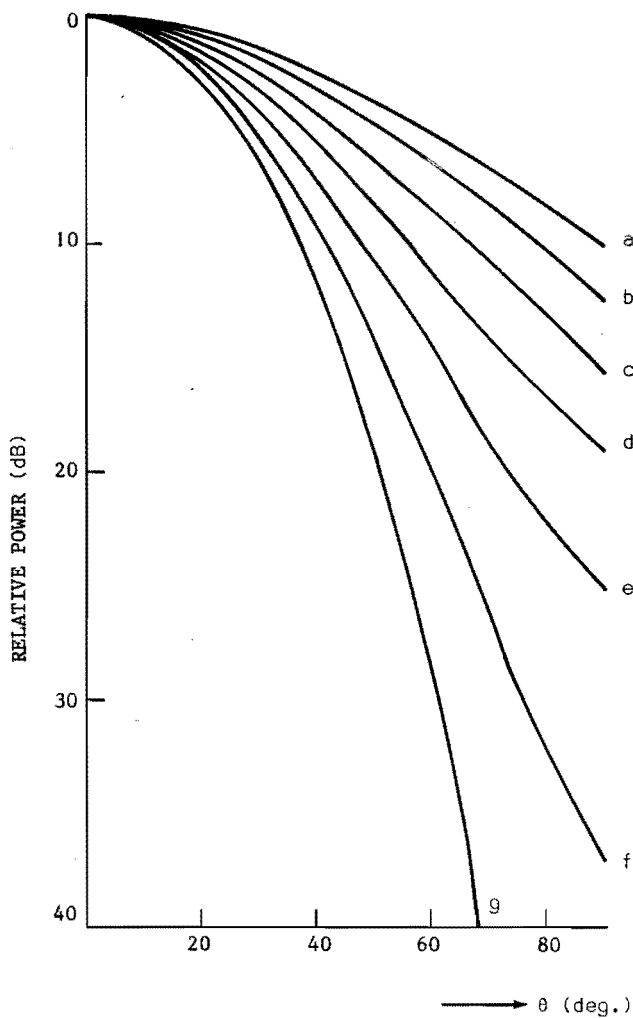
(3.81)

103

Fig. 3.12. Power radiation pattern of radiating circular waveguide with anisotropic boundary.

a: $2a/\lambda = 0.6$; b: $2a/\lambda = 0.8$; c: $2a/\lambda = 1.0$;

d: $2a/\lambda = 1.2$; e: $2a/\lambda = 1.4$; f: $2a/\lambda = 1.6$;

g: $2a/\lambda = 1.8$.
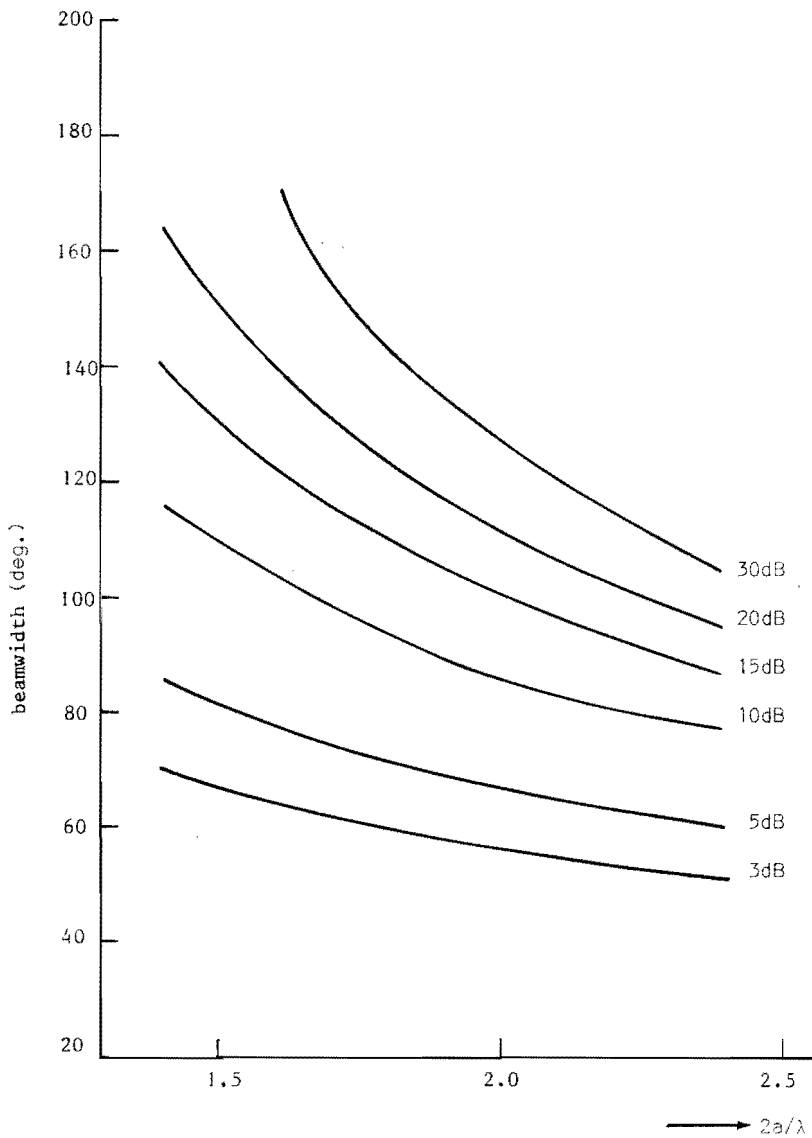
Fig. 3.13.   Beamwidth against $2a/\lambda$ of radiating circular waveguide with anisotropic boundary.

In the formula for $F(\theta)$ we have used the abbrevation

$$\alpha = \frac{1 - \beta/k}{1 + \beta/k}.$$ (3.82)

It may be recalled that the function $F(\theta)$ represents the power radiation pattern of an open circular waveguide with aperture fields equal to the transverse part of the electromagnetic field of the $HE_{11}^{(1)}$-mode. We are now able to calculate this pattern for several values of $2a/\lambda$. The procedure, which has been adopted is as follows. Choose the value of $2a/\lambda$. From Fig. 3.5 or Fig. 3.7 we find β/k. After calculating α and a_1 we can find the function $F(\theta)$. In Fig. 3.12 we have plotted the function $10^{10}\log F(\theta)$ for several values of $2a/\lambda$ between 0.6 and 1.8, whereas in Fig. 3.13 we have plotted the 3, 5,10,15,20 and 30dB points for several values of $2a/\lambda$ between 1.4 and 2.4. These figures can be used as a design chart. For instance, suppose that we wish to design a feed for a parabolic reflector antenna. Suppose further that this feed should have a symmetrical power pattern with a 20-dB beamwidth of 120°. (Among other factors this choice depends, of course, on the ratio of the focal distance and the diameter of the reflector). Then we see that this requirement can be met with a feed having $2a/\lambda = 1.6$. So, after specifying the frequency for which this feed will be used, we can find the diameter of the radiating waveguide.

The next task then is to find a physical structure which acts as a waveguide with the anisotropic boundary defined in the previous section by the relation (3.21), with $Z_\phi = 0$ and $Z_z = \infty$. This question will be discussed in the following section.

3.4   Circular corrugated waveguide.

In this section we shall prove that a circular corrugated waveguide in a limited frequency region acts as an anisotropic waveguide as discussed in the preceding sections (Fig. 3.14).
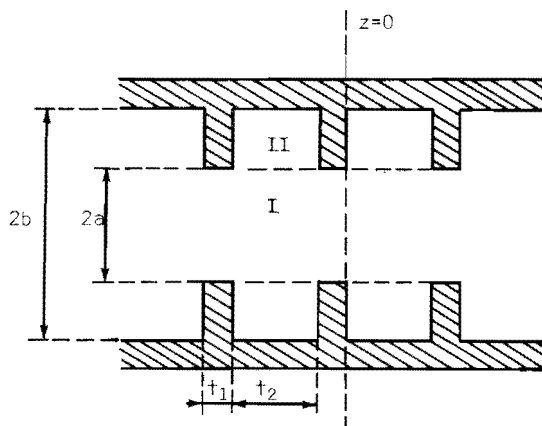
Fig. 3.14.   Circular corrugated waveguide.

A corrugated waveguide consists of a central part (I) and equally spaced grooves (II). Such a waveguide is a periodic structure and an exact theory of it should start by writing down the electromagnetic fields in the central part in the form of a series of space harmonics. The following step is then to find the electromagnetic fields in the grooves. After applying the boundary conditions at $r' = a$ a dispersion equation is obtained. The solution of the equation is a difficult task. This procedure has been followed ·in the design of linear accelerators [55], [56], where the distance between two consecutive grooves is of the order of half a wavelength. In our case, however, the distance between two consecutive grooves is so short that there are many grooves per wavelength. This implies that it is permissible to ignore the periodic nature of the waveguide. The electromagnetic fields in the central part of the waveguide can now be determined by treating the structure as a waveguide with an impedance boundary. In the following we shall indicate a second reason for abandoning the treatment of the corrugated waveguide as a periodic structure. In section 3.5 we shall deal with conical horn antennas of which the boundary consists of

closely spaced grooves. They have no periodic nature and therefore we expect that a theory of them can be developed only if we describe the properties of the boundary in terms of an impedance boundary. Our next task is to prove that the waveguide, sketched in Fig. 3.14, exhibits indeed the property that $Z_\phi = 0$ and $Z_z = \infty$ for $r' = a$. Therefore, we observe that the region II between $r' = a$ and $r' = b$ is in fact a radial waveguide, which is short-circuited at $r' = b$. The electromagnetic fields in a radial waveguide can be derived in a way similar to the one in which we have found the electromagnetic fields in a circular waveguide. The modes which can exist in a radial waveguide (Fig. 3.15) represent waves propagating in the direction $+ r'$ or $- r'$.
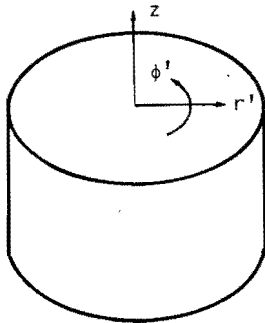
Fig. 3.15.   Radial waveguide.

They are TE—modes and TM—modes with respect to the z-axis. The TM—modes can be derived from the generating function [57]

$$\psi_{TM}(r',\phi',z) = f_n(k_c r') \cos n\phi' \cos \frac{m\pi z}{t_2} , \qquad (3.83)$$

$$k_c^2 = k^2 - \left(\frac{m\pi}{t_2}\right)^2 .$$

We shall specify the function $f_n(k_c r')$ later on.
The components of the electromagnetic field of this mode can now be found using (3.26).

The results are:

$$E_r' = \frac{-1}{j\omega\varepsilon_0} \; \frac{m\pi}{t_2} \; \frac{df_n(k_c r')}{dr'} \; \cos n\phi' \; \sin \frac{m\pi z}{t_2} \tag{3.84}$$

$$E_\phi' = \frac{1}{j\omega\varepsilon_0} \; \frac{n}{r'} \; \frac{m\pi}{t_2} \; f_n(k_c r') \; \sin n\phi' \; \sin \frac{m\pi z}{t_2} \;, \tag{3.85}$$

$$E_z' = \frac{1}{j\omega\varepsilon_0} \left\{ k^2 - \left(\frac{m\pi}{t_2}\right)^2 \right\} f_n(k_c r') \; \cos n\phi' \; \cos \frac{m\pi z}{t_2} \;, \tag{3.86}$$

$$H_r' = -\frac{n}{r'} \; f_n(k_c r') \; \sin n\phi' \; \cos \frac{m\pi z}{t_2} \;, \tag{3.87}$$

$$H_\phi' = -\frac{df_n(k_c r')}{dr'} \; \cos n\phi' \; \cos \frac{m\pi z}{t_2} \;, \tag{3.88}$$

$$H_z' = 0. \tag{3.89}$$

By inspection we see that the boundary conditions at $z = 0$ and $z = t_2$ are satisfied. The components of the electromagnetic field of the TE-mode can be derived from the generating function:

$$\psi_{TE}(r',\phi',z) = f_n(k_c r') \; \cos n\phi' \; \sin \frac{m\pi z}{t_2} \tag{3.90}$$

and (3.25). The results are:

$$E_r' = \frac{n}{r'} \; f_n(k_c r') \; \sin n\phi' \; \sin \frac{m\pi z}{t_2} \;, \tag{3.91}$$

$$E_\phi' = \frac{df_n(k_c r')}{dr'} \; \cos n\phi' \; \sin \frac{m\pi z}{t_2} \;, \tag{3.92}$$

$$E_z' = 0, \tag{3.93}$$

$$H_r' = \frac{1}{j\omega\mu_0} \; \frac{m\pi}{t_2} \; \frac{df_n(k_c r')}{dr'} \; \cos n\phi' \; \cos \frac{m\pi z}{t_2} \;, \tag{3.94}$$

$$H_\phi' = \frac{-1}{j\omega\mu_0} \; \frac{m\pi}{t_2} \; \frac{n}{r'} \; f_n(k_c r') \; \sin n\phi' \; \cos \frac{m\pi z}{t_2} \;, \tag{3.95}$$

$$H_z' = \frac{1}{j\omega\mu_0} \left\{ k^2 - \left(\frac{m\pi}{t_2}\right)^2 \right\} f_n(k_c r') \; \cos n\phi' \; \sin \frac{m\pi z}{t_2} \;. \tag{3.96}$$

109

In this case too, the boundary conditions at $z = 0$ and $z = t_2$ are satisfied. For waves propagating in the positive r'-direction we have to take $f_n(k_c r') = H_n^{(2)}(k_c r')$ whereas for waves propagating in the negative r-direction $f_n(k_c r') = H_n^{(1)}(k_c r')$. So we see that for propagating waves $k_c^2 > 0$ or $k^2 > \left(\frac{m\pi}{t_2}\right)^2$. From the expressions (3.84) to (3.96) incl. we conclude that the dominant mode is the TM-mode with the components E_z', H_ϕ' and H_r'. If we choose $t_2 < \frac{\lambda}{2}$ then only the dominant mode can propagate. Under these conditions we find for the electromagnetic field in the radial waveguide with a short-circuit at $r' = b$:

$$E_z' = -j\omega\mu_o \left\{ A\, H_n^{(1)}(kr') + B\, H_n^{(2)}(kr') \right\} \cos n\phi' ,\qquad (3.97)$$

$$H_r' = -\frac{n}{r'} \left\{ A\, H_n^{(1)}(kr') + B\, H_n^{(2)}(kr') \right\} \sin n\phi' ,\qquad (3.98)$$

$$H_\phi' = -\left\{ A\, \frac{dH_n^{(1)}(kr')}{dr'} + B\, \frac{dH_n^{(2)}(kr')}{dr'} \right\} \cos n\phi' .\qquad (3.99)$$

Applying the boundary condition $E_z = 0$ for $r' = b$ and using the relations

$$H_n^{(1)}(kr') = J_n(kr') + j\, Y_n(kr') ,\qquad (3.100)$$

$$H_n^{(2)}(kr') = J_n(kr') - j\, Y_n(kr') ,\qquad (3.101)$$

we obtain the final result:

$$E_z' = E_o \left\{ J_n(kb')\, Y_n(kr') - J_n(kr')\, Y_n(kb) \right\} \cos n\phi',\qquad (3.102)$$

$$Z_o H_\phi' = -jE_o \left\{ J_n(kb)\, Y_n'(kr') - J_n'(kr')\, Y_n(kb) \right\} \cos n\phi',\qquad (3.103)$$

$$Z_o H_r' = \frac{n}{jkr'} E_o \left\{ J_n(kb)\, Y_n(kr') - J_n(kr')\, Y_n(kb) \right\} \sin n\phi'.\qquad (3.104)$$

The primes in $J_n'(kr')$ and $Y_n'(kr')$ (3.103) means differentiating with respect to the argument kr'. E_o is a new constant and $Y_n(kr')$ is the Neumann function [58]. Next we define Z_ϕ by the relation

110

$$Z_\phi = \frac{\displaystyle\int_0^{t_1+t_2} E_\phi^! \, dz}{\displaystyle\int_0^{t_1+t_2} H_\phi^! \, dz} \qquad\qquad (3.105)$$

and Z_z by the relation

$$Z_z = \frac{\displaystyle\int_0^{t_1+t_2} E_z^! \, dz}{\displaystyle\int_0^{t_1+t_2} H_\phi^! \, dz} \qquad\qquad (3.106)$$

So Z_ϕ and Z_z are average values over one period of the structure. From the expressions (3.102) to (3.104) incl. we see that there exists no $E_\phi^!$ at the opening of the groove. $E_\phi^!$ is also zero on the dams between the grooves. However, $H_z^!$ is non-zero at the dams, because there flows a current in the ϕ-direction. So $Z_\phi = 0$. $E_z^!$ is non-zero at the opening of the groove. If we assume that the width of the dams is negligible, then we can conclude that $Z_z = \infty$, provided we choose the frequency in such a way that $H_\phi^!$ is zero at the opening of the groove.

The conditions $Z_\phi = 0$ and $Z_z = \infty$ are just the conditions under which the considerations of the preceding sections are valid. However, some remarks should be made in order to indicate the restrictions of the theory:

(i) the electromagnetic field at the opening of the grooves is very complicated, because apart from the propagating TM-mode, there exist also evanescent modes, which are not taken into account;

(ii) the quantity t_1 does not appear in our theory;

(iii) the condition $H_\phi^! = 0$ at the opening of the grooves depends on the frequency. In the sections 3.2 and 3.3 we have assumed that Z_z and Z_ϕ were independent of the frequency. So the theory is valid only at frequencies for which $H_\phi^! = 0$. However, the condition $H_\phi^!=0$ is approximately satisfied in limited frequency bands. In other words, symmetrical radiation patterns can be obtained only in limited frequency bands.

Within the restrictions of our theory the condition $Z_\phi = 0$ offers no difficulty, whereas the condition $Z_z = \infty$ is equivalent with

$$J_n(kb) \; Y_n'(ka) - J_n'(ka) \; Y_n(kb) = 0. \tag{3.107}$$

If we assume that $ka \gg 1$ and $kb \gg 1$, which means that we are dealing with a waveguide with large diameter, then it is permissible to apply the following approximations [60]:

$$J_n(z) \cong \left(\frac{2}{\pi z}\right)^{\frac{1}{2}} \cos\left(z - \frac{n\pi}{2} - \frac{\pi}{4}\right) ,$$
$$Y_n(z) \cong \left(\frac{2}{\pi z}\right)^{\frac{1}{2}} \sin\left(z - \frac{n\pi}{2} - \frac{\pi}{4}\right) . \tag{3.108}$$

Substituting (3.108) in (3.107) and using the recurrence relations

$$Z_\nu'(z) = \frac{-\nu}{z} Z_\nu(z) + Z_{\nu-1}(z) \tag{3.109}$$

where $Z_\nu(z)$ stands for $J_\nu(z)$, $Y_\nu(z)$ resp., we obtain the equation

$$\tan k(b-a) = - \frac{ka}{n}. \tag{3.110}$$

If the diameter of the waveguide is large, for instance $ka > 5\pi$, then we may use the approximation $k(b-a) = \frac{\pi}{2}$ if $n = 1$. From section 3.1 we know that the case $n = 1$ is the most important one and we shall restrict our further considerations to that case. An exact solution of equation
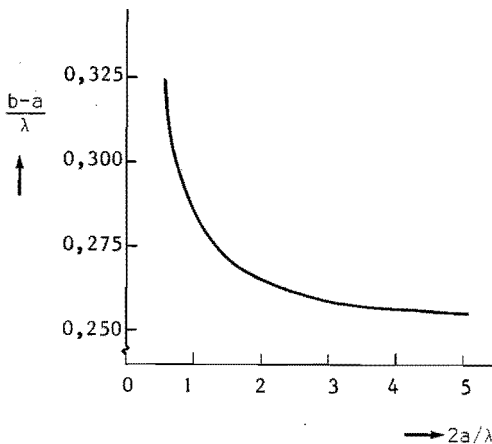

Fig. 3.16.
Depth of the grooves against diameter of waveguide; fixed frequency.

(3.107) can be found by prescribing the value of ka and solving the
equation for kb. For $\frac{2a}{\lambda} < 5$ the results are collected in Fig. 3.16. For
values of $2a/\lambda > 5$ equation (3.110) can be used. The main conclusion is
that for fixed frequency the depth of the grooves increases if the dia-
meter or the waveguide decreases. We shall return to this phenomenon in
the following section, where we shall apply the theory of this section.
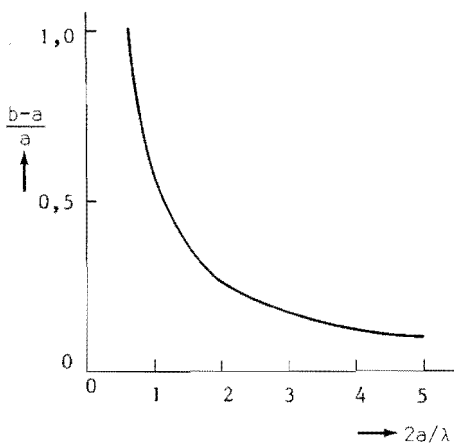
Fig. 3.17.
Depth of the grooves against frequency;
fixed diameter of waveguide.

In Fig. 3.17 we have plotted the same numerical results, but in a some-
what different way. From Fig. 3.17 we may derive the depth of the grooves,
and we can see that this depth is a function of the frequency if the
diameter is fixed. To obtain some insight into the frequency-dependent
behaviour of the corrugated waveguide, one has to solve Maxwell's equa-
tion for various combinations of ka and kb. Substitution of the trans -
verse part of the electromagnetic field in the formulae which represent
the radiation field, offers the possibility to investigate the frequen-
cy-dependence behaviour of the corrugated conical horn antenna. However,
this is a comprehensive task. In addition, in order to be complete, one
should also compute the transmission coefficient of the $HE_{11}^{(1)}$-mode in
the corrugated waveguide and the reflection coefficient of the TE_{11}-
mode in the perfectly conducting waveguide. To obtain quickly insight
into the frequency-dependent behaviour of corrugated conical horn an-
tennas, we have used an experimental approach, although it is desirable
that the solutions of the above problems should be found.
So in the following sections of this study we shall describe some expe-
riments, which will give some idea about the usefulness of the corru-
gated conical horn antennas.

3.5 The power radiation pattern of the corrugated conical horn antennas with small flare angle and small aperture.

The purpose of this section is to study the power radiation pattern of conical horn antennas with a corrugated boundary of the same type as discussed in section 3.4. As in chapter 2, we shall restrict our considerations to conical horn antennas with a flare angle $\alpha_0 < 15^\circ$. This offers the possibility to treat the antenna as an open circular waveguide radiator. The radiation pattern of this radiator can be computed rather easily; if necessary a quadratic phase field distribution across the aperture may be assumed. In addition, it is now possible to use the results of the preceding section, because the conical horn antenna can be considered to be a cylindrical waveguide with a cross-section which increases only slightly from the top of the cone towards the aperture. It should be noted that the grooves are assumed to be perpendicular to the wall of the antenna. However, the angle $\alpha_0 < 15^\circ$ and, consequently, the theory of the preceding section can still be applied. This implies that a theory of corrugated conical horn antennas with small flare angle can be formulated, but only for the frequency which satisfies equation (3.107).

From Fig. 3.16 one may conclude that for a fixed frequency the depth of the grooves increases towards the apex of the cone. However, it is desirable to advoid the mechanical difficulties of constructing horn antennas with variable depth of the grooves. In fact, this depth was chosen constant. A consequence of this procedure is that the depth of the first grooves at the throat of the horn are not optimised with respect to the matching of the transition from perfectly conducting waveguide to corrugated waveguide and with respect to the excitation of the $HE_{11}^{(1)}$-mode. Especially one is not sure that no unwanted modes are excited.

The difficulties described above are in fact of the same type, as has already been noticed at the end of section 3.4. So an experimental approach to the solution of the above problems has been adopted. However, further theoretical investigation is necessary. In this connection we remark that some preliminary results concerning these problems have been published by Bryant [61].

To investigate whether the theory of section 3.4 is valid, one has to
measure the power radiation pattern of corrugated conical horn antennas
as a function of the frequency. If the theory is valid, then one should
observe a symmetrical power radiation pattern for the frequency which
satisfies (3.107), provided the depth of the groove at the aperture and
the diameter of the aperture are substituted in (3.107). With a view to
carrying out the above investigation, three antennas with different
aperture diameter have been constructed. (Fig. 3.18). The dimensions
of these antennas are summarised in Table III.
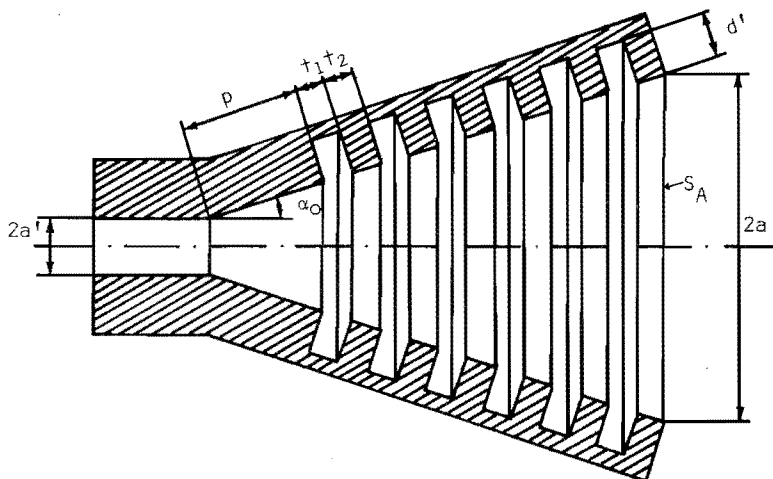
Fig. 3.18. Corrugated conical horn antenna.

In Fig. 3.18 we may distinguish three regions. The first is the circu-
lar waveguide and the first part of the conical horn antenna, where the
boundary is perfectly conducting. The second region is that part of the
horn antenna which consists of the corrugated boundary. The third part
is the radiating aperture S_A. The length p has been determined experi-
mentally. The criterion that has been used for this purpose was that
the reflection coefficient should be below 20 dB.

115

TABLE III

antenna	2a [mm]	2a' [mm]	α_o	β [mm]	t_1 [mm]	t_2 [mm]	d' [mm]	n
1	62.3	28	15°	12.4	2	2	9	14
2	91	28	15°	12	2	2	9	28
3	121.3	28	15°	13.5	2	2	9	42

n is the number of the grooves.

The power radiation pattern of the three antennas of table III has been measured as a function of the frequency. Moreover, the pattern has been calculated for the frequency which satisfies (3.107). These calculations are performed by multiplying the integrand of (3.71) and of (3.72) by exp $[-j\nu\rho^2]$; ν has the same meaning as in chapter 2. For the substitution of (3.65) and (3.66) in (3.71) and (3.72) one needs the value of β/k, which has been found by solving (3.40). The results of the measurements and the computations are given in Fig. 3.19 to Fig. 3.21 incl. In addition these also show the reflection coefficient of the antennas as a function of the frequency. The information concerning the reflection coefficient has been obtained by means of a sweep-technique.
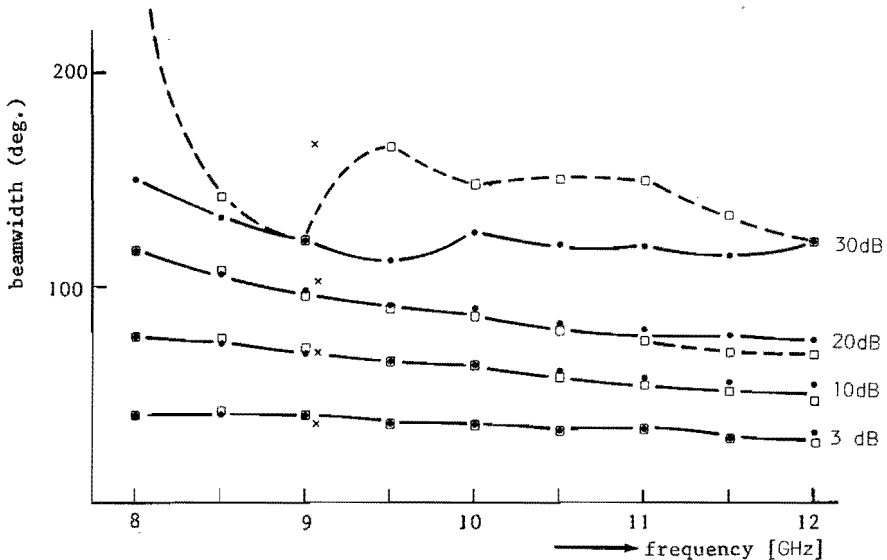

Fig. 3.19. Beamwidth against frequency for antenna 1.
        ×,theoretical , H-plane and E-plane,
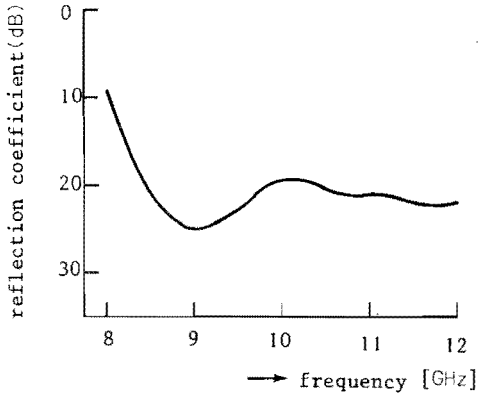   •,experimental, H-plane,   □,experimental, E-plane.

Fig. 3.19^a.

Reflection coefficient against frequency for antenna 1.

The conclusions that can be drawn from Fig. 3.19 to Fig. 3.21 incl. are:

(i) The power radiation patterns are symmetrical for the frequency
     that satisfies equation (3.107);

(ii) the power radiation patterns are approximately symmetrical in a
     rather large frequency band; the lowest frequency in this band is
     the one of (i). It should be noted that this conclusion is only
     valid if we restrict ourselves to the 3,10 and 20 dB points;

(iii) the antennas 2 and 3 possess a power radiation pattern that is
     symmetrical within the 30 dB points and in the same large fre-
     quency band as mentioned in conclusion (ii);

(iv) the beamwidth of the antennas 1, 2 and 3 is a function of the
     frequency. This is not surprising, because the phase difference
     between rim and centre of the aperture is too small to give rise
     to a frequency-independent antenna. In fact, even for antenna 3
     we find from (2.31) that $d/\lambda = 0.26$ at 10 GHz.

The argumentation which has been used in (iv) to make plausible that
antenna 3 cannot possess frequency-independent properties, is not com-
pletely satisfactory for the following reason. Fig. 2.8 and Fig. 2.9
show that the beamwidth of a conical horn antenna cannot be independent
of the frequency if $d/\lambda = 0.26$. However, in the derivation of the theory
which underlies Fig. 2.8 and Fig. 2.9 the amplitude distribution cor-
responding to the $TE_{1\nu}$-mode has been assumed. In general, this distri-
bution differs from the one which exists in the aperture of antenna 3.

117

Fig. 3.20. Beamwidth against frequency for antenna 2.
×,theoretical , H-plane and E-plane,
•,experimental, H-plane, □,experimental, E-plane.
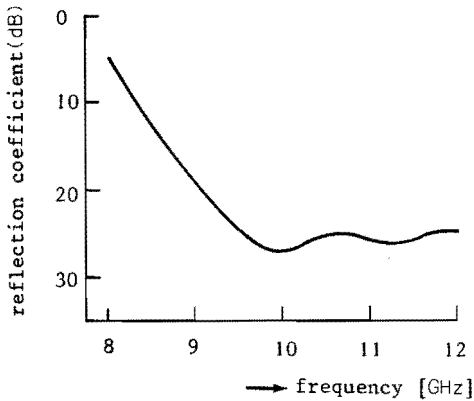
Fig. 3.20^{a}.

Reflection coefficient against frequency of antenna 2.

Moreover, Fig. 2.8 and Fig. 2.9 are valid only if the amplitude distribution is independent of the frequency. Obviously, this is not the case for the aperture fields of a corrugated conical horn antenna, as can be concluded from Fig. 3.6. It should be noted that the diagrams of Fig. 3.6 have been composed under the assumption that Z_z and Z_ϕ are independent of the frequency, which is not the case for a corrugated conical horn antenna. This is a second reason for supposing that the aperture fields of corrugated conical horn antennas are dependent on the frequency.
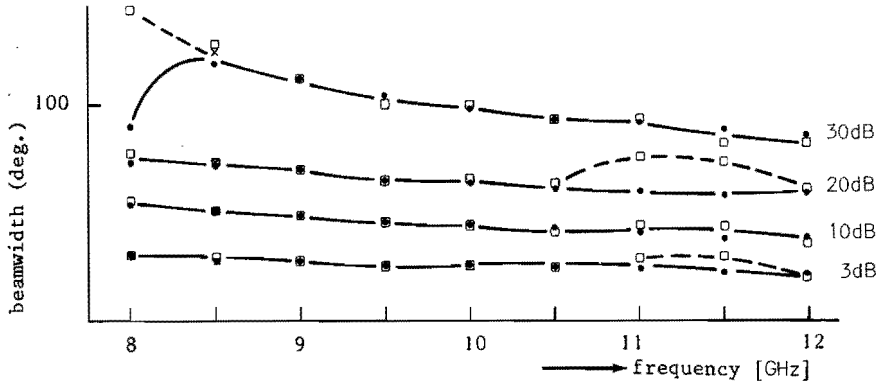
Fig. 3.21. Beamwidth against frequency for antenna 3.
        ×,theoretical , H-plane and E-plane,
        •,experimental, H-plane,   □,experimental, E-plane.
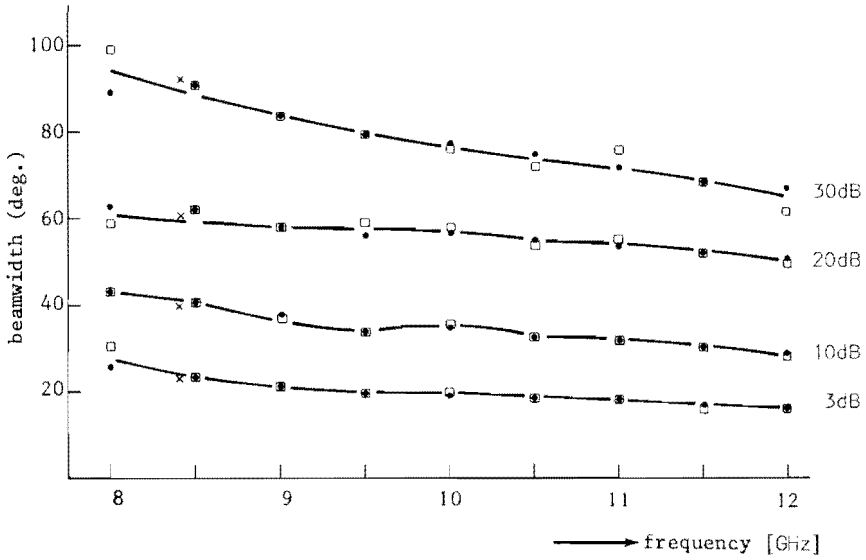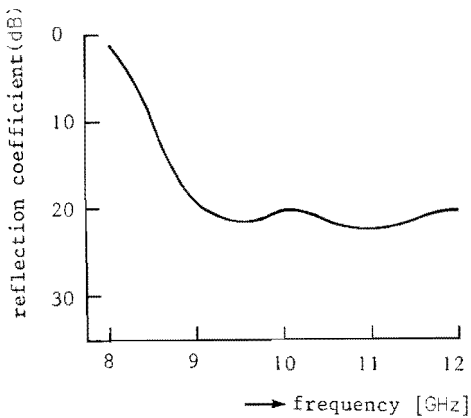

Fig. 3.21^{a}.
Reflection coefficient against
frequency for antenna 3.

119

3.6 Theoretical investigation of frequency – independent conical horn antennas with small flare angle and anisotropic boundary.

The results of the preceding section indicate that a symmetrical power radiation pattern can be obtained with a corrugated conical horn antenna, at least for the frequency which satisfies (3.107). If the diameter of the aperture is not too small a symmetrical radiation pattern is obtained in a rather large frequency band. These results raise the question whether it is possible to combine the frequency-independent properties of the conical horn antenna with perfectly conducting boundary and the symmetry properties od the corrugated conical horn antenna of the preceding section.

In this section we shall perform calculations concerning the above question and in the last section of this study some experimental results will be described. The theoretical considerations start with the assumption that

$$Z_\phi = 0 \quad \text{and} \quad Z_z = \infty. \tag{3.111}$$

These assumptions imply that Z_ϕ and Z_z are independent of the frequency. Although the assumptions (3.111) are not valid for a corrugated conical horn antenna as described in section (3.4) and (3.5) it is still useful to start with them for the following two reasons:

(i) the results of this section will show that useful antennas can be designed, provided the above assumptions are valid. This will stimulate investigations with the aim to synthesise a boundary with the above properties,

(ii) in the next section we shall show that the above assumptions are acceptable for corrugated conical horn antennas, but only in a limited frequency range.

It is very interesting to compare the results of this section with results described in chapter 2. Therefore we assume that the flare angle $\alpha_0 \leqslant 15^\circ$. Then we know from (2.75) that

$$\frac{d}{a} \cong \frac{\alpha_0}{2} \tag{2.75}$$

Suppose that $\frac{d}{\lambda} > \frac{1}{4}$, then $\frac{2a}{\lambda} = 2 \frac{2}{\alpha_0} \frac{1}{4} > 3.8$ \qquad (3.112)

From Fig. 3.7 we observe that $\beta/k \geqslant 0.98$. The equation (3.40) now reduce to the following one

$$J_0(k_c a) = 0 \tag{3.113}$$

So

$$k_c a = j_{01} = a(k^2 - \beta^2)^{\frac{1}{2}}, \tag{3.114}$$

where j_{01} is the first zero of $J_0(x)$

Substitution of

$$(k^2 - \beta^2)^{\frac{1}{2}} = \frac{j_{01}}{a} \tag{3.115}$$

and

$$k_c r' = j_{01} \frac{r'}{a} \tag{3.116}$$

together with $\beta/k = 1$ in the expressions (3.61) to (3.66) incl. gives

$$E_r' = - Z_0 A_2 \frac{j_{01}}{a} J_0 (j_{01} \frac{r'}{a}) \cos \phi', \tag{3.117}$$

$$E_\phi' = Z_0 A_2 \frac{j_{01}}{a} J_0 (j_{01} \frac{r'}{a}) \sin \phi', \tag{3.118}$$

$$Z_0 H_r' = - Z_0 A_2 \frac{j_{01}}{a} J_0 (j_{01} \frac{r'}{a}) \sin \phi', \tag{3.119}$$

$$Z_0 H_\phi' = - Z_0 A_2 \frac{j_{01}}{a} J_0 (j_{01} \frac{r'}{a}) \cos \phi'. \tag{3.120}$$

The electric field lines and the magnetic field lines of this mode can be constructed easily. This has been done in Fig. 3.22.
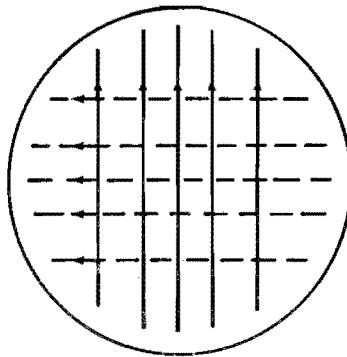

Fig. 3.22. Transverse electric field lines and transverse magnetic field lines of the $HE_{11}^{(1)}$-mode for large value of $2a/\lambda$.

A comparison of Fig. 3.8 with Fig. 3.22 shows that for large value of $2a/\lambda$ the field lines become straight lines. This fact demonstrates again that the transverse electric field and the transverse magnetic field of the $HE_{11}^{(1)}$-mode depend on the value of $2a/\lambda$. This is not the case for modes in a perfectly conducting waveguide.
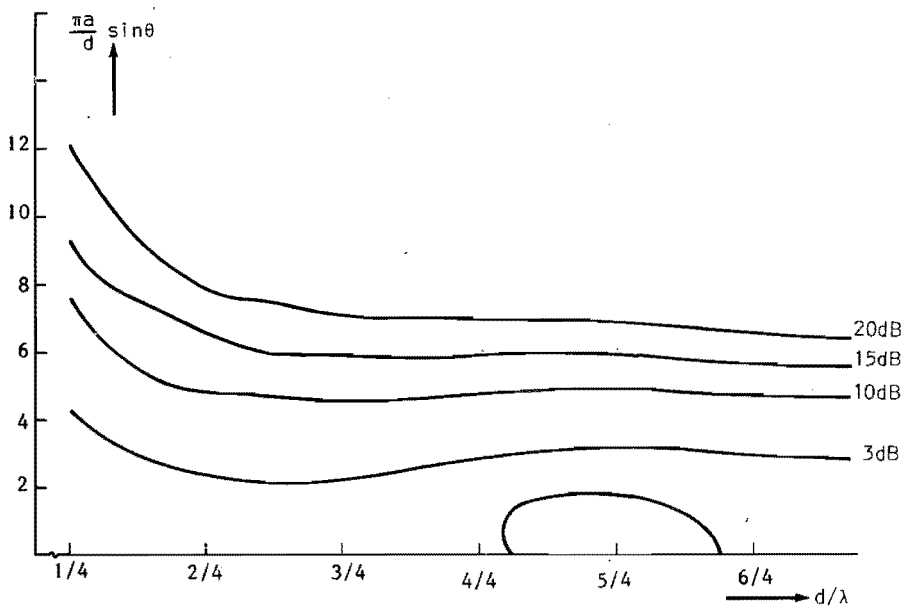
Fig. 3.23. Beamwidth of conical horn antenna with small flare angle and anisotropic boundary.

Substitution of (3.117) to (3.120) incl. in (2.24) and (2.25) gives the radiation field. It should be noted that in (2.24) and (2.25) now $v=kd$. Following the same procedure as in chapter 2 a similar diagram as in Fig. 2.8 has been composed and is given in Fig. 3.23. We note that this diagram has already been published elsewhere. [62]. As we are concerned with symmetrical power radiation pattern, it is sufficient to compose one diagram. From Fig. 3.23 we observe that indeed a frequency-independent antenna with a symmetrical power radiation pattern can be obtained, provided it is possible to design a boundary which is described by frequency-independent Z_ϕ and Z_z, satisfying the relation (3.111). Furthermore, we observe that there exist no sidelobes in the pattern and beamsplitting occurs for a larger value of d/λ compared with the situation of Fig. 2.9.

122

For the sake of completeness we have also composed a diagram similar to
the one of Fig. 2.21. This diagram is given in Fig. 3.24. From this
diagram the equiphase surfaces can be constructed. It is obvious that
the equiphase surfaces are independent of the frequency too. The cur-
ves of Fig. 3.24 are of the same form as the curves of Fig. 2.21. So
we may conclude that the antennas studied in this section have no
phasecentre.
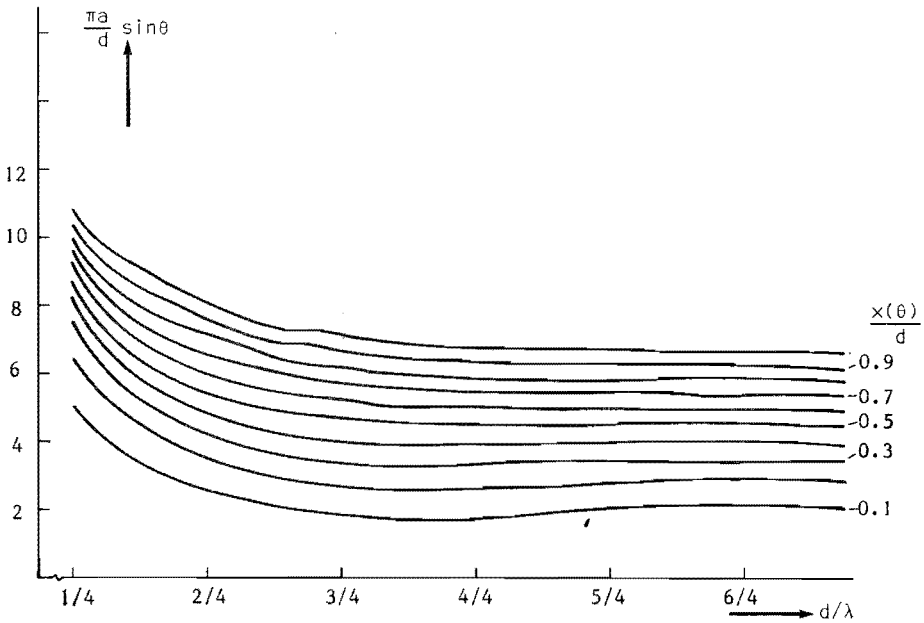
Fig. 3.24 Curves of constant $x(\theta)/d$-value against d/λ for conical horn
antenna with small flare angle and anisotropic boundary.

In Fig. 3.2 we have plotted the fraction of the total energy which is
radiated within the cone-angle θ for various values of θ. These data
are related to the antenna of Fig. 2.15 and are given for 8 GHz.
The same information has been plotted in Fig. 3.25 for an antenna with
the same dimensions as the antenna of Fig. 2.15 but with a boundary,
specified by (3.111). Fig. 3.25 is also only valid for 8 GHz. In con-

clusion we see that in this case a larger fraction of the total energy
is radiated between the angles -θ and θ as in the corresponding case
of the antenna of Fig. 2.15.
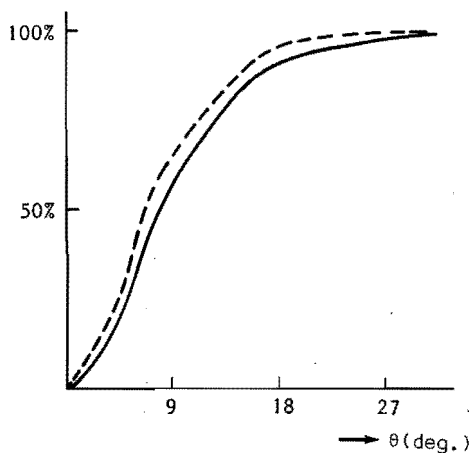
Fig. 3.25.

Fraction of the energy radiated within the cone-angle θ against θ.

　　——, conical horn antenna with small flare angle and perfectly
　　　　conducting boundary,
　　----, conical horn antenna with small flare angle and anisotropic
　　　　boundary.

The dimensions are identical with those of the antenna of Fig. 2.15.

3.7　Experimental investigation of frequency-independent corrugated conical horn antennas with small flare angle.

The purpose of this section is to investigate whether frequency-inde-
pendent radiation patterns can be obtained with a corrugated conical
horn antenna. The idea is to choose the dimensions of the horn in such
a way that a frequency-independent horn antenna is obtained provided
the corrugated boundary can be described by (3.111). The next step is
to measure the radiation pattern of this antenna as a function of the
frequency. Then it is possible to investigate in which frequency band
a symmetrical radiation pattern exists.

In order to carry out these measurements and to facilitate the compar-
ison with the results of chapter 2 an antenna was constructed with the
same flare angle and aperture as the antenna of Fig. 2.15. The inside
of the antenna consists of a corrugated boundary. The dimensions of
the antenna are given in Table IV and the symbols have the same meaning
as in Fig. 3.18. The value of p was chosen experimentally in order to
obtain a good matching.

TABLE IV

antenna	2a [mm]	2a' [mm]	α_o	p [mm]	t_1 [mm]	t_2 [mm]	d' [mm]	n
4	264	28	15°	26	10.2	2.3	9	34

The power radiation pattern was measured using the antenna test range
described in chapter 2. The results are given in Fig. 3.26 and the con-
clusion can be drawn that indeed a symmetrical power radiation pattern
can be obtained in the frequency band from about 7GHz to 10 GHz.

Fig. 3.26.   Beamwidth against frequency for antenna 4.

    •, experimental, H-plane,

    □, experimental, E-plane,

    ×, theoretical , H-plane and E-plane.
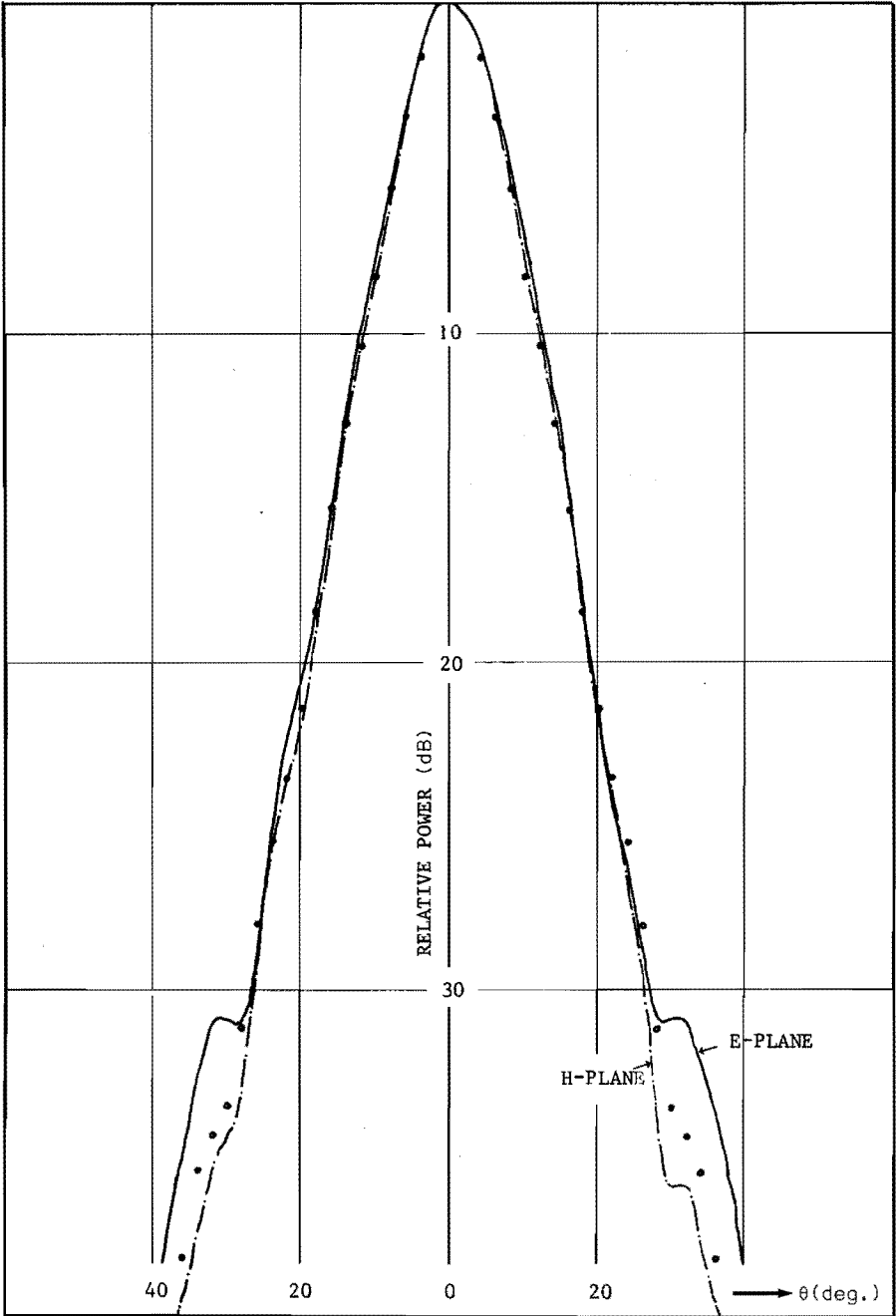
Fig. 3.27. Power radiation pattern of antenna 4 at 8.3 GHz.

The second conclusion is that the beamwidth in the H-plane is virtually independent of the frequency in the band from 7 GHz to 15,5 GHz. However the pattern in the E-plane exhibits a rather large variation as a function of the frequency. Finally the theoretically predicted beamwidth has also been plotted in the diagram. This value can be calculated for the frequency that satisfies (3.107) and we see that a symmetrical power radiation pattern is obtained in a frequency range around this frequency. A complete power radiation pattern has been included also in Fig. 3.27 and shows good agreement between theory and experiment.

Note that in the above antenna the width of the dams is about twice the width of the grooves, which is not in accordance with the assumption made in section 3.4. The dimensions of the grooves and the dams has been chosen in the same way as has been done by Kay [63]. In this report the results of an experimental study concerning corrugated conical horn antennas with large flare angle are described.
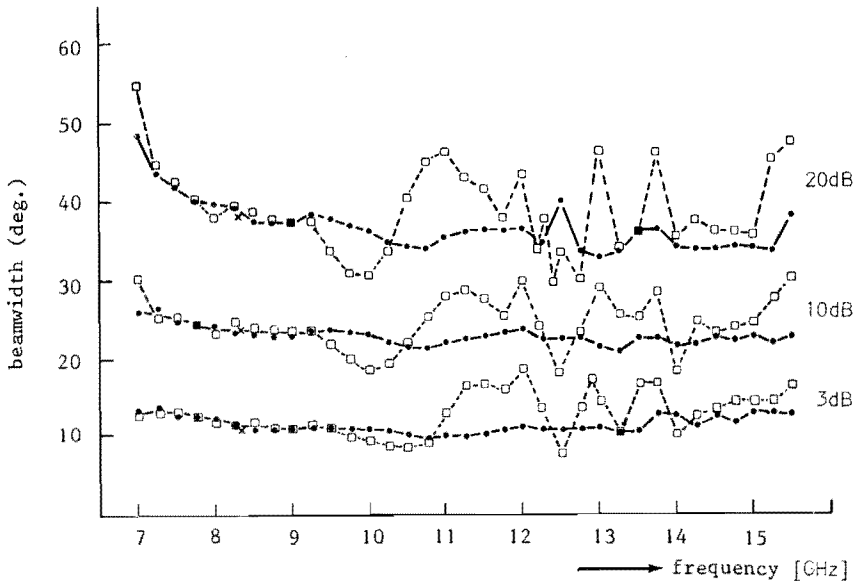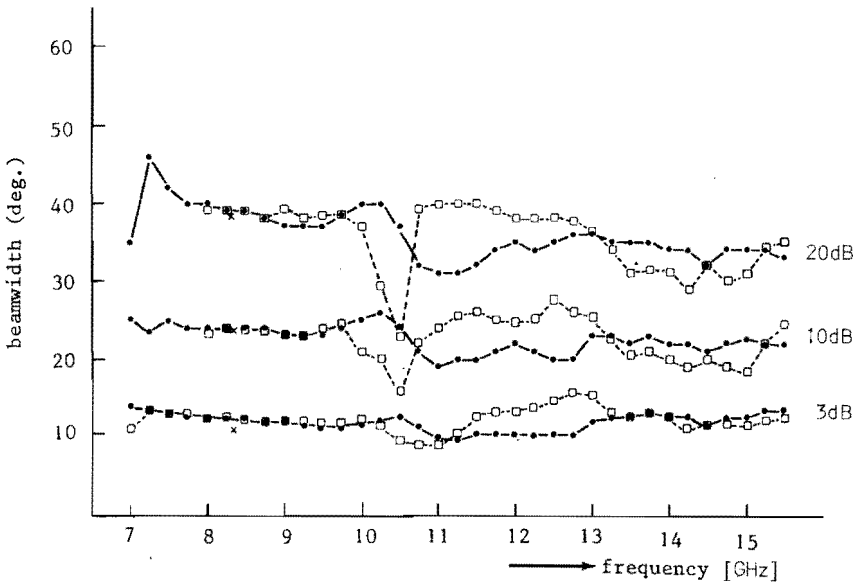

Fig. 3.28. Beamwidth against frequency for antenna 5.

        •, experimental, H-plane,

        □, experimental, E-plane,

        ×, theoretical , H-plane and E-plane.
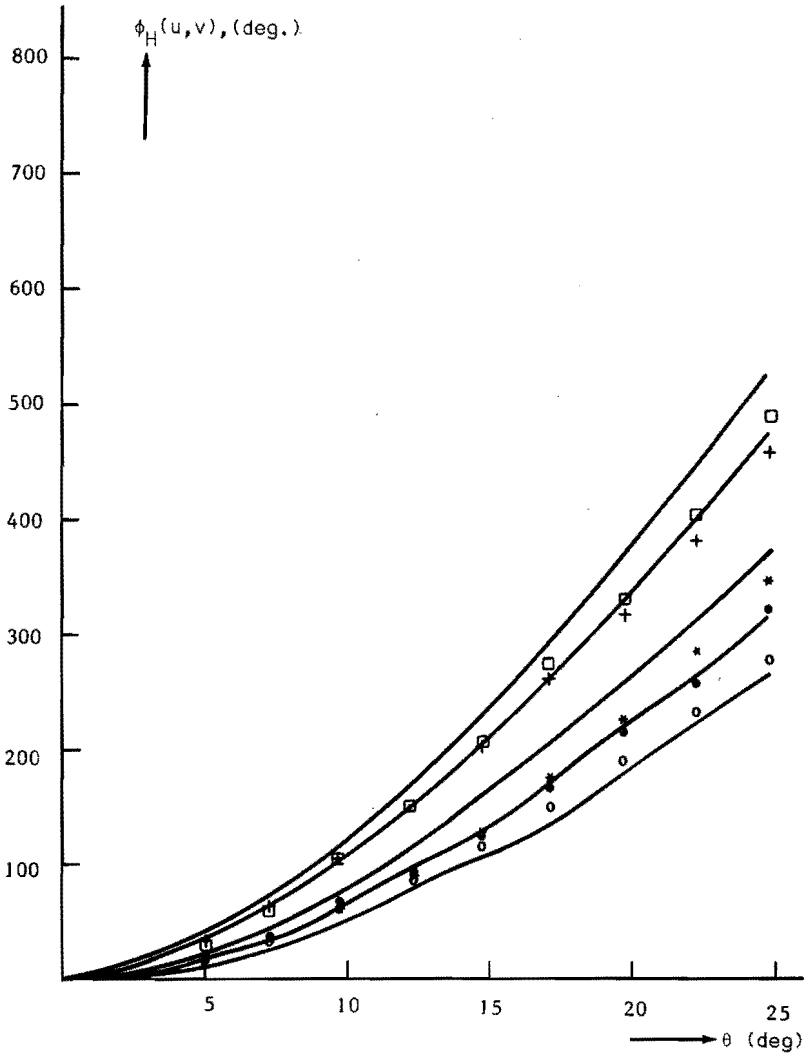
Fig. 3.29. Measured phase variations in H-plane of antenna 5.

o $\frac{d}{\lambda} = 0.5000,$ + $\frac{d}{\lambda} = 0.7500,$

• $\frac{d}{\lambda} = 0.5625,$ □ $\frac{d}{\lambda} = 0.8125,$

* $\frac{d}{\lambda} = 0.6250,$ —— theoretical.
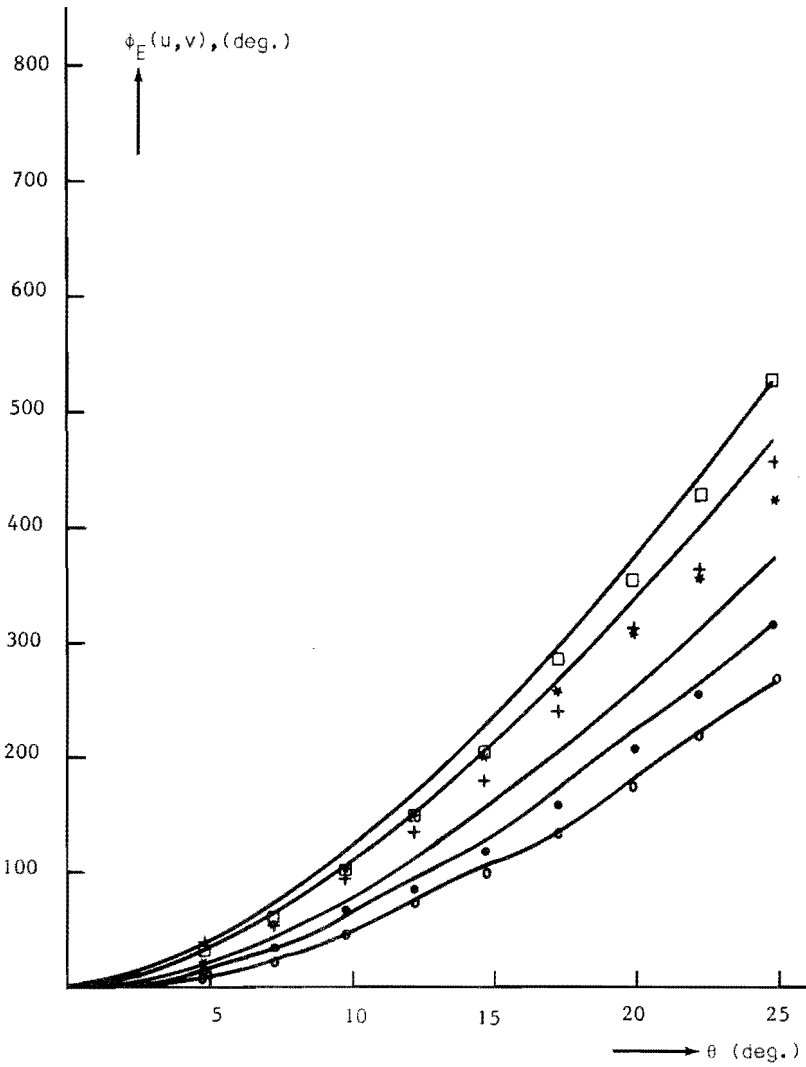
Fig. 3.30. Measured phase variations in E-plane of antenna 5.

o $\frac{d}{\lambda}$ = 0.5000,   + $\frac{d}{\lambda}$ = 0.7500,

• $\frac{d}{\lambda}$ = 0.5625,   □ $\frac{d}{\lambda}$ = 0.8125,

* $\frac{d}{\lambda}$ = 0.6250,   ——— theoretical.

In order to have better agreement with the theoretical assumptions of section (3.4) a new antenna was constructed. This antenna has the same flare angle and aperture as the above antenna, but the width of the dams was chosen as small as possible. The dimensions of this antenna are collected in Table V.

TABLE V

antenna	$2a$ [mm]	$2a'$ [mm]	α_0	p [mm]	t_1 [mm]	t_2 [mm]	d' [mm]	n
5	264	28	15°	26	3.8	2.3	9	67

The power radiation pattern of this antenna has been measured also and the results are given in Fig. 3.28. The main conclusion is that the results are virtually the same as for the former antenna, although the variations in beamwidth as a function of the frequency are a little smoother except for the dip at 10.5 GHz in the 10-dB and 20-dB curves. For the frequency band from 7 GHz to 8 GHz we observed a very broad beam in the E-plane. These results are not plotted in the diagram. We have also measured the phase variation along a circle with a centre that coincides with the centre of the aperture of the antenna. The measurements have been performed in the same way as described in section 2.5. The results are collected in Fig. 3.29 and Fig. 3.30 and good agreement with the theoretical predicted values, at least for the frequency for which the depth of the grooves was a quarter of a wavelength.

APPENDIX A

The expression for the electric field in the far field region is repre-
sented by

$$E(\underline{r}) = \frac{-jk}{4\pi} \frac{e^{-jkr}}{r} \underline{a}_r \times \int_{S_A} \left(\underline{n} \times \underline{E}(\underline{r}') - Z_o \left[\underline{a}_r \times \{ \underline{n} \times \underline{H}(\underline{r}') \} \right] \right) \times$$

$$e^{jkr' \sin \theta \cos(\phi - \phi') -jk \frac{(r')^2}{2r}} \, dS \, . \tag{2.21}$$

This can be written in the abbreviated form

$$E_\theta = \frac{jk}{4\pi} \frac{e^{-jkr}}{r} I_\phi \, , \tag{A.1}$$

$$E_\phi = -\frac{jk}{4\pi} \frac{e^{-jkr}}{r} I_\theta \tag{A.2}$$

with

$$\underline{I} = \int_{S_A} \left(\underline{n} \times \underline{E}(\underline{r}') - Z_o \left[\underline{a}_r \times \{ \underline{n} \times \underline{H}(\underline{r}') \} \right] \right) \times$$

$$e^{jkr' \sin \theta \cos(\phi - \phi') -jk \frac{(r')^2}{2r}} \, dS \, .$$

Using the abbreviation $M = \underline{n} \times \underline{E}(\underline{r}') - Z_o \left[\underline{a}_r \times \{ \underline{n} \times \underline{H}(\underline{r}') \} \right]$
we see that

$$I_\theta = \int_{S_A} M_\theta \, e^{jkr' \sin \theta \cos(\phi - \phi') -jk \frac{(r')^2}{2r}} \, dS \tag{A.3}$$

and

$$I_\phi = \int_{S_A} M_\phi \, e^{jkr' \sin \theta \cos(\phi - \phi') -jk \frac{(r')^2}{2r}} \, dS \, . \tag{A.4}$$

The calculation of M_θ and M_ϕ can be carried out easily if we use Fig.
2.4. Then we find

$$E(\underline{r}') = (E_r' \cos \phi' - E_\phi' \sin \phi') \underline{a}_x + (E_r' \sin \phi' + E_\phi' \cos \phi') \underline{a}_y \, , \tag{A.5}$$

$\underline{a}_x$, $\underline{a}_y$ and $\underline{a}_z$ are unit vectors in a rectangular coordinate system.

Moreover we see that the vector $\underline{n}$ equals $\underline{a}_z$. So

$$\underline{n} \times \underline{E}(\underline{r}') = -(E_r' \sin \phi' + E_\phi' \cos \phi') \, \underline{a}_x + (E_r' \cos\phi' - E_\phi' \sin \phi')\underline{a}_y \, .$$

(A.6)

In a similar way we derive that

$$\underline{n} \times \underline{H}(\underline{r}') = -(H_r' \sin \phi' + H_\phi' \cos \phi') \, \underline{a}_x + (H_r' \cos\phi' - H_\phi' \sin \phi')\underline{a}_y \, .$$

(A.7)

We know that

$$M_\theta = \{\underline{a}_z \times \underline{E}(\underline{r}')\} \cdot \underline{a}_\theta - Z_0 \Big[\underline{a}_r \times \{\underline{a}_z \times \underline{H}(\underline{r}')\}\Big]\underline{a}_\theta =$$

$$\{\underline{a}_z \times \underline{E}(\underline{r}')\} \cdot \underline{a}_\theta + Z_0 \{\underline{a}_z \times \underline{H}(\underline{r}')\} \cdot \underline{a}_\phi$$

(A.8)

and

$$M_\phi = \{\underline{a}_z \times \underline{E}(\underline{r}')\} \cdot \underline{a}_\phi - Z_0 \Big[\underline{a}_r \times \{\underline{a}_z \times \underline{H}(\underline{r}')\}\Big] \cdot \underline{a}_\phi =$$

$$\{\underline{a}_z \times \underline{E}(\underline{r}')\} \cdot \underline{a}_\phi - Z_0 \{\underline{a}_z \times \underline{H}(\underline{r}')\} \cdot \underline{a}_\theta \, .$$

(A.9)

Substitution of the relations

$$\underline{a}_r = \sin \theta \cos \phi \, \underline{a}_x + \sin \theta \sin \phi \, \underline{a}_y + \cos \theta \, \underline{a}_z \, ,$$

$$\underline{a}_\theta = \cos \theta \cos \phi \, \underline{a}_x + \cos \theta \sin \phi \, \underline{a}_y - \sin \theta \, \underline{a}_z \, ,$$

$$\underline{a}_\phi = - \sin \phi \, \underline{a}_x + \cos \phi \, \underline{a}_y$$

and (A.6) and (A.7) in (A.8) and (A.9) gives the following result:

$$M_\theta = \cos(\phi-\phi') \, [-E_\phi' \cos \theta + Z_0 H_r'] + \sin(\phi-\phi') \, [E_r' \cos\theta + Z_0 H_\phi'] \, ,$$

(A.10)

$$M_\phi = \cos(\phi-\phi') \, [E_r' + Z_0 H_\phi' \cos \theta] + \sin(\phi-\phi') \, [E_\phi' - Z_0 H_r' \cos\theta] \, .$$

(A.11)

Combining (A.11) with (A.1) and (A.4) we obtain

$$E_\theta = \frac{jk}{4\pi} \frac{e^{-jkr}}{r} \int_{S_A} \left[\{E'_r + Z_o H'_\phi \cos\theta\} \cos(\phi-\phi') + \{E'_\phi - Z_o H'_r \cos\theta\} \sin(\phi-\phi') \right]$$

$$\times e^{jkr' \sin\theta \cos(\phi-\phi')} - jk \frac{(r')^2}{2r} \, dS \; . \tag{A.12}$$

The combination of (A.10) with (A.2) and (A.3) results in

$$E_\phi = \frac{jk}{4\pi} \frac{e^{-jkr}}{r} \int_{S_A} \left[\{E'_\phi \cos\theta - Z_o H'_r\} \cos(\phi-\phi') - \{E'_r \cos\theta + Z_o H'_\phi\} \sin(\phi-\phi') \right] \times$$

$$e^{jkr' \sin\theta \cos(\phi-\phi')} - jk \frac{(r')^2}{2r} \, dS \; . \tag{A.13}$$

After applying the substitutions $r' = \rho \underline{a}$, $dS = a^2 \rho d\rho d\phi'$,
$u = ka \sin\theta$ and $v = ka^2/2r$ in (A.12) and (A.13) we find the expressions
(2.24) and (2.25)

APPENDIX B

The purpose of this appendix is to summarise the results of De Hoop's
paper [46] and to use them as a theoretical foundation of the method
of phase measurement as has been described in section 2.5. In [46] an
antenna has been considered as a transmitting as well as a receiving
antenna. Let us first summarise the results of [46] for the case that
the antenna is considered to be transmitting. The starting points are
the formulae (2.11) and (2.12). We use essentially the notation of chap-
ter 2, but some minor changes will be made to facilitate the comparison
with [46].

Point P is assumed to be in the far field region of the antenna. Then the following approximation of $r_o = |\underline{r} - \underline{r}'|$ is valid:

$$r_o = |\underline{r} - \underline{r}'| = [(\underline{r},\underline{r}) - 2(\underline{r},\underline{r}') + (\underline{r}',\underline{r}')]^{\frac{1}{2}} \cong r - (\underline{r}^{(1)},\underline{r}') \quad (B.1)$$

where $r = (\underline{r},\underline{r})^{\frac{1}{2}}$ and $\underline{r}^{(1)} = \dfrac{\underline{r}}{r}$.
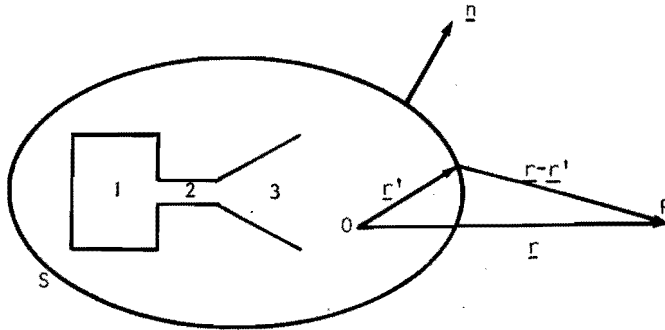
1: generator
2: waveguide
3: antenna

Fig. B.1.   Antenna with closed surface S.

Then we write for the electric field in P

$$E_T(\underline{r}) = \frac{-jk}{4\pi} \frac{e^{-jkr}}{r} \underline{r}^{(1)} \times \int_S \left[\{\underline{n} \times \underline{E}_T(\underline{r}')\} + \right.$$

$$\left. - Z_o \underline{r}^{(1)} \times \{\underline{n} \times \underline{H}_T(\underline{r}')\} \right] e^{jk(\underline{r}^{(1)},\underline{r}')} \, dS$$

$$\underline{E}_T(\underline{r}) = \frac{-jk}{4\pi} \frac{e^{-jkr}}{r} \underline{F}_T(\underline{r}^{(1)}). \quad (B.2)$$

The subscript T denotes the transmitting situation and S represents any closed surface surrounding the antenna. For the magnetic field in P we find

$$Z_o \underline{H}_T(\underline{r}) = \frac{-jk}{4\pi} \frac{e^{-jkr}}{r} \underline{r}^{(1)} \times \underline{F}_T(\underline{r}^{(1)}) . \quad (B.3)$$

134 .

Suppose now that a plane wave is incident upon the antenna from the direction $-\underline{r}^{(1)}$. The plane wave is represented by

$$\underline{E}_i = \underline{B} \, e^{jk(\underline{r}^{(1)}, \underline{r}')} \quad ,$$

(B.4)

$$Z_o \underline{H}_i = \underline{B} \times \underline{r}^{(1)} \, e^{jk(\underline{r}^{(1)}, \underline{r}')} \; .$$

$\underline{B}$ specifies the amplitude and the state of polarisation.

Apart from the incident field there exists a scattered field denoted by $\underline{E}_S$ and $\underline{H}_S$, and the total field in case of receiving is given by

$$\underline{E}_R = \underline{E}_i + \underline{E}_S \; ,$$

$$\underline{H}_R = \underline{H}_i + \underline{H}_S \; .$$

(B.5)

The subscript R denotes the receiving case.

In [46] the following reciprocity relation has been proved:

$$\int_S (\underline{E}_T \times \underline{H}_R - \underline{E}_R \times \underline{H}_T) \cdot \underline{n} \; dS = Z_o^{-1} \, \underline{B} \cdot \underline{f}_T(\underline{r}^{(1)}) \; .$$

(B.6)

It should be noted that the constant in the right-hand side of (B.6) differs somewhat from the one in equation (5.4) in [46]. This is caused by a slightly different definition of the function $\underline{f}_T(\underline{r}^{(1)})$. Again, S denotes any closed surface surrounding the antenna.
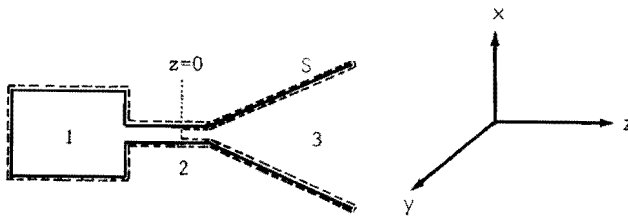
1: generator in case of transmitting

1: load in case of receiving

2: waveguide

3: antenna

4: coordinate system.

Fig. B.2.   Antenna and coordinate system.

If we choose S as indicated in Fig. B.2 and assume that the antenna
system is perfectly conducting, we may restrict the integration in the
left-hand side of (B.6) to a cross-section of the waveguide at z = 0.If
the waveguide between the generator/load and the antenna is long enough,
then we can find a reference plane z = 0 where only the dominant mode
exists. It is then possible to perform the integration of the left-hand
side of (B.6). For this purpose a rectangular coordinate system is in-
troduced. (Fig. B.2). The positive z direction points towards the an-
tenna. The coordinates x and y determine the position of a point in a
given cross-section of the waveguide.

From the theory of wave propagation in cylindrical waveguides [59] we
know that the transverse part $\underline{E}_+$ of the electric field vector and the
transverse part $\underline{H}_+$ of the magnetic field vector can be written as

$$\underline{E}_+(x,y,z) = V(z) \underline{e}(x,y) ,$$

$$\underline{H}_+(x,y,z) = I(z) \underline{h}(x,y) ,$$

(B.7)

where the voltage V(z) and the current I(z) describe the longitudinal
dependence, and $\underline{e}(x,y)$ and $\underline{h}(x,y)$ are the transverse vector functions
of the mode. If a waveguide is analysed on an impedance basis, the
vector functions $\underline{e}(x,y)$ and $\underline{h}(x,y)$ are normalised in such a way that

$$\int \left\{ \underline{e}(x,y) \times \underline{h}(x,y) \right\} . \underline{i}_z \, dxdy = 1 .$$

(B.8)

Substitution of (B.7) and (B.8) in the left-hand side of (B.6) gives
the following result:

$$\int_S (\underline{E}_T \times \underline{H}_R - \underline{E}_R \times \underline{H}_T) . \underline{n} \, dS = V_T I_R - V_R I_T .$$

(B.9)

After introducing the impedance Z_T of the antenna system observed at
z = 0 and the impedance Z_L of the load observed at z = 0, we may write

$$V_T = Z_T I_T ,$$

$$V_R = - Z_R I_R ,$$

(B.10)

where the minus sign in the second expression of (B.10) is due to the

136

fact that the positive z-direction has been chosen towards the antenna.

Substitution of (B.10) in (B.9) gives

$$\int_S (\underline{E}_T \times \underline{H}_R - \underline{E}_R \times \underline{H}_T) \cdot \underline{n} \; dS = (Z_T + Z_R) \; I_R \; I_T \; , \tag{B.11}$$

$$\int_S (\underline{E}_T \times \underline{H}_R - \underline{E}_R \times \underline{H}_T) \cdot \underline{n} \; dS = -(\frac{1}{Z_R} + \frac{1}{Z_T}) \; V_T \; V_R \; . \tag{B.12}$$

Combining (B.6) with (B.11) results in

$$Z_0^{-1} \; \underline{\underline{B}} \cdot \underline{F}_T(\underline{r}^{(1)}) = (Z_T + Z_R) \; I_T \; I_R \; . \tag{B.13}$$

Combining (B.6) with (B.12) gives

$$Z_0^{-1} \; \underline{\underline{B}} \cdot \underline{F}_T(\underline{r}^{(1)}) = -(\frac{1}{Z_R} + \frac{1}{Z_T}) \; V_T \; V_R \; . \tag{B.14}$$

Let us now assume that the point 0 in Fig. B.1 coincides with the centre of the aperture of the antenna.

Then the equations (B.13) and (B.14) give rise to the formulation of the following theorem.

Suppose that a plane wave is incident upon an antenna successively from different directions given by the vector $-\underline{r}^{(1)}$. Suppose further that the phase variations of the transverse part of the electric field vector or the transverse part of the magnetic field vector are measured with respect to the phase in case the plane wave is incident perpendiculary upon the antenna. Then (B.13) and (B.14) show that these phase variations are identical with the phase variations of $\underline{F}_T(\underline{r}^{(1)})$.

If the phase variations are measured in the above way, one should take care that the antenna under test rotates around an axis through the aperture, because the calculations of $F_T(\underline{r}^{(1)})$ are performed in a coordinate system, the origin of which coincides with the centre of the aperture.

The measurements described in section 2.5 are based on the above theorem.

Finally, the author wishes to express his appreciation to De Hoop for making available some unpublished notes, which were relevant to our problem.

SUMMARY

This thesis refers to feeds for reflector antennas. In the introduction
an attempt has been made to describe the properties which a good feed
should possess. Subsequently a review of the recent literature concern-
ing feeds has been given.

In chapter 2 the properties of conical horn antennas with small flare
angles are studied. The slant length of the horn has been chosen in
such a way that the phase distribution across the aperture of the horn
antenna is a quadratic function of the length of the radiusvector in
the aperture. It has been proved in section 2.2 that these antennas
have power radiation patterns which are independent of the frequency
in a rather large frequency band. The theory of the preceding section
has been verified in section 2.3. and it has been shown that frequency-
independent conical horn antennas can be designed in a relative fre-
quency range 1 : 2. The phase radiation patterns of the above antennas
have been studied theoretically in section 2.4. The conclusion is that
the phase radiation pattern is independent of the frequency as well.
Moreover, it turns out that these antennas do not possess a phase centre.
An experimental study of the phase radiation pattern has been under-
taken and is described in section 2.5. For this study a new method of
measurement has been developed. Good agreement between theory and ex-
periment was obtained.
It should be noted that the theory of chapter 2 applies to conical horn
antennas with a perfectly conducting boundary. A property of these an-
tennas is that their radiation patterns are not symmetrical with respect
to the antenna-axis. Moreover, there exist rather high sidelobes in the
E-plane. For some applications these sidelobes and the asymmetry are
undesirable.

In the first section of chapter 3 a theory concerning symmetrical ra-
diation patterns of circular apertures is developed. In section 3.2
wave propagation in a cylindrical waveguide with a special anisotropic
boundary is discussed and it is proved that the transverse part of the

electromagnetic fields is of the same type as the aperture fields found
in section 3.1. So an open radiating cylindrical waveguide with the
anisotropic boundary, specified in section 3.2, gives rise to a symme-
trical radiation pattern. These patterns are discussed in section 3.3.
In the next section a corrugated cylindrical waveguide is studied and
it is proved that this waveguide possesses the special anisotropic
boundary discussed in section 3.2, however, only for one frequency. It
may be expected that the theory of the sections 3.3 and 3.4 is also
valid for corrugated conical horn antennas with small flare angle.
Section 3.5 contains some experimental results of corrugated conical
horn antennas with small flare angle. These results confirm the theory
of the preceding sections. Moreover, it is shown that symmetrical power
radiation patterns are obtained in a rather large frequency range, es-
pecially if the aperture is not small.
The frequency-independent properties of the conical horn antenna with
perfectly conducting boundary are obtained by a right choice of the
dimensions of the antenna. This raises the question whether it is
possible to combine the frequency-independent properties of the conical
horn antenna with perfectly conducting boundary and the symmetry pro-
perties of the conical horn antenna with anisotropic boundary. Calcula-
tions concerning this question are given in section 3.6 and show that
frequency-independent conical horn antennas with a symmetrical radia-
tion pattern can be obtained provided the anisotropic boundary which
has been assumed in section 3.6 can be realised independent of the
frequency. This question has been investigated experimentally in sec-
tion 3.7. In this section the properties of corrugated conical horn
antennas with small flare angles and large apertures are studied. The
dimensions of the antennas are chosen in such a way that again the
phase distribution across the aperture is a quadratic function of the
length of the radiusvector in the aperture. The experimental results
show that indeed a symmetrical radiation pattern can be obtained in a
frequency range from 8 GHz to 10 GHz, while acceptable patterns are
obtained in the frequency range from 10 GHz to 15GHz with the excep-
tion of a small frequency range around 10.5 GHz. Finally the phase
radiation pattern of the above antenna has been studied and good
agreement with the theoretical predictions was found, at least for the
frequency for which the depth of the grooves is a quarter of a wave-
length.

X

SAMENVATTING

Dit proefschrift heeft betrekking op belichters voor reflector anten-
nes. In de inleiding is een poging gedaan de eigenschappen te beschrij-
van, die een goede belichter dient te bezitten. Vervolgens is een over-
zicht van de recente literatuur over belichters gegeven.

In hoofdstuk 2 worden de eigenschappen van conische hoorn antennes met
een kleine tophoek bestudeerd. De lengte van de hoorn antenne is zoda-
nig gekozen dat de faseverdeling over de apertuur een kwadratische
funktie is van de lengte van de radiusvector in de apertuur. In para-
graaf 2.2 wordt bewezen dat deze antennes een vermogensstralingsdia -
gram bezitten, dat onafhankelijk is van de frequentie in een tamelijk
grote frequentieband. De theorie van de vorige paragraaf is geverifi-
eerd in paragraaf 2.3 en er is aangetoond dat inderdaad frequentie -
onafhankelijke conische hoorn antennes ontworpen kunnen worden in een
relatieve frequentieband 2 : 1. Het fasestralingsdiagram is theoretisch
onderzocht in paragraaf 2.4. De conclusie is dat het fasestralingsdia-
gram eveneens onafhankelijk is van de frequentie. Bovendien blijkt dat
deze antennes geen fasecentrum bezitten. Een experimenteel onderzoek
naar het fasestralingsdiagram is in paragraaf 2.5 beschreven. Het was
nodig voor dit onderzoek een nieuwe meetmethode te ontwikkelen. De
overeenstemming tussen theoretische en experimentele resultaten was
goed.

De theorie van hoofdstuk 2 is geldig voor conische hoorn antennes met
een perfect geleidende wand. Een eigenschap van deze antennes is dat
het stralingsdiagram niet symmetrisch is met betrekking tot de antenne-
as. Bovendien bezitten deze antennes hoge zijlussen in het E-vlak van
het stralingsdiagram. Voor sommige toepassingen zijn deze zijlussen en
de asymmetrie ongewenst. In de eerste paragraaf van hoofdstuk 3 is een
theorie betreffende symmetrische stralingsdiagrammen van cirkelvormige
aperturen ontwikkeld.

Het onderwerp van paragraaf 3.2 is golfvoortplanting in een cirkel-
cylindrische golfgeleider met een anisotrope wand. Er wordt bewezen

dat de transversale veldverdeling van hetzelfde type is als de aper-
tuurvelden, die in paragraaf 3.1 gevonden zijn. Dus een open cirkel-
cylindrische golfgeleider met de anisotrope wand, die in paragraaf 3.2
nader gespecificeerd is, heeft een symmetrisch stralingsdiagram. Deze
diagrammen zijn onderwerp van discussie in paragraaf 3.3. In de vol-
gende paragraaf worden cirkelcylindrische golfgeleiders met groeven
in de wand bestudeerd en de conclusie is dat deze golfgeleiders een
anisotrope wand bezitten met dezelfde eigenschappen als in paragraaf
3.2 verondersteld werd, echter slechts voor een frequentie. Men mag
verwachten dat de theorie van de paragrafen 3.3 en 3.4 ook geldig is
voor conische gegroefde hoorn antennes met kleine tophoek. Paragraaf
3.5 bevat enige experimentele resultaten verkregen met conische ge-
groefde hoorn antennes met kleine tophoek. Deze resultaten bevestigen
de theorie van de vorige paragrafen. Bovendien is aangetoond dat
symmetrische stralingsdiagrammen kunnen worden verkregen in een tame-
lijke grote frequentieband, speciaal als de apertuur niet te klein is.

De frequentie-onafhankelijke eigenschappen van de conische hoorn an-
tenne met perfect geleidende wand worden verkregen door een juiste
keuze van de afmetingen van de antenne. Men kan zich nu afvragen of
het mogelijk is de frequentie-onafhankelijke eigenschappen van de
normale conische hoorn antenne met perfect geleidende wand te combi-
neren met de symmetrie eigenschappen van de conische gegroefde hoorn
antenne. Berekeningen betreffende deze kwestie zijn in paragraaf 3.6
opgenomen en de conclusie is dat frequentie-onafhankelijke conische
hoorn antennes met een symmetrisch stralingsdiagram inderdaad ontworpen
kunnen worden onder voorwaarde dat de anisotrope wand, die in paragraaf
3.6 verondersteld werd, gerealiseerd kan worden voor iedere frequentie.
De laatste kwestie is experimenteel onderzocht in paragraaf 3.7. In
deze paragraaf worden de eigenschappen van conisch gegroefde hoorn
antennes met kleine tophoek en grote apertuur bestudeerd.
De afmetingen van de antennes zijn weer zodanig gekozen dat een fase-
verdeling over de apertuur ontstaat, die een kwadratische functie is
van de lengte van de radiusvector in de apertuur. De experimentele re-
sultaten laten zien dat inderdaad symmetrische stralingsdiagrammen
worden verkregen in een frequentieband van 8GHz tot 10 GHz, terwijl
acceptabele diagrammen worden verkregen in een frequentieband van
10 GHz tot 15 GHz met uitzondering van een kleine frequentieband om

10,5 GHz. Tenslotte werd het fasestralingsdiagram van de bovengenoemde antenne bestudeerd en een goede overeenstemming werd gevonden tussen de experimentele resultaten en de theoretische resultaten, tenminste voor de frequentie waarvoor de diepte van de groeven een kwart van de golflengte was.

✕

REFERENCES

[1] Jasik, H.,"Antenna Engineering Handbook", p 1 - 4, p 17 - 22.

[2] Geyer, H.,"Runder Hornstrahler mit ringförmigen Sperrtöpfen usw",
Frequenz 20 (1966),S. 22 - 28.

[3] Galindo, V., "Design of Dual-Reflector Antennas with Arbitrary
Phase and Amplitude Distributions", I.E.E.E. AP - 12, 1964,
pp 403 - 408.

[4] Dijk, J., Jeuken, M. and Maanders, E.J., "An Antenna for a Satel-
lite Communication Groundstation", T.H.-report 68-E-01, March 1968,
Technological University Eindhoven, Netherlands.

[5] Muller, C.A., "Polarization Measurements in Radio Astronomy",
Progress in radio science 1963-1966. Proceedings during XV general
assembly of U.R.S.I. Munich, september 1966.

[6] Van Binsbergen, P.R.M., "Een studie betreffende de kruispolarisa-
tie bij grote paraboloïdale reflector antennes",
Verslag ETA-31-1968, december 1968, Technische Hogeschool, Eind-
hoven.

[7] Koch, G.F., "A new Feed For Low Noise Paraboloid Antennas",
Conference On Design And Construction Of Large Steerable Aerials,
I.E.E. Conference Publication 21.

[8] Koch, G.F., "Koaxialstrahler als Erreger für rauscharme Parabol-
antennen", N.T.G.-U.S.R.I. Tagung Antennen und Elektromagnetische
Felder, Darmstadt 17 - 20 Okt. 1967.

[9] Geyer, H., ibid.

[10] Thust, P., "Hornstrahler mit sektorähnlichem Richtdiagramm usw.",
Frequenz 20 (1966), S. 148 - 155.

[11] Potter, P.D., "A new Horn Antenna with Suppressed Sidelobes and
Equal Beamwidths", The microwave journal, June 1963, pp. 71 - 78.

[12] Nagelberg,E.R., and Shefer,J., "Mode Conversion in Circular Wave-
guides", B.S.T.J. 1965. pp 1321 - 1338.

[13] Reitzig, R., "Anwendung des Variationprinzips zur Ermittlung des
Einflusses kleiner Unstetigkeitsstellen im Rundhohlleiter",
Frequenz 22 (1968), S. 45 - 52.

[14] Ludwig, A.C., "Radiation Pattern Synthesis for Circular Aperture
Horn Antennas",I.E.E.E. AP - 14, 1966, pp 434 - 440.

[15] Minett, H.C., and Mac A. Thomas, "A Method of Synthesising Radiation Patterns with Axial Symmetry", I.E.E.E. AP - 14, 1966, pp 654 - 656.

[16] Rumsey, V.H., "Horn Antennas with Uniform Power Pattern Around Their Axis", I.E.E.E. AP - 14, 1966, pp 656 - 658.

[17] Simmons, A.J. and Kay A.F., "The Scalar Feed - A High - Performance Feed For Large Paraboloid Reflectors". Conference on Design and Construction of Large Steerable Aerials, I.E.E. Conference Publication 21.

[18] Silver, S.,"Microwave Antenna Theory and Design", Chap. 10, McGraw-Hill 1949.

[19] Jasik, H.,"Antenna Engineering Handbook", Chap.10, McGraw-Hill 1961.

[20] Trentini, G. von, "Erregersysteme für Cassegrain-Antennen", Frequenz/Sonderausgabe, 17, S. 491 - 499, Dec. 1965.

[21] Trentini, G. von, Romeiser, K.P. und Jatsch, E., "Dimensioniering und Elektrische Eigenschaften der 25-M-Antenne der Erdefunkstelle Raisting usw.", Frequenz 19, Nr. 12,S. 402 - 421, Dec. 1965.

[22] Trentini, G. von, Romeiser, K.P. Reitzer, R., "Anderungs- und Verbesserungsmöglichkeiten im Aufbau groszer Cassegrain-Antennen mit Hornparabolspeisung", Frequenz 22, August 1968, S. 216 - 223.

[23] Jasik, H., ibid, pp 10 - 11 etc.

[24] Schorr, M.G. and Beck, F.J., "Electromagnetic Field of The Conical Horn". Journal of Applied Physics 21,1950,pp 795 - 801.

[25] Flügge, S., "Handbuch der Physik", Bd.25, S. 238 - S. 240, Springer-Verlag, Berlin, Göttingen, Heidelberg 1961.

[26] Hoop, A.T. de. "Propagatie en Diffractie van Electromagnetische Golven" p 105 - 109, T.H.Delft 1966.

[27] Hansen, R.C., "Microwave Scanning Antennas". p 26, Academic Press New York and London 1964.

[28] Ming-Kuei Hu, "Fresnel Region Fields of Circular Aperture Antennas" Journal of Research of the N.B.S.-D, Radio Propagation vol. 65 D no. 2, March - April 1961.

[29] Hansen, R.C., ibid. p. 32.

[30] Hansen, R.C., ibid. p. 22.

[31] Kikkert, J.S., "Een onderzoek naar de frequentie-afhankelijkheid van apertuurantennes", report graduate work, Eindhoven ETA-15-1968.

[32] Hansen, R.C., ibid. p. 38.

[33] Harrington, R.F.,"Time-harmonic electromagnetic fields", New York 1961.

[34] Fradin, A.Z., "Microwave Antennas", p 224, Pergarnon Press, Oxford, London, New York, Paris 1961.

[35] Bateman, H., "Higher Trancedental Functions". vol. I. p. 144, McGraw-Hill, New York, Toronto, London 1953.

[36] Robin, Louis, "Functions spheriques de Legendre et functions spheroidales", p. 34 et p. 242, tome II, Gauthier villars, Paris 1958.

[37] Stratton, J.A., "Electromagnetic Theory", p. 372, MacGraw-Hill, New York and London 1941.

[38] Irving, J. and Mullineux N., "Mathematics in Physics and Engineering". p. 156, Academic Press, New York and London 1959.

[39] Jasik, H., ibid. p. 10 - 11.

[40] King, A.P., "The Radiation Characteristics of Conical Horn Antennas", Proceedings of the I.R.E. vol.38 pp. 249 - 251. March 1950.

[41] Hamid, M.A.K., "Diffraction by a Conical Horn". I.E.E.E. AP - 16, 1968, pp 520 - 527.

[42] Dijk, J., Jeuken, M.E.J. and Maanders, E.J., "Blocking and diffraction in cassegrain antenna systems", De Ingenieur no. 27 1968, pp. 079 - 091.

[43] Silver, S., ibid. chap. 15.

[44] I.E.E.E. Test Procedure for Antennas, Transactions on Antennas and Propagation, vol. 13, 1965; pp. 437 - 466.

[45] Silver, S., ibid. p. 431.

[46] de Hoop, A.T., "A Reciprocity Relation Between the Transmitting And The Receiving Properties Of An Antenna", Appl. Sci. Res. 19, 1968, pp. 90 - 96.

[47] Rumsey, V.H., "Frequency Independent Antennas", Academic Press. New York and London 1966.

[48] Cook, J.S. and Lowell, R., "The Autotrack System". B.S.T.J. 42, no. 4, pt. 2, pp. 1283 - 1307, July 1963.

[49] Nakahashi, N., Kakinuma, Y. and Shirai, T., "A multimode Autotrack System Employing the Circular TE_{11} and TE_{21} mode", Journal of the Radio Research Laboratories. vol. 14, no. 73, pp. 129 - 152.

[50] Flügge, S. ibid p. 225.

[51] Harrington, R.F., ibid p. 204.

[52] Harrington, R.F., ibid p. 203.

[53] Abramowitz, M. and Stegun I.A., "Handbook of Mathematical Functions". p. 374. Dover Publication, Inc. New York 1964.

[54] Collin, R.E., "Field Theory of Guided Waves", p. 198, McGraw-Hill Book Company New York, Toronto, London 1960.

[55] Saxon, G., Jarns, T.R. and White, I., "Angular-dependent modes in circular corrugated waveguide", Proceedings I.E.E., vol. 110, no.8, August 1963.

[56] Davies, J.B. and Goldsmith, B.J., "An Analysis of General Mode Propagation And The Puls-shortening Phenomenon In Electron Linear Accelerators". Philips Res. Reports vol. 23 pp. 207 - 232, 1968.

[57] Harrington, R.F., ibid p. 208.

[58] Harrington, R.F., ibid p. 199.

[59] Silver, S., ibid p. 210.

[60] Abramowitz, M. and Stegun I.A., ibid p. 364.

[61] Bryant, G.H., "Propagation in corrugated waveguides", Proc. I.E.E. vol. 116, pp 203 - 213, 1969.

[62] Jeuken, M.E.J. and Kikkert, J.S., "A broadband aperture antenna with a narrow beam" Alta Frequenza, 38, 1969, Numero Speciale pp. 270 - 276.

[63] Kay, A.F., "The scalar feed", TRG report, contract AF 19(604) - 8057, March 1964.

146

ACKNOWLEDGEMENTS

LEVENSBERICHT

Geboortedatum:	24 februari 1935
juni 1951	Eindexamen Mulo A+B te Venray
juni 1953	Eindexamen Rijks H.B.S. B te Venlo
december 1955	Kandidaatsexamen Wis- en Natuurkunde Rijks Universiteit te Utrecht
maart 1960	Doctoraalexamen Wis- en Natuurkunde Rijks Universi - teit te Utrect. Hoofdvak experimentele natuurkunde; bijvakken wiskunde en theoretische natuurkunde
maart 1960 - augustus 1961	Docent natuurkunde bij het V.W.O.
september 1961	In dienst getreden bij de afdeling Elektrotechniek van de Technische Hogeschool te Eindhoven. Aanvankelijk gewerkt aan golfvoortplanting in anisotrope media. Vervolgens de inrichting van een antennelaboratorium in het toen nog in aanbouw zijnde laboratorium voor elektrotechniek ter hand genomen. Een tiental afstudeerprojekten begeleid. De resultaten van vier hiervan zijn gepubliceerd in vaktijdschriften. Het onderwerp van dit proefschrift werd eveneens in het antennelaboratorium bewerkt. Daarnaast werd meegewerkt aan een voorlopig ontwerp van een antenne voor satellietkommunikatie. Tenslotte werden diverse antennes ontwikkeld ten behoeve van de nederlandse radioastronomen.

Errata

p. 23: 2nd line: "fase" should be "phase".

p. 77: 15th line: "(3.1) is" should be "(3.1) are".

p. 100: k_C should be Γ_C.

p. 111: formula (3.105): H_ϕ' should be H_z'.

STELLINGEN

1.

De symmetrie eigenschappen van het stralingsdiagram van hoorn anten-
nes kunnen niet gevonden worden door uit te gaan van een model van de
antenne waarbij het apertuurvlak uitgebreid wordt met een oneindig
grote vlakke plaat die perfekt geleidend is.

> *Collin R.E. and Zucker F.J., "Antenna Theory", part 1, page 73,*
> *formulae (3.27^a) and (3.27^b).*

2.

Tegen de wijze waarop Shih en Bergstein de resultaten van hun bereke-
ningen presenteren zijn bedenkingen aan te voeren.

> *Shih S.L. and Bergstein L., "Synthesis of nonuniform antenna*
> *arrays using lambda functions", Proc. I.E.E., vol. 114, no. 9,*
> *sept. 1967, pp 1237 - 1241.*
> *Reinders M., "Niet uniform belichte lineaire configuraties met*
> *een sinusvormige positieverdeling en een optimaal stralingsdia-*
> *gram". Verslag afstudeerwerk ETA-6, oktober 1965.*

3.

De afleiding die Clarricoats geeft van de randvoorwaarden die toege-
past moeten worden om de modes in een gegroefde conische golfgeleider
met grote tophoek te vinden is niet korrekt.

> *Clarricoats P.J.B., "Analysis of spherical hybrid modes in a*
> *corrugated conical horn". Electronic Letters, 1st May 1969,*
> *vol. 5, no. 9, p. 189.*

De randvoorwaarden, die toegepast moeten worden om de modes in een ge-
groefde conische golfgeleider te vinden, kunnen gevonden worden door in
het theoretische model de groeven te vervangen door sferische groeven.

*Jansen J.K.M., Jeuken M.E.J. and Lambrechtse C.W., "The scalar
feed", T.H. report 70-E-12, december 1969.*

<div align="center">5.</div>

De meetmethode welke door Maxum is toegepast ter bepaling van de reso-
nantielengte van een komplexe gleuf in de bovenkant van een rechthoe -
kige golfgeleider is niet korrekt, omdat de gleuf in het transmissie -
lijnmodel wordt voorgesteld als een shunt element.

*Maxum B.J., "Resonant Slots with Independent Control of Ampli-
tude and Phase", I.E.E.E., AP-8, 1960, pp 384 - 389.
Van Gemert J.J.A., "Een niet-uniform belichte, ongelijk gespa-
tieerde gleufantenne, met optimaal stralingsdiagram", Verslag
afstudeerwerk ETA-12, juni 1967.*

<div align="center">6.</div>

Om radio-astronomische antennes met een lage ruistemperatuur te verkrij-
gen verdienen conische gegroefde hoorn antennes met grote tophoek als
belichter de voorkeur boven open gegroefde cylindrische golfpijpen waar-
in meerdere modes toegepast worden.

*Vu T.B. and Vu Q.H., "Optimum feed for large radio-telescopes:
experimental results". Electronic Letters 19th March 1970, vol.6,
p.159.*

<div align="center">7.</div>

In verband met de toenemende urbanisatie en de voortdurend stijgende
vraag naar elektrische energie is het gewenst dat het onderzoek naar
transportmiddelen voor elektrische energie, welke ondergronds kunnen
worden aangebracht, wordt gestimuleerd. De centrale overheid dient
hierbij het initiatief te nemen. De benodigde fondsen zouden gevonden

kunnen worden door een temporisering van het onderzoek aan kernenergie-
centrales toe te passen.

8.

Het is gewenst dat de voorlichtingsorganen van verenigingen ter be-
scherming van landschapsschoon bij publikatie van alternatieve voor-
stellen met betrekking tot vestiging van nieuwe elektrische centrales
niet na laten de financiële konsekwenties van hun alternatieve oplos-
singen aan te geven.

*Natuurbescherming 1968 - 1969. Verslag van de werkzaamheden
van de Contact-Commissie voor Natuur- en Landschapsbescherming.*

9.

Het feit dat in de monumentenwet niet is voorgeschreven binnen welke
termijn de Kroon een beslissing dient te nemen met betrekking tot een
ingediend bezwaarschrift schept een ongewenste rechtsonzekerheid.

10.

Nu de laatste stukken woeste grond van het voormalige moerasgebied de
Peel ontgonnen zijn en bovendien de archieven van de dorpen, die om
dit gebied liggen, geordend en toegankelijk gemaakt worden ontstaat
de behoefte aan een monografie waarin de geschiedenis van de Peel be-
schreven wordt. Deze monografie dient tenminste de volgende onderwer-
pen te bevatten: een beschrijving van het gebruik van de Peel, van de
eigendomsrechten en van de ontginningen.

*Philips J., Jansen J. en Claessens Th., "Geschiedenis van de
landbouw in Limburg 1750-1914", Van Gorcum, Assen 1965.
Van Emstede E., "Varia Peellandiae Historiae ex fontibus",
Deurne, 1965 t/m 1970.*

Eindhoven, 8 september 1970.   M.E.J. Jeuken.